

Capacity Optimization for Self-organizing Networks: Analysis and Algorithms

Dem Fachbereich 18
Elektrotechnik und Informationstechnik
der Technischen Universität Darmstadt
zur Erlangung der Würde eines
Doktor-Ingenieurs (Dr.-Ing.)
vorgelegte Dissertation

von
Dipl.-Ing. Philipp Paul Hasselbach
geboren am 4. März 1980 in Wetzlar

| | |
|-----------------------------|------------------------------|
| Referent: | Prof. Dr.-Ing. Anja Klein |
| Korreferent: | Prof. Dr.-Ing. Thomas Kürner |
| Tag der Einreichung: | 22. September 2011 |
| Tag der mündlichen Prüfung: | |

Kurzfassung

Mobilfunknetze sind heutzutage allgegenwärtig. Die große Popularität mobiler Kommunikation und die schnelle Verbreitung moderner Endgeräten haben in den letzten Jahren zu einer stetig wachsenden Beliebtheit von mobilen Datendiensten geführt. Um die steigende Kapazitätsnachfrage zu bedienen, müssen Netzbetreiber ihre Netzinfrastruktur ausbauen, was zu einem Anstieg der Investitionskosten führt. Gleichzeitig führt der technische Fortschritt zu immer komplexeren Systemen und zu der Notwendigkeit, mehrere Mobilfunknetze unterschiedlicher Technologien gleichzeitig zu betreiben, wodurch der Aufwand für die Netzsteuerung stark ansteigt und sich in erhöhten Betriebskosten der Netzbetreiber niederschlägt. Um wettbewerbsfähig zu bleiben, sind Netzbetreiber daher zu Kostensenkungen gezwungen, ohne dabei die Netz- und Dienstqualität zu verringern.

Selbstorganisierende Netze (SONs) werden als Schlüsseltechnologie für zukünftige Mobilfunknetze betrachtet. Sie haben im Gegensatz zu herkömmlichen Mobilfunknetzen die Fähigkeit, viele Aufgaben aus dem Bereich Betrieb und Steuerung automatisch und autonom mit qualitativ hochwertigen Ergebnissen auszuführen. Von der Einführung von SONs wird daher erwartet, dass einerseits die Effizienz von Mobilfunknetzen zunimmt und damit die Netzkapazität steigt und so die zunehmenden Investitionskosten relativiert werden. Andererseits werden autonome Funktionen den benötigten Aufwand für die derzeit hauptsächlich manuell ausgeführten Aufgaben aus Betrieb und Steuerung reduzieren und die Betriebskosten senken. Allerdings stellen die hohe Komplexität und die verteilte Struktur von Mobilfunknetzen insbesondere im Zusammenhang mit hohen Anforderungen an Echtzeitfähigkeit und Zuverlässigkeit von SONs große Herausforderungen an die Entwicklung von Algorithmen für den automatischen Betrieb von Mobilfunknetzen dar. SONs erfordern daher neue Ansätze und Konzepte für den automatischen Betrieb von Mobilfunknetzen.

Diese Arbeit erforscht die automatische Anpassung eines zellularen Mobilfunknetzes an schwankende Kapazitätsanforderungen durch die adaptive Zuweisung von Funkressourcen. Dazu wird ein hierarchisches Konzept mit zwei Ebenen vorgeschlagen. Das Konzept trennt die Anpassung des Netzes an die Kapazitätsanforderungen von der Ressourcenzuweisung an einzelne Nutzer und reduziert damit die Komplexität der Netzanpassung soweit, dass ein effizienter automatischer Betrieb in Echtzeit möglich wird. Für die Ressourcenzuweisung an einzelne Nutzer in der zweiten Ebene werden bestehende Verfahren verwendet. Die automatische Anpassung des Netzes findet in der ersten Ebene statt. In diesem Zusammenhang wird ein neues Netzmodell, das

zellzentrische Netzmodell, vorgeschlagen. Das Modell stellt den Zusammenhang zwischen der Kapazität einer Zelle und der Ressourcenallokation der Zelle in Form von Zellbandbreite und Sendeleistung her und berücksichtigt die Verteilung und die Kapazitätsanforderungen der Nutzer, anstatt die Nutzer einzeln zu modellieren, wie in bisherigen Netzmodellen üblich. Es abstrahiert damit von einzelnen Nutzern und betrachtet ganze Zellen, so dass die Modellkomplexität stark verringert wird und effiziente selbstorganisierende Ansätze möglich werden. Außerdem werden der Einfluss der Umgebung auf die Signalausbreitung und die Interferenz durch andere Zellen berücksichtigt, so dass das Modell eine hohe Genauigkeit aufweist.

Das zellzentrische Netzmodell wird verwendet, um verschiedene Optimierungsprobleme für die automatische Kapazitätsoptimierung in SONS aufzustellen. Die Optimierungsprobleme haben verschiedene Optimierungsziele und erreichen die Kapazitätsoptimierung mit Hilfe einer Anpassung der Zellbandbreiten oder der Sendeleistungen oder der gleichzeitigen Anpassung von beidem. Für die Lösung der Optimierungsprobleme werden Algorithmen mit zentraler und mit verteilter Implementierung vorgeschlagen. Zentrale Algorithmen sind im Allgemeinen für die Simulation und die Analyse geeignet. Verteilte Algorithmen sind von großer Bedeutung für SONS, da sie aufgrund der verteilten Implementierung der Struktur von Mobilfunknetzen gerecht werden und damit effizient umgesetzt werden können und robust gegenüber Störungen sind.

Für die Validierung der vorgeschlagenen Ansätze zur automatischen Kapazitätsoptimierung und zur Leistungsevaluation der Ansätze wird ein Simulationsansatz mit Szenarien mit sogenannten Hotspots in der Kapazitätsnachfrage vorgestellt. Der Simulationsansatz wird verwendet, um die grundsätzliche Anwendbarkeit und Eignung der Ansätze für die automatische Kapazitätsoptimierung von zellularen Mobilfunknetzen zu untersuchen und um ihre Stärken und Schwächen zu identifizieren. Die Untersuchungen vergleichen den Stand der Technik mit den vorgeschlagenen neuen Ansätzen, zeigen, welcher Optimierungsansatz in welchen Szenarien die beste Leistung erzielt und verdeutlichen den Einfluss des Diensttyps.

Schließlich wird ein Ansatz zur Ableitung eines Simulationsszenarios, das auf einem realen Netz basiert und mit Hilfe von Messungen des Zelldurchsatzes gewonnen wird, vorgestellt. Die vorgeschlagenen Ansätze zur automatischen Kapazitätsoptimierung werden auf ein mit Hilfe dieses Ansatzes gewonnenes reales Szenario angewendet und im Hinblick auf ihre Anwendbarkeit in der Praxis untersucht. Die Simulationsergebnisse bestätigen die Erkenntnisse aus den Untersuchungen in den Hotspot-Szenarien und bestätigen die Praxistauglichkeit der Ansätze. Um eine detaillierte Analyse durchzuführen, wird das reale Szenario im Hinblick auf Bereiche, in denen Hotspots in

der Kapazitätsnachfrage auftauchen, untersucht. Die vorgeschlagenen Ansätze zur automatischen Kapazitätsoptimierung werden speziell für diese Bereiche betrachtet und es wird gezeigt, dass die vorgeschlagenen Ansätze lokal in Gegenden mit inhomogener Kapazitätsnachfrage erhebliche Gewinne erzielen.

Abstract

Mobile radio networks are ubiquitous nowadays. The large popularity of mobile communication and the fast proliferation of advanced mobile devices have led to a significant increase in the use of mobile data services. Network operators, therefore, have to extend the capacity of their networks in order to meet the increasing capacity demand, causing high capital expenditures (CAPEX). At the same time, technical progress leads to increasingly complex networks and to the need to operate several networks of different technologies in parallel, causing high effort in operation and management of mobile communication networks, which leads to high operational expenditures (OPEX). As a consequence, in order to stay economically competitive, network operators need to lower costs without sacrificing network and service quality.

Self-organizing networks (SONs) are considered a key technology for future mobile radio networks. In contrast to conventional mobile radio networks, they are able to carry out a wide range of tasks in the field of operation and management in an automatic and autonomous way and with a high level of sophistication. SONs, thus, promise to increase the efficiency of mobile radio networks, leading to higher capacity of the network and counteracting the increase in CAPEX. The autonomous operation furthermore reduces the effort required to carry out operation and management tasks which are currently done mostly manually and, therefore, lowers OPEX. The high complexity and the distributed structure of mobile radio networks, on the other hand, pose in connection with the high demands on real-time capability and reliability of SONs great challenges on the development of algorithms for the automatic operation of mobile radio networks. As a consequence, SONs require new approaches and concepts in order to enable the automatic operation of mobile radio networks.

In this thesis, the automatic adaptation of a cellular mobile radio network to varying capacity demands by adapting the radio resource allocation is investigated. For this purpose, a hierarchic concept with two planes of hierarchy is proposed. The concept separates the capacity demand adaptation of the network from the resource allocation to individual users and reduces the complexity of the network adaptation to an extent that allows efficient automatic operation in real time. For the allocation of resources to individual users, as done in the lower plane, existing methods are applied. The automatic adaptation of the network is carried out in the upper plane. In this context, a new network model, the cell-centric network model, is proposed. It models the relation between the capacity of a cell and the resource allocation of the cell in terms of cell bandwidth and transmit power and considers the distribution of the users and their capacity demands, instead of modeling the individual users, as it is done in current

network models. This way, the model abstracts from individual users and considers whole cells, such that the modeling complexity is reduced significantly, making efficient self-organizing approaches possible. Furthermore, interference from other cells and the influence of the environment on signal propagation are considered, such that the model achieves high accuracy.

Using the cell-centric network model, different optimization problems for the automatic capacity optimization for SONs are developed. The optimization problems have different optimization goals and achieve the capacity optimization by allocating cell bandwidth, transmit power or both, cell bandwidth and transmit power, jointly. For the solution of the optimization problems, different algorithms with central as well as distributed implementations are proposed. Central algorithms are in general suited for simulation and analysis purposes. Distributed algorithms are of practical relevance for SONs since their implementation corresponds to the structure of mobile radio networks, such that they can be implemented efficiently and provide robustness against failure.

For verification of the proposed automatic capacity optimization approaches for SONs and for performance evaluation of the approaches, a simulation approach with scenarios with capacity demand hotspots is presented. Using this simulation approach, the proposed automatic capacity optimization approaches for SONs are investigated in order to gain insight into their behavior and in order to identify their strengths and weaknesses. The simulations are used to compare the state of the art with the proposed new approaches, show which capacity optimization approach performs best with the different distributions of the capacity hotspots and illustrate the influence of the service type.

Finally, an approach for the derivation of a real-world simulation scenario that is based on a real network and obtained using throughput measurements is presented. The proposed approaches for automatic capacity optimization are applied to a real-world scenario obtained using this approach and are evaluated with respect to their performance in practical application. The simulation results confirm the findings from the simulations in the hotspot scenarios and verify the applicability of the approaches in practice. For a more detailed analysis, the real-world scenario is investigated with respect to the areas in which the capacity hotspots appear. The performance of the proposed automatic capacity optimization approaches for SONs are investigated specifically for these hotspot areas and it is shown that the proposed approaches are able to achieve significant capacity gains locally in areas of inhomogeneous capacity demand.

Contents

| | | |
|----------|--|-----------|
| 1 | Introduction | 1 |
| 1.1 | Self-organizing Cellular Mobile Radio Networks | 1 |
| 1.2 | Automatic Capacity Optimization of Cellular Radio Networks | 4 |
| 1.3 | State of the Art | 7 |
| 1.4 | Problem Statement | 9 |
| 1.5 | Contributions and Overview | 11 |
| 2 | The Cell-centric Network Model | 13 |
| 2.1 | Motivation | 13 |
| 2.2 | Coordination of Automatic Capacity Optimization and Scheduling | 14 |
| 2.3 | System and Environment | 15 |
| 2.4 | Theoretic Derivation | 19 |
| 2.4.1 | Power Ratio and Average ICI Power | 19 |
| 2.4.2 | Achieved Cell Throughput and Required Cell Bandwidth | 21 |
| 2.4.3 | PBR-Characteristic | 28 |
| 2.4.4 | PBN-Characteristic | 30 |
| 2.4.5 | Adaptive Fair Resource Scheduling | 32 |
| 2.4.6 | Fair Throughput Scheduling | 35 |
| 2.4.7 | Fractional Frequency Reuse | 38 |
| 2.4.8 | Sources of Inaccuracies | 40 |
| 2.5 | Implementation Aspects | 43 |
| 2.5.1 | Measurement Based Determination of Achieved Cell Throughput and Required Cell Bandwidth | 43 |
| 2.5.2 | Measurement Based Determination of the Average ICI Power | 45 |
| 2.6 | Areas of Application | 46 |
| 3 | Automatic Capacity Optimization | 49 |
| 3.1 | Introduction and Self-organizing Approach | 49 |
| 3.2 | Coordination of Bandwidth Allocations | 50 |
| 3.3 | Optimization Goals | 52 |
| 3.3.1 | Network Throughput | 52 |
| 3.3.2 | Total Number of Users | 53 |
| 3.4 | Resource Allocation Techniques | 53 |
| 3.4.1 | Cell Bandwidth Allocation | 54 |
| 3.4.2 | Transmit Power Allocation | 55 |
| 3.4.3 | Joint Power and Bandwidth Allocation | 57 |
| 3.5 | Principles of Operation of Capacity Optimization | 59 |

| | | |
|----------|--|------------|
| 3.6 | Optimization Problems | 61 |
| 4 | Algorithms for Automatic Capacity Optimization | 65 |
| 4.1 | Introduction | 65 |
| 4.2 | Central Algorithms | 65 |
| 4.2.1 | Introduction | 65 |
| 4.2.2 | Convex Optimization | 66 |
| 4.2.3 | Cell Bandwidth Allocation | 68 |
| 4.2.4 | Transmit Power Allocation | 69 |
| 4.2.5 | Joint Power and Bandwidth Allocation | 72 |
| 4.3 | Distributed Algorithms | 74 |
| 4.3.1 | Introduction and General Approach | 74 |
| 4.3.2 | General Linear Network Throughput Optimization | 75 |
| 4.3.3 | Distributed Simplex Algorithm | 77 |
| 4.3.4 | Sequential Linear Programming | 79 |
| 4.3.5 | Distributed Power Allocation | 80 |
| 4.4 | Local Approach | 82 |
| 5 | Performance Analysis | 85 |
| 5.1 | Introduction | 85 |
| 5.2 | Functional Analysis | 85 |
| 5.2.1 | Simulation Approach and Scenarios | 86 |
| 5.2.2 | Comparison of Capacity Optimization Approaches | 91 |
| 5.2.3 | The Effect of Scheduling | 96 |
| 5.2.4 | Influence of the HS Distribution | 97 |
| 5.2.5 | QoS Performance Evaluation | 101 |
| 5.3 | Real-world Analysis | 104 |
| 5.3.1 | Simulation Approach and Modeling Data | 104 |
| 5.3.2 | Performance Results | 107 |
| 6 | Summary and Outlook | 115 |
| | Appendix | 119 |
| A.1 | Analytical Derivation of Achievable User Bit Rate and Required User Bandwidth | 119 |
| A.2 | Further Simulation Results | 122 |
| A.2.1 | Influence of the HS Distribution | 122 |
| A.2.2 | QoS Performance Evaluation for PF scheduling | 123 |
| A.2.3 | QoS Performance Evaluation for FT scheduling | 125 |
| | List of Acronyms | 129 |

| | |
|------------------------|------------|
| List of Symbols | 131 |
| Bibliography | 135 |
| Lebenslauf | 143 |

Chapter 1

Introduction

1.1 Self-organizing Cellular Mobile Radio Networks

In recent years, mobile communication has become truly ubiquitous. Significant technological development has led to advanced devices, such as smartphones, PC data cards and USB modems, for example, that provide easy access to the internet and to other data services. New operational concepts and software development platforms for smartphones enable a large crowd of developers to mobile application development and boost the invention of new services and new applications. All of these developments together have caused mobile communication to fully merge into private as well as business life, such that mobile communication now belongs to everyday life.

Modern communication systems provide great flexibility with respect to the bit rate requirements of data services. As a consequence, data services are manifold and while some require the transmission of only few bytes, several others require high transmission volumes and high transmission speeds. Popularity and availability of data services on modern user equipment and the great variety of data services cause a strong increase of the throughput demanded by the users from the network, such that network operators are forced to invest in their infrastructure in order to extend the capacity of their networks, which causes increasing capital expenditures (CAPEX) [vLE⁺08].

At the same time, infrastructure complexity of mobile radio networks increases due to the use of advanced transmission technologies with a multitude of tunable parameters with complex dependencies, and due to the simultaneous operation of several networks based on different technologies, such as 2nd generation (2G), 3rd generation (3G) and Long Term Evolution (LTE) [3GP11b], for example. As a consequence, complexity of maintenance, operation and optimization increases, such that more and more manpower is required for the in general manually carried out operation and management tasks and in order to assure efficient and reliable operation of the network, which leads to increasing operational expenditures (OPEX) [Leh07a, vLE⁺08].

While expenditures of the network operators rise due to increasing CAPEX and increasing OPEX, revenues stagnate under the influence of competition and new billing

models, such as flat-rates, for example. Operators, thus, feel the pressure to reduce costs and look for new ways to cut CAPEX as well as OPEX without reducing the reliability of their networks and the quality of the services [vLE⁺08].

A major role, in this context, plays the surrounding in which mobile radio networks operate. It is characterized by inhomogeneous capacity demand distributions and strong dynamics of the capacity demand resulting from, for example, rush hour traffic or events such as concerts or sports tournaments. The capacity demand dynamics in connection with the inhomogeneous capacity demand distribution offer much room for optimization, which is, however, very complex and tedious due to the large number of users and base stations (BSs) of cellular radio networks. As a consequence, it has been found in recent years that dynamic, autonomously operating processes are required in order to adapt cellular mobile radio networks to the large capacity demand variations they experience. Since such processes run autonomously and are carried out automatically in a self-organizing manner, a network containing functionality of the described nature is called a self-organizing network (SON) [Moi06, vLE⁺08].

Due to their self-organizing capabilities, SONs are considered a key technology to enable further development of mobile communication technology while assuring economic success. They are expected to be able to reduce the need for costly human interaction in many areas of operation and management of the network and, thus, to lead to a strong reduction of the operator's OPEX. Furthermore, the optimization gains achieved by the introduction of self-organizing functionality are expected to exceed the gains obtainable with the current, mostly manual, optimization methods. Spectral efficiency and capacity of the network are, consequently, expected to increase and will reduce the number of sites required to provide coverage and capacity, which decreases the CAPEX of the network operator. The introduction of SONs is, therefore, considered a key factor in achieving significant cost reductions while increasing network performance [Moi06, vLE⁺08].

Self-organizing functionality is relevant for different fields in the area of operation and management of cellular radio networks. Depending on the respective operation and management task, the following fields of self-organizing functionality are identified [Moi06, vLE⁺08]:

- self-configuration, which is the process of automatically determining parameters for the initial configuration or a reconfiguration of a BS,
- self-optimization, which is the process of automatically adjusting parameters in order to adapt the network to changing operating conditions and environments,

- self-healing, which is the process of automatically resolving coverage and capacity problems resulting from failures.

Hence, self-organizing functionality is envisioned for application in a wide range of tasks of operation and management of cellular radio networks. Great care and thorough investigation is required in the development of self-organizing functionality since major network parameters are affected to an extent that may be critical for reliable and stable operation of the network.

Apart from reliability and stability, which are required for all self-organizing approaches equally, there exist different requirements concerning spatial and temporal aspects depending on the field of self-organizing functionality. Figure 1.1 classifies the different fields of self-organizing functionality with respect to execution speed. The figure shows that especially for self-healing, tight temporal constraints apply since coverage or capacity holes arising due to failures have to be resolved as soon as possible in order to assure high service quality. The temporal constraints on self-optimizing functionality are more relaxed, they depend on the speed at which capacity demand dynamics, such as rush-hour traffic, for example, evolve. For self-optimizing functionality, the temporal requirements, thus, range between several minutes and few hours. Self-configuration functionality has the most relaxed temporal requirements. Here, the desired time until self-configuring infrastructure can be fully included in normal operation is the deciding factor, it can be up to several hours, depending on the requirements of the network operator.

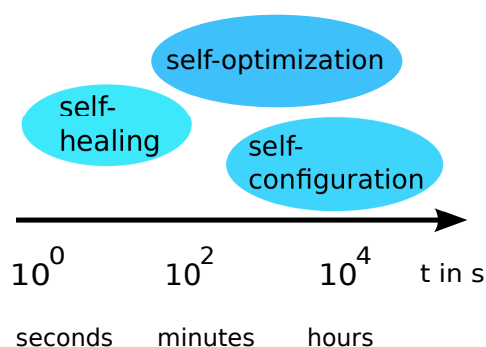


Figure 1.1. Temporal aspects of self-organizing functionality.

The spatial classification of the different fields of self-organizing functionality is shown in Figure 1.2. The figure illustrates to which spatial extent the self-organizing functionality influences the network. For self-configuring functionality, influence may be local since it may affect only a single BS. On the other hand, the configuration of a new BS

or the reconfiguration of an existing BS may force further BSs to adjust their configurations, such that self-configuring functionality may also have influence on a cluster of BSs. Self-healing, on the other hand, cannot be carried out by a single BS. Instead, a cluster of several BSs is required in general in order to resolve capacity and coverage holes caused by failure of a single BS. Thus, self-healing affects a cluster of cells. Also for self-optimizing functionality, several BSs will be adjusted in order to optimize a small area of a cellular network. Furthermore, also the optimization of large parts of a network may be required since certain phenomena that trigger the optimization of a network, such as rush-hour traffic, for example, take place at the same time in different places of the network. Thus, self-optimizing approaches will have influence on a cluster of cells or on even larger areas.

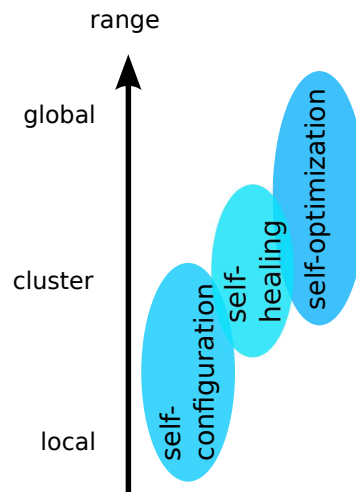


Figure 1.2. Spatial aspects of self-organizing functionality.

Note that above spatial and temporal classifications are of great relevance for self-organizing functionality. Any approach that does not comply with both, temporal and spatial requirements of the respective field of self-organizing functionality, is likely to fail when applied in SONS since it will not be able to successfully complete the assigned operation and management task in a self-organizing way.

1.2 Automatic Capacity Optimization of Cellular Radio Networks

Several goals exist in the field of self-optimization, such as optimizing service quality, handover (HO) performance, call admission performance or network capacity, for

example [JBT⁺10,LSJB10]. The optimization of the network capacity is of great relevance since the network capacity correlates with the income of the network operator, such that network operators seek to maximize the capacity of their networks.

This thesis investigates the automatic optimization of the network capacity of the downlink for SONs. The capacity optimization is achieved by adapting the capacity that is delivered by the network to the inhomogeneously distributed capacity demand such that at all times and all places, only as much capacity as required is delivered. The resource allocation of the cells in terms of cell bandwidth and transmit power are well suited to adapt the capacity that is delivered by the network, such that in this thesis, cell bandwidth and transmit power are the parameters that are adapted in order to optimize the network. In this section, an introduction to capacity optimization in cellular mobile radio networks is given. The focus of the introduction is put on the aspects that are critical for automatic capacity optimization for SONs.

The capacity that is delivered by a cellular radio network depends on the capacity of the individual radio links and is influenced by multiple factors. These factors can be divided into the group of propagation conditions related factors and the group of service related factors, as illustrated by Figure 1.3. The propagation conditions related factors have great impact on the network capacity since they determine the signal quality at the receiver, which is the deciding factor for the capacity of a radio link. Among the propagation conditions related factors is the mobile radio channel, which determines the attenuation of the radio signal and which is composed of a path loss component and fading components. While fading is usually considered to be random, the path loss is determined by the distance between transmitter and receiver [Rap02]. As a consequence, the layout of the network with the number of BSs and the locations of the BSs as well as the distribution of the users have influence on the propagation conditions, since they together determine the distances between transmitters and receivers.

The service related factors influence the capacity of a cellular radio network since they decide how the radio resources are used. Most important in this context is the scheduling, which carries out the allocation of the resources to the individual users. Scheduling can be channel adaptive, such that the channel fluctuations caused by fading can be exploited to maximize the network capacity. At the same time, however, Quality Of Service (QoS) requirements, which depend on the service type, have to be considered and may require actions that counteract capacity maximization [CL01]. As a consequence, also the service type has influence on the network capacity of cellular radio networks.

In addition, inter-cell interference (ICI) exists in cellular radio networks. It arises due to the reuse of resources and is an inherent effect in cellular radio networks. ICI is of great

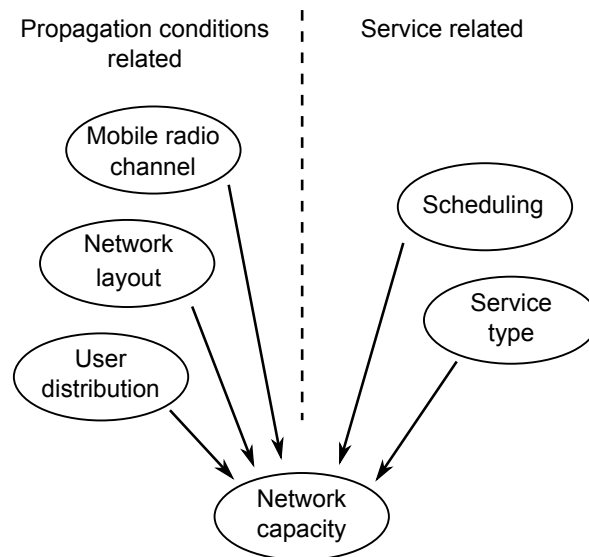


Figure 1.3. Influencing factors of the network capacity in cellular radio networks.

relevance in the context of network capacity optimization since it causes interrelations between the cells and between the influencing factors of the network capacity. These interrelations are very complex and make cellular radio networks very complex systems and the optimization of the capacity of cellular radio networks a very challenging task. Furthermore, ICI has influence on the signal quality and, thus, on the network capacity. The influencing factors of ICI are the same as for the network capacity [Rap02].

As a consequence, the challenge in capacity optimization is the large complexity arising from the existence of ICI. Mathematical optimization is usually applied for capacity optimization of cellular radio networks since, given an adequate model of the network, mathematical optimization problems are capable of dealing with the great complexity arising in capacity optimization of cellular radio networks. Thus, the development of adequate models of the network is a key aspect in the context of capacity optimization of cellular radio networks. This is especially true in connection with automatic capacity optimization for SONs since certain requirements concerning execution speed of automatic capacity optimization algorithms for SONs have to be fulfilled, according to Section 1.1 and Figures 1.1 and 1.2. Furthermore, the network model largely determines the complexity of an optimization problem and the methods that are suited to solve the optimization problem and, thus, affects efficiency and speed of an automatic capacity optimization algorithm.

Another important aspect in the context of automatic capacity optimization for SONs is the practical implementation of the automatic capacity optimization algorithms. Distributed implementation approaches are in this context of special relevance due to

the distributed nature of a cellular radio network and since they provide advantages in terms of robustness and reliability compared to central implementations. Note that the network model used in the capacity optimization of cellular radio networks also has great influence on implementation related issues of automatic capacity optimization for SONs since it may facilitate or complicate or even inhibit a distributed implementation.

1.3 State of the Art

This section introduces previous works that constitute the technical background of this thesis. The section discusses the development of cellular radio network optimization and the step to the change of paradigm in operation and management of cellular radio networks that lead to SONs and it reviews the literature relevant for this thesis.

Early mobile radio networks were circuit switched networks based on frequency division multiple access (FDMA) and time division multiple access (TDMA). First works for the capacity optimization of such networks investigate the allocation of frequencies to the cells in order to achieve optimum static network configuration [Hal80, Gam86]. The adaptation of circuit switched networks to changing capacity demands is done using dynamic channel allocation techniques and channel borrowing techniques that intend to shift frequencies from cells with low traffic load to cells with high traffic load. A wide overview of dynamic channel allocation schemes and channel borrowing schemes for circuit switched cellular mobile radio networks is given in [KN96].

With the emergence of code division multiple access (CDMA) based 3G cellular mobile radio networks, and with the migration to multiple services with different data rates and different QoS requirements, the number of parameters that had to be controlled increased. Optimization complexity increased accordingly, requiring new approaches and tools to enable and support manual interaction [EGJ⁺03, NDA06, Gee08]. Furthermore, CDMA based networks have to be actively managed due to the short term variations of the operating conditions. For this, parameters from the areas of admission control, power control, load control, neighbor cell list and packet scheduling have to be adapted such that key performance indicators (KPIs) [LWN02] are held at certain levels. This adaptation was initially carried out manually. In the course of competition among network operators, however, process automation became a key element and the manually carried out optimization using KPIs was automated, called auto-tuning [LWN02]. In the context of this process, automatic tuning of radio resource management (RRM) [LWN02] parameters using fuzzy logic and reinforcement learning, for example, was introduced, implementing the automation of a part of the traditional

tool-based planning and optimization process [LWN02, DAD⁺05, NAD06, NADN06]. Further approaches for automated optimization were investigated in the MONOTAS project, where simulation based optimization for 3G and 4th generation (4G) networks was considered. The project aimed at dramatically decreasing the optimization cycle time of typically several months by using simulations in the optimization loop [ABB⁺08]. In the Celtic Gandalf project, techniques for the automation of management tasks in systems applying several different mobile radio technologies were investigated [SAD⁺05].

With the convergence of mobile systems and internet protocol (IP) networks and the resulting evolution of fully packet-switched 4G systems, first and foremost LTE, and based on the promising results obtained in previous research on auto-tuning, a shift of paradigm in operation and management of cellular radio networks took place. The new paradigm of optimization and management of cellular mobile radio networks envisions SONs, which are networks that widely automate configuration and optimization of their infrastructure in a self-organizing way, circumventing classical planning and optimization [PB05, SPI05, BBD⁺05]. This vision was adopted by industry organizations, such as the next generation mobile networks (NGMN) Alliance, by research groups, such as FP7 SOCRATES, and by standardization groups, such as the 3rd Generation Partnership Project (3GPP), for example. Each of them developed their own concept and vision of SONs, but due to the mutual dependence and cooperation between industry, research and standardization, the individual concepts and visions show only minor deviations [Leh07b, vLE⁺08, 3GP11b]. Much effort has been spent to establish frameworks containing requirements, assessment criteria and use cases that are indispensable for definition, development and evaluation of SON functionality [3GP11a, Leh08, ALS⁺08, S⁺08a, S⁺08b, S⁺08c].

Among the use cases specified by [3GP11a, Leh08, S⁺08b], the one treating inter-cell interference coordination (ICIC) is the relevant one for this thesis. ICIC refers to the coordination of the radio resource allocations of different cells such that ICI can be controlled and that the network can offer good QoS while providing high network capacity. Thus, ICIC is inherently a problem of radio resource allocation and good ICIC increases the network capacity. Currently, scheduling based approaches are usually applied in order to achieve ICIC. Channel aware scheduling [LZ06] usually schedules resource blocks with low attenuation and low interference and, thus, achieves ICIC to a certain extent [SCR05, SV08, FCS07]. More sophisticated methods reduce interference by applying beamforming or using several BSs to support a single user, thus implementing virtual multiple input multiple output (MIMO) [Nec08, PB09]. All of these approaches, however, rely on measurements of the instantaneous interference and on estimates of the transmission channel. Due to short scheduling intervals and fast channel

variations, which are in the order of milliseconds, the effort required to distribute information on interference and channel conditions is significant and causes much signaling traffic. Furthermore, obtaining up-to-date and accurate information about interference and channel conditions is a big challenge, due to the fast changes [Nec08, GKGO07].

Much research has been carried out to overcome the challenge of large signaling traffic and to reduce the effect of inaccurate and outdated knowledge on channel and interference conditions. In [BBP05, AYM06], the signaling effort is reduced by considering the spatial positions of the users and identifying the interferers with the most significant impact. Only the resource allocations of these so-called dominant interferers are coordinated, leading to good results and greatly reduced signaling traffic. Also the resource allocation itself can be structured in order to achieve ICIC as in [FHL⁺98, LS99], for example, where resources are allocated in a certain order which is chosen such that the probability that neighbored cells use the same resources is low if the cells are not fully loaded and use the available spectrum only partially. Another approach is the shaping of the transmit power profile either over time or over space such that different slots or beams, respectively, are affected differently by interference. This way, slots or beams, respectively, can be assigned according to the amount of interference each user can tolerate [TVZ04, VTZZ06, CQ99]. A comparable approach is pursued in [LL06, ZTH⁺10], which introduce a super frame that extends over several scheduling periods. For each super frame, transmit power limits are set which have to be observed by the scheduling process, such that ICI can be controlled.

1.4 Problem Statement

Despite the existing approaches for ICIC summarized in Section 1.3, it is believed that further capacity gains can be achieved by self-organizing functionality [3GP11a, Leh08, S⁺08b]. Thus, automatic capacity optimization for SONS is a current research topic of high interest. This section summarizes the research that is required for automatic capacity optimization for SONS. The specific aspects of the research are as follows:

- Automatic capacity optimization for SONS adapts the network to inhomogeneous capacity demand distributions, as introduced in Section 1.2. The corresponding effects develop over timescales of minutes and occur in large areas that may contain many cells, according to Section 1.1. As a consequence, new modeling approaches of cellular radio networks are required in order to be able to model large parts of a network and in order to consider time intervals of several minutes

or even hours while keeping complexity low. At the same time, these new modeling approaches should consider the QoS requirements of the individual users in order to be able to provide good QoS to the users.

- The automatic capacity optimization for SONs has to coexist with current state of the art scheduling, which assigns the resources allocated to a cell to the users of the cell. Ideally, not only coexistence is desired, but a contribution of the automatic capacity optimization to achieve improved ICIC. For this purpose, a new concept that coordinates the new automatic capacity optimization approaches for SONs and the scheduling of resources to the users is required.
- Specific approaches for automatic capacity optimization for SONs are required. Depending on the capacity optimization goal and on the parameters that are manipulated to achieve the capacity optimization, several different approaches are required. It is favorable to consider implementational aspects in the development of approaches for automatic capacity optimization for SONs such that efficient algorithms for the implementation of the approaches can be established.
- Implementations of the approaches for automatic capacity optimization for SONs resulting in optimization algorithms have to be established. In this context, two different fields can be distinguished. One field concerns algorithms that are suited for simulation and analysis purposes. These algorithms should allow the simulation and analysis of the automatic capacity optimization approaches for SONs as well as the state of the art scheduling based approaches in order to be able to make comparisons. The second field concerns the practical implementation in real systems. Suited algorithms are preferably of distributed nature. Note that in order to obtain analysis results that are valid for practical implementation, the distributed algorithms should obtain solution that are the same or at least very close to the solutions obtained with the central algorithms.
- Finally, analysis of the different approaches for automatic capacity optimization for SONs have to be carried out and the new automatic capacity optimization approaches for SONs have to be compared to the state of the art scheduling based approaches. A fundamental analysis that generally assesses behavior, performance and stability of the different capacity optimization approaches has to be carried out using realistic scenarios. Additionally, the investigation of the capacity optimization approaches in real-world scenarios is required in order to be able to assess the performance that can be expected in practice. For this purpose, an approach for obtaining real-world scenarios based on measurement data has to be established and the capacity optimization approaches have to be evaluated in the real-world scenario.

1.5 Contributions and Overview

This section introduces the solutions developed in this thesis for the problems stated in Section 1.4. It summarizes the main contributions and gives an overview of the thesis. The contributions are addressed in the order of appearance in the thesis and according to the order of presentation of the aspects of Section 1.4. In particular, the main contributions are as follows:

- Chapter 2 presents a new model for the downlink of cellular radio networks which focuses on the cells rather than on individual users. It is, thus, called cell-centric network model and is capable of greatly reducing the modeling complexity, such that large numbers of cells and long time intervals can be considered efficiently. At the same time, the model is capable of considering the QoS requirements of the individual users, which is important to be able to assure good QoS of the users. The cell-centric network model considers ICI and the dependencies among the cells as well as the effect of the environment on the signal propagation, such that the model achieves high accuracy.
- Chapter 2 furthermore introduces a hierarchic concept for the coordination of capacity optimization approaches and scheduling. The concept enables both approaches to complement each other, such that ICIC is enhanced. Furthermore, it provides the possibility to consider state of the art scheduling based approaches as well as new approaches for automatic capacity optimization for SONs.
- Chapter 3 introduces several approaches for automatic capacity optimization for SONs by defining different optimization problems that are capable of maximizing the network capacity in terms of the number of users or the network throughput. According to Section 1.2, the optimization is achieved by allocating cell bandwidth or transmit power or cell bandwidth and transmit power jointly.
- Chapter 4 presents different algorithms that solve the optimization problems proposed for automatic capacity optimization for SONs. Central implementations suitable for analysis and simulation purposes are presented as well as distributed implementations that are intended for implementation in practice.
- Chapter 5 analyses and evaluates the approaches for automatic capacity optimization for SONs using simulations. It proposes a simulation approach for performance evaluation in scenarios with inhomogeneous capacity demand. The simulation approach is used to generally investigate the behavior and the performance of the approaches for automatic capacity optimization for SONs and

to compare the results with the state of the art scheduling based approaches. Furthermore, an approach for deriving measurement based real world scenarios is presented and applied for performance analysis of the proposed capacity optimization approaches in practical implementation.

Chapter 6 concludes the thesis. It summarizes the content and the achievements of the thesis and presents an outlook on related further research.

Chapter 2

The Cell-centric Network Model

2.1 Motivation

Automatic capacity optimization for SONs reacts to effects that occur in large areas containing many cells and that develop over long time intervals of minutes or even hours, as discussed in Section 1.1. According to Section 1.4, new low complexity modeling approaches of cellular radio networks are required in order to be able to efficiently optimize and simulate large parts of a network over long time intervals. At the same time, the accuracy of the modeling approach must be high, which means that influencing factors on the network performance, the dependencies between the cells of the network and the QoS requirements of the users have to be considered.

This chapter presents a new network model that fulfills above requirements. The focus of the model is on the cells, rather than on the individual users. As a consequence of this cell-centric view, a network can be modeled with very low complexity compared to the usual user-centric modeling. Thus, efficient approaches for automatic capacity optimization and the simulative verification of such approaches are enabled. The model describes the relation between the resources transmit power and cell bandwidth on one side and the performance metrics cell throughput and number of supported users on the other side. The respective modeling equations can be obtained by two different approaches, as shown by Figure 2.1. The theoretical approach is based on analytical derivations. It requires some simplifying assumption and is used in special scenarios and for the detailed description of the cell-centric network model. The practical approach uses measurements to obtain the modeling equations. It is generally applicable, such that it is preferably used for practical application.

In both cases, the model achieves high accuracy since ICI and the relations between the cells are regarded and since the effect of the environment on the radio propagation is considered, either by the environment model and the user distribution, as for the theoretic approach, or by the measurement data, as for the practical approach. Also, the distribution of the users and the individual QoS requirements of the users are regarded. The model is, therefore, suited for the application in automatic capacity optimization for SONs. Furthermore, it allows to develop approaches that can be efficiently combined with the scheduling of resources to the users in the cells.

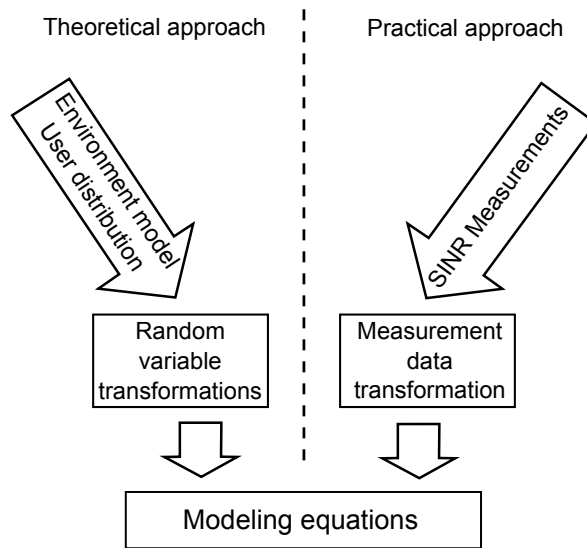


Figure 2.1. Theoretical and practical approach of the cell-centric network model for obtaining the modeling equations.

The chapter is structured as follows. Section 2.2 introduces a concept that allows the combination of automatic capacity optimization approaches with the scheduling of resources to the users in the cells. General considerations concerning the system and the environment and their modeling are presented in Section 2.3. Section 2.4 derives the cell-centric network model analytically using the theoretical approach. The practical approach of the model for implementation in practice is presented in Section 2.5 and the main areas of application of the cell-centric network model are introduced in Section 2.6. Several parts of this chapter have been originally published by the author in [HK08, HKS08, HKG09b].

2.2 Coordination of Automatic Capacity Optimization and Scheduling

Automatic capacity optimization is capable of making resource allocation decisions considering several cells and their interactions. This way, automatic capacity optimization has influence on ICIC, such that in order to assure the success of automatic capacity optimization, it has to be coordinated with the scheduling of resources to the users in the cells. This section presents a hierarchic concept that coordinates automatic capacity optimization approaches and scheduling.

The hierarchic concept for the coordination of automatic capacity optimization approaches and scheduling consists of two planes. The upper plane contains the auto-

matic capacity optimization approaches that consider the whole network and which react to changes in the environment that require the optimization of the network, such as rush-hour traffic, for example. The lower plane considers only single cells and contains the cell scheduling. The concept is hierarchic because the approaches of the upper plane establish limits and requirements concerning the allocation of resources that have to be observed by the scheduling of the lower plane.

Using this hierarchic concept, different effects with different temporal and spatial properties can be treated separately in the different planes and appropriate approaches can be developed. Clearly, the automatic capacity optimization approaches of the upper plane can react to effects such as rush-hour traffic, for example, that develop over time intervals of minutes or hours and that require a fundamental adjustment of the network. The high complexity arising from the need to consider large areas of a network, cf. Section 1.1, can be reduced using appropriate approaches and models since the treated effects develop slowly. In the lower plane, the network is adapted to effects such as fast fading, which require action in short time intervals in the order of milliseconds. Here, the quick variations of the channel are challenging, due to the hierarchic concept, however, the view of the approaches of the second layer can be limited to a single cell such that the complexity of the task is limited.

The hierarchic concept furthermore enables the consideration and comparison of state of the art scheduling based approaches for network capacity optimization and new automatic capacity optimization approaches for SONs in simulations. This is achieved by considering coordination of the bandwidth allocations of the cells. The bandwidth allocations of two cells are in this thesis referred to as being coordinated if the two cells do not use the same frequencies. ICI can, thus, be avoided between two cells that coordinate their bandwidth allocations. The coordination of bandwidth allocations, however, requires the consideration of several cells in the allocation of resources to the cells, which is only possible with new capacity optimization approaches for SONs. As a consequence, with the consideration of coordinated bandwidth allocations in connection with the hierarchic concept, the new capacity optimization approaches for SONs are considered. Assuming no coordinations in the bandwidth allocations, the network is adapted exclusively by the action of the schedulers of the cells, such that state of the art scheduling based approaches are modeled.

2.3 System and Environment

In Section 1.2, different aspects from the system and the environment in which the system is placed are introduced as the main influencing factors of the capacity of

cellular radio networks. These factors are also for the cell-centric network model of this chapter of primary importance. This section discusses the influencing factors of the capacity of cellular radio networks in more detail and introduces how they are considered in the cell-centric network model.

Network capacity can be measured in terms of the total network throughput, for example. With user index n , N_i the number of users in cell i and N_c the number of cells in the scenario, the total network throughput R_{nw} is given by the sum of the user throughputs $R_{u,n}^{(i)}$ of all users of the network according to

$$R_{\text{nw}} = \sum_{i=1}^{N_c} \sum_{n=1}^{N_i} R_{u,n}^{(i)}. \quad (2.1)$$

The user throughput depends on the signal quality at the receiver [Sha48]. The signal quality greatly depends on ICI, which occurs in cellular radio networks since the same frequencies are used by several cells in order to be able to provide high capacity. The reuse distance D expresses the degree of frequency reuse. It gives the distance between two cells that use the same frequencies and decreases if more cells use the same frequencies since then, cells that use the same resources are located closer. Thus, ICI increases with the decreasing reuse distance [Rap02]. With the assumption that ICI can be modeled by a Gaussian process, as it is valid in unsynchronized multi-carrier transmission, according to [ADSK03], the user bit rate $R_{u,n}^{(i)}$ of user n of cell i depends on the user bandwidth $B_{u,n}^{(i)}$ and on the Signal to Interference plus Noise Ratio (SINR) $\gamma_n^{(i)}$ at the receiver of user n of cell i and is given by [Sha48]

$$R_{u,n}^{(i)} = B_{u,n}^{(i)} \cdot \log_2 (1 + \gamma_n^{(i)}) . \quad (2.2)$$

In practice, adaptive modulation and coding (AMC) [GC97, GC98], which adapts the modulation scheme and the coding rate to the SINR at the receiver using a discrete number of different Modulation and Coding Schemes (MCSs), creates a stepwise continuous relation between SINR $\gamma_n^{(i)}$ and the user bit rate $R_{u,n}^{(i)}$. If the number of different MCSs is sufficiently large, (2.2) is approached [MNK⁺07].

The SINR $\gamma_n^{(i)}$ at the receiver depends on the transmit power $P_{\text{tx},i}$ of cell i , the noise power P_N at the receiver, the ICI power $P_{1,n}^{(i)}$ received by user n of cell i and the attenuation $a_n^{(ii)}$ of the mobile radio channel from the BS of cell i to user n of cell i according to

$$\gamma_n^{(i)} = \frac{P_{\text{tx},i}}{a_n^{(ii)}} \cdot \frac{1}{P_N + P_{1,n}^{(i)}}. \quad (2.3)$$

With the attenuation $a_n^{(ij)}$ from the BS of cell j to user n of cell i and factor $\beta_n^{(ij)} \in \{0, \dots, 1\}$, which specifies the overlap of the bandwidth of user n of cell i with the

bandwidth of cell j , the ICI power $P_{I,n}^{(i)}$ received by user n of cell i is defined by

$$P_{I,n}^{(i)} = \sum_{j \neq i} \frac{P_{\text{tx},i}}{a_n^{(ij)}} \cdot \beta_n^{(ij)}. \quad (2.4)$$

The attenuation $a_n^{(ij)}$ is composed of the path loss $a_{\text{pl}}(d_n^{(ij)})$, the shadow fading component a_{sf} and the fast fading component a_{ff} . In logarithmic scale, attenuation $a_n^{(ij)}$ is given by

$$a_n^{(ij)} = a_{\text{pl}}(d_n^{(ij)}) + a_{\text{sf}} + a_{\text{ff}}. \quad (2.5)$$

The pathloss $a_{\text{pl}}(d_n^{(ij)})$ depends on the distance $d_n^{(ij)}$ between the BS of cell j and the user n of cell i and is modeled by an exponential pathloss model with a propagation coefficient α larger than two, as it is implemented in the Hata pathloss model [Hat80, Rap02], for example. In this thesis, the Urban Macro Scenario model from the 3GPP Spatial Channel Model (SCM) is used to determine the pathloss $a_{\text{pl}}(d_n^{(ij)})$ in dB for a distance $d_n^{(ij)}$ in meters. With a_0 the attenuation in dB for a distance $d_n^{(ij)}$ of one meter, the pathloss model of the 3GPP Urban Macro Scenario is given by [3GPP09]

$$a_{\text{pl}}(d_n^{(ij)}) = a_0 + \alpha \cdot 10 \log_{10}(d_n^{(ij)}). \quad (2.6)$$

Shadow fading is a random process that results from environmental effects, such as shadowing through hills and buildings, for example. The shadow fading attenuation a_{sf} in dB is a realization of the random variable (RV) \mathbf{a}_{sf} . The probability density function (pdf) of \mathbf{a}_{sf} is assumed to be lognormal with zero mean and variance σ_{sf}^2 in dB and is given by [Rap02]

$$f_{\mathbf{a}_{\text{sf}}}(a_{\text{sf}}) = \frac{1}{\sigma_{\text{sf}} \sqrt{2\pi}} \cdot e^{-\frac{a_{\text{sf}}^2}{2\sigma_{\text{sf}}^2}}. \quad (2.7)$$

Fast fading accounts for strong amplitude fluctuations resulting from multi-path propagation. It is a random process, too. The fast fading attenuation a_{ff} is a realization of the Rayleigh distributed RV \mathbf{a}_{ff} with pdf [Mol03]

$$f_{\mathbf{a}_{\text{ff}}}(a_{\text{ff}}) = \frac{a_{\text{ff}}}{\sigma_{\text{ff}}^2} \cdot e^{-\frac{a_{\text{ff}}^2}{2\sigma_{\text{ff}}^2}}, \quad \sigma_{\text{ff}}^2 = \frac{1}{2}. \quad (2.8)$$

The network layout and the distribution of the users determine the distances $d_n^{(ij)}$ between transmitters and receivers and, thus, have significant effect on the path loss

$a_{\text{pl}}(d_n^{(ij)})$. The locations of the BSs and their sector configuration and antenna configuration is assumed to be given, as well as the distribution of the users over the complete considered area. Furthermore, the cell borders are assumed to be known and fixed. With these information, the position of the users over the cell area of a cell i is a RV. With r and φ radius and angle relative to a reference point, for example the position of BS i , the density $p_{\mathbf{r},\varphi}^{(i)}(r, \varphi)$ of the users over the cell area of cell i can be determined for each cell i . In this thesis, it is assumed that $p_{\mathbf{r},\varphi}^{(i)}(r, \varphi)$ is given.

In packet switched networks, the scheduler allocates radio resources to the users and has great effect on the capacity of the cell. Different scheduling strategies can be pursued, priority can be given to certain users or groups of users or fairness among the users can be aimed at, for example. Two basic scheduling strategies are Fair Resource (FR) scheduling and Fair Throughput (FT) scheduling [Fer10]. In FR scheduling, the scheduler allocates on average the same amount of resources in terms of bandwidth, for example, to each of the users. Depending on the signal quality at the receiver, the users achieve different user throughputs, according to (2.2). In FT scheduling, the scheduler assures that each user achieves in average the same user bit rate. According to (2.2), this requires that more resources are scheduled to users with low SINR at the receiver. In any case, the user bandwidth $B_{\text{u},n}^{(i)}$ of (2.2) is given by the average sum of the bandwidth that is allocated to user n of cell i per time unit.

Furthermore, advanced scheduling approaches are capable of exploiting the channel fluctuations caused by fast fading in order to maximize the cell throughput [CL01, VTL02, LCS03]. One popular approach is Proportional Fair (PF) scheduling [Kel97, LZ06], for example, which allocates resources to the user which has the highest ratio of instantaneous SINR to average SINR [LZ06]. Assuming the subcarriers to be independent, the analysis of PF scheduling can be simplified by considering a single subcarrier and extending the results to all other subcarriers. Further simplification of the analysis is possible if the shadow fading process is assumed to vary much slower than the fast fading process. Since with this assumption, the scheduling strategy can be treated as selecting for each subcarrier the user which has the highest fast fading channel power gain $g_{\text{ff}} = a_{\text{ff}}^2$. Using these assumptions, order statistics [Dav81] can be applied to derive the cumulative distribution function (cdf) of the fast fading channel power gain $\mathbf{g}_{\text{pf}}^{(i)}$ due to PF scheduling of cell i . Assuming fast fading to be Rayleigh distributed with pdf of (2.8), the fast fading channel power gain g_{ff} follows an exponential distribution [PP02] and the cdf of fast fading channel power gain due to PF scheduling yields [Dav81]

$$F_{\mathbf{g}_{\text{pf}}^{(i)}}(g_{\text{pf}}^{(i)}) = \left(1 - e^{-\frac{g_{\text{pf}}^{(i)}}{2\sigma_{\text{ff}}^2}}\right)^{N_i}. \quad (2.9)$$

With the assumption that the slow fading process varies much slower than the fast fading process, it can furthermore be concluded that PF scheduling is a FR approach, since it allocates the same amount of resources to all users because the same fast fading process is assumed for each of the users.

2.4 Theoretic Derivation

This section presents the theoretic derivation of the cell-centric network model. Section 2.4.1 defines the cell-centric equivalents to SINR $\gamma_n^{(i)}$ and interference $P_{I,n}^{(i)}$ at the receiver of a single user. A stochastic approach that allows to consider user-specific effects, such as the user positions, the propagation conditions to the user positions and the interference conditions at the user positions in a cell-centric model is presented in Section 2.4.2. Using this stochastic approach, the cell throughput a cell can achieve for a given cell bandwidth or, vice versa, the bandwidth a cell requires in order to support all its users with a certain QoS are derived. Sections 2.4.3 and 2.4.4 use these results to derive characteristic representations of the relation between the resource allocation of a cell and the cell performance for channel non-adaptive FR scheduling. Sections 2.4.5 and 2.4.6 show how to incorporate different scheduling strategies into the presented model and Section 2.4.7 extends the cell-centric network model to fractional reuse system designs. Section 2.4.8 finally discusses inherent inaccuracies that may arise in the model.

2.4.1 Power Ratio and Average ICI Power

Establishing a model with focus on the cells of a network, rather than on the users, requires the definition of some basic parameters, which are conventionally linked with individual users, for whole cells. Furthermore, certain assumptions have to be established in order to assure that the minimum QoS requirements of the individual users are observed in a cell-centric network model. This section provides all necessary definitions and introduces the required assumptions.

In the cell-centric network model, an equivalent to the SINR $\gamma_n^{(i)}$ at the receiver of the user is required in order to be able to assess the transmit power allocation of the cell with respect to noise and ICI. For this purpose, the power ratio Γ_i of cell i is introduced. The Power ratio Γ_i expresses the situation of a cell concerning transmit power, ICI power and noise power and has to be representative for the whole cell considering all

its users. It is, therefore, defined using the average ICI power $\bar{P}_{1,i}$ of all users of cell i and is given by

$$\Gamma_i = \frac{P_{\text{tx},i}}{\bar{P}_{1,i} + P_N}. \quad (2.10)$$

The SINR $\gamma_n^{(i)}$ at the receiver of a user of (2.3) and the power ratio Γ_i from (2.10) are related by a user specific factor $\psi_n^{(i)}$, that accounts for the attenuation $a_n^{(ii)}$ and the difference between the ICI power $P_{1,n}^{(i)}$ at the receiver of the user of (2.4) and the average ICI power $\bar{P}_{1,i}$, according to

$$\gamma_n^{(i)} = \psi_n^{(i)} \cdot \Gamma_i. \quad (2.11)$$

In order to model ICI without knowing the exact allocation of frequencies to the cells, the average transmit power $P_{\text{tx},j}$ of a cell j over the system bandwidth B_{sys} is considered in the determination of ICI power. The ICI power a cell i receives then depends on its cell bandwidth B_i . With this in mind, the relative cell bandwidth β_i is defined by

$$\beta_i = \frac{B_i}{B_{\text{sys}}}. \quad (2.12)$$

According to above considerations, (2.12) specifies the ratio of the transmit power $P_{\text{tx},j}$ of an interfering cell j that is received by cell i as ICI over the frequencies cell i uses. Furthermore, the average channel gain g_{ij} is introduced, it is defined as the expected value of the channel gain from BS j over the cell area of cell i according to

$$g_{ij} = \int_0^{S_i} \int_0^{2\pi} \frac{p_{\mathbf{r},\varphi}^{(i)}(r, \varphi)}{a_{ij}(r, \varphi)} d\varphi dr. \quad (2.13)$$

With β_i and g_{ij} from (2.12) and (2.13), respectively, and S_i the radius of cell i in terms of the distance from the BS to the most remote point within the cell area, the average ICI $\bar{P}_{1,i}$ of all users of cell i is determined by calculating the expected value of the ICI over the cell area of cell i according to

$$\begin{aligned} \bar{P}_{1,i} &= \int_0^{S_i} \int_0^{2\pi} \sum_{i \neq j} \frac{P_{\text{tx},j}}{a_{ij}(r, \varphi)} \cdot \beta_i \cdot p_{\mathbf{r},\varphi}^{(i)}(r, \varphi) d\varphi dr \\ &= \sum_{i \neq j} P_{\text{tx},j} \cdot \beta_i \cdot \int_0^{S_i} \int_0^{2\pi} \frac{p_{\mathbf{r},\varphi}^{(i)}(r, \varphi)}{a_{ij}(r, \varphi)} d\varphi dr \\ &= \sum_{i \neq j} P_{\text{tx},j} \cdot \beta_i \cdot g_{ij}. \end{aligned} \quad (2.14)$$

Variable $\bar{P}_{1,i}$ of (2.14) is a measure for the strength of ICI considering the whole cell and, thus, expresses the interference situation of the cell.

In a cell-centric network model, user-specific parameters cannot be directly obtained or optimized for. As a consequence, an approach for dealing with user-specific parameters

has to be established. This concerns in particular the treatment of QoS requirements, which are commonly expressed as user specific parameters. In order to be able to consider user-specific QoS requirements, the so called Scheduler Assumption is made. It states that with sufficient resources allocated to a cell, all QoS requirements of all users can be met by the cell. Thus, the determination of the amount of resources that are sufficient to fulfill the QoS requirements of the users is an important aspect of the cell-centric network model. It depends on the QoS requirements of the users, such that in the cell-centric network model, the number of required resources is determined depending on the minimum required user bit rate. All QoS definitions in the cell-centric network model are, therefore, always expressed in terms of minimum user bit rate.

Note that the downlink of a cellular radio system is considered throughout this thesis. In the uplink, however, the fundamental relations that are represented by the model do not change since the same users share resources as in the downlink. The difference between up- and downlink is in the determination of ICI, which comes in the uplink from the users, rather than from the BSs. Considering this difference together with the fact that in the uplink, the interferers are moving and adapting (2.4) and (2.14) accordingly, the cell-centric network model can also be applied to the uplink of cellular radio networks.

Concerning the denomination of variables throughout this chapter, the cell indices are used as sub index with any variable that relates to a cell. In variables that relate to individual users, cell indices will be carried as super index in parentheses. Variables with tildes denote given targets and variable with primes denote measurements or values obtained from measurements.

2.4.2 Achieved Cell Throughput and Required Cell Bandwidth

In the scope of the cell-centric network model, a cell-centric equivalent of the relation between link capacity and user bandwidth, as it is used in user-centric approaches and given by (2.2) is required. This cell-centric equivalent of (2.2), consequently, relates cell bandwidth and cell throughput. This section presents a stochastic approach to obtain this relation.

Since the position of the users within the cell area is a RV, according to Section 2.3, the cell throughput \mathbf{R}_i that is achieved by cell i is a RV, too. It depends on the sum

of the bit rates $\mathbf{R}_{u,n}^{(i)}$ achieved by the users of cell i and is given by

$$\mathbf{R}_i = \sum_{n=1}^{N_i} \mathbf{R}_{u,n}^{(i)}. \quad (2.15)$$

The same way, the cell bandwidth \mathbf{B}_i that is required by a cell i to support its users with a certain QoS is a RV. It depends on the sum of the bandwidths $\mathbf{B}_{u,n}^{(i)}$ required by the users and yields

$$\mathbf{B}_i = \sum_{n=1}^{N_i} \mathbf{B}_{u,n}^{(i)}. \quad (2.16)$$

In order to find a relation between cell bandwidth \mathbf{B}_i and cell throughput \mathbf{R}_i , the stochastic properties of the RVs are required.

The first step in obtaining the stochastic properties of cell bandwidth \mathbf{B}_i and cell throughput \mathbf{R}_i is the derivation of the pdfs $f_{\mathbf{R}_{u,n}^{(i)}}(R_{u,n}^{(i)})$ and $f_{\mathbf{B}_{u,n}^{(i)}}(B_{u,n}^{(i)})$ of achieved user bit rate $\mathbf{R}_{u,n}^{(i)}$ and required user bandwidth $\mathbf{B}_{u,n}^{(i)}$, respectively. For this purpose, the relation between user bit rate $R_{u,n}^{(i)}$, receiver SINR $\gamma_n^{(i)}$ and user bandwidth $B_{u,n}^{(i)}$, as introduced in Section 2.3, has to be considered. Let $R_{u,n}^{(i)} = g(B_{u,n}^{(i)}, \gamma_n^{(i)})$ denote this relation and assume that its inverse $\gamma_n^{(i)} = g^{-1}(B_{u,n}^{(i)}, R_{u,n}^{(i)})$ exists, which is true if the relation is monotonic and which can be assumed to hold for such a relation. Furthermore, it is assumed that the pdf $f_{\gamma_n^{(i)}}(\gamma_n^{(i)})$ of the SINR $\gamma_n^{(i)}$ is known. The pdf $f_{\mathbf{R}_{u,n}^{(i)}}(R_{u,n}^{(i)})$ of the user bit rate $R_{u,n}^{(i)}$ achievable by user n of cell i with bandwidth $B_{u,n}^{(i)}$ and the pdf $f_{\mathbf{B}_{u,n}^{(i)}}(B_{u,n}^{(i)})$ of the bandwidth required by user n of cell i to achieve a bit rate of $R_{u,n}^{(i)}$, respectively, can then be obtained using RV transformation [Hän01,PP02] and yield

$$f_{\mathbf{R}_{u,n}^{(i)}}(R_{u,n}^{(i)}) = f_{\gamma_n^{(i)}}(g^{-1}(B_{u,n}^{(i)}, R_{u,n}^{(i)})) \cdot \left| \frac{\partial g^{-1}(B_{u,n}^{(i)}, R_{u,n}^{(i)})}{\partial R_{u,n}^{(i)}} \right| \quad (2.17)$$

$$f_{\mathbf{B}_{u,n}^{(i)}}(B_{u,n}^{(i)}) = f_{\gamma_n^{(i)}}(g^{-1}(B_{u,n}^{(i)}, R_{u,n}^{(i)})) \cdot \left| \frac{\partial g^{-1}(B_{u,n}^{(i)}, R_{u,n}^{(i)})}{\partial B_{u,n}^{(i)}} \right|. \quad (2.18)$$

Setting $g(B_{u,n}^{(i)}, \gamma_n^{(i)})$ equal to the Shannon bound of (2.2), (2.17) and (2.18) results in

$$f_{\mathbf{R}_{u,n}^{(i)}}(R_{u,n}^{(i)}) = f_{\gamma_n^{(i)}} \left(2^{\frac{R_{u,n}^{(i)}}{B_{u,n}^{(i)}}} - 1 \right) \cdot 2^{\frac{R_{u,n}^{(i)}}{B_{u,n}^{(i)}}} \ln(2) \frac{1}{B_{u,n}^{(i)}} \quad (2.19)$$

$$f_{\mathbf{B}_{u,n}^{(i)}}(B_{u,n}^{(i)}) = f_{\gamma_n^{(i)}} \left(2^{\frac{R_{u,n}^{(i)}}{B_{u,n}^{(i)}}} - 1 \right) \cdot 2^{\frac{R_{u,n}^{(i)}}{B_{u,n}^{(i)}}} \ln(2) \frac{R_{u,n}^{(i)}}{B_{u,n}^{(i)2}}. \quad (2.20)$$

Note that (2.19) and (2.20) are applicable for systems that dispose of a large number of MCSs, such as LTE, for example [3GP11b,MNK⁺07]. In other systems, the relation of (2.2) might not be approached, depending on the applied MCSs, such that other relations than (2.2) may have to be applied to (2.17) and (2.18), cf. Section 2.3.

Now, the pdfs of cell throughput \mathbf{R}_i and cell bandwidth \mathbf{B}_i are derived. According to (2.15) and (2.16), both are sums of other RVs. Assuming all RVs $\mathbf{R}_{u,n}^{(i)}$ and $\mathbf{B}_{u,n}^{(i)}$ to be independent and identical distributed [PP02], which can be assumed for channel non-adaptive FR and FT scheduling, the Central Limit Theorem (CLT) [PP02] can be applied. As a consequence, both, achieved cell throughput \mathbf{R}_i and required cell bandwidth \mathbf{B}_i , are Normal distributed with pdfs

$$f_{\mathbf{R}_i}(R_i) \sim \mathcal{N}(\mu_{\mathbf{R}_i}, \sigma_{\mathbf{R}_i}^2), \quad (2.21)$$

$$f_{\mathbf{B}_i}(B_i) \sim \mathcal{N}(\mu_{\mathbf{B}_i}, \sigma_{\mathbf{B}_i}^2). \quad (2.22)$$

Mean and variance of (2.21) and (2.22) depend on mean and variance of (2.17) and (2.18), respectively, and are given by

$$\mu_{\{\mathbf{R},\mathbf{B}\}_i} = \sum_{n=1}^{N_i} \mu_{\{R_{u,n}^{(i)}, B_{u,n}^{(i)}\}}, \quad \sigma_{\{\mathbf{R},\mathbf{B}\}_i}^2 = \sum_{n=1}^{N_i} \sigma_{\{R_{u,n}^{(i)}, B_{u,n}^{(i)}\}}^2. \quad (2.23)$$

In order to avoid the calculation of $\mu_{\{R_{u,n}^{(i)}, B_{u,n}^{(i)}\}}$ and $\sigma_{\{R_{u,n}^{(i)}, B_{u,n}^{(i)}\}}^2$ for each user separately, it is assumed that the density $p_{\mathbf{r},\varphi}^{(i)}(r, \varphi)$ holds for each user of cell i , i.e. that $p_{\mathbf{r},\varphi}^{(i)}(r, \varphi)$ gives for each user the probability to appear at location (r, φ) . This may not hold in practice, because different users preferably sojourn in different areas, but from the point of view of resource use, however, it is a valid assumption. As a consequence of this assumption, pdfs derived for a single user of a cell hold in general for each user of the cell. Different QoS requirements of the users can then be considered by calculating mean $\mu_{B_u^{(i)}|R_u^{(i)}=1}$ and variance $\sigma_{B_u^{(i)}|R_u^{(i)}=1}^2$ of the bandwidth required by a user to transmit one bit/s and by multiplying them with the QoS target $\tilde{R}_{u,n}^{(i)}$ of user n of cell i , such that (2.23) yields

$$\mu_{\mathbf{B}_i} = \sum_{n=1}^{N_i} \tilde{R}_{u,n}^{(i)} \cdot \mu_{B_u^{(i)}|R_u^{(i)}=1}, \quad \sigma_{\mathbf{B}_i}^2 = \sum_{n=1}^{N_i} \tilde{R}_{u,n}^{(i)2} \cdot \sigma_{B_u^{(i)}|R_u^{(i)}=1}^2. \quad (2.24)$$

The same way, different amounts of bandwidth for different users can be realized by calculating mean $\mu_{R_u^{(i)}|B_u^{(i)}=1}$ and variance $\sigma_{R_u^{(i)}|B_u^{(i)}=1}^2$ of the user bit rate achievable for one Hertz of user bandwidth and by multiplying them with the bandwidth target $\tilde{B}_{u,n}^{(i)}$ of user n of cell i . Thus, (2.23) can be rewritten to

$$\mu_{\mathbf{R}_i} = \sum_{n=1}^{N_i} \tilde{B}_{u,n}^{(i)} \cdot \mu_{R_u^{(i)}|B_u^{(i)}=1}, \quad \sigma_{\mathbf{R}_i}^2 = \sum_{n=1}^{N_i} \tilde{B}_{u,n}^{(i)2} \cdot \sigma_{R_u^{(i)}|B_u^{(i)}=1}^2. \quad (2.25)$$

Since with this method, the calculation of $\mu_{\{R_{u,n}^{(i)}, B_{u,n}^{(i)}\}}$ and $\sigma_{\{R_{u,n}^{(i)}, B_{u,n}^{(i)}\}}^2$ for each user separately is avoided, also the pdfs for user specific variables, such as SINR $\gamma_n^{(i)}$, achieved user bit rate $\mathbf{R}_{u,n}^{(i)}$ and required user bandwidth $\mathbf{B}_{u,n}^{(i)}$, for example, are no longer required for each user separately. Instead, only the pdfs for calculating mean $\mu_{B_u^{(i)}|R_u^{(i)}=1}$ and variance $\sigma_{B_u^{(i)}|R_u^{(i)}=1}^2$ of the bandwidth required by a user to transmit one bit/s as well as mean $\mu_{R_u^{(i)}|B_u^{(i)}=1}$ and variance $\sigma_{R_u^{(i)}|B_u^{(i)}=1}^2$ of the user bit rate achieved for one Hertz of user bandwidth are required. As a consequence, pdfs that are originally user specific, such as $f_{\gamma_n^{(i)}}(\gamma_n^{(i)})$, $f_{\mathbf{R}_{u,n}^{(i)}}(R_{u,n}^{(i)})$ and $f_{\mathbf{B}_{u,n}^{(i)}}(B_{u,n}^{(i)})$, for example, are now user independent and are, therefore, used without user index in the following.

With these considerations, the pdf of the SINR, which is required in above derivations and was up to now assumed to be known, can be derived conveniently. An important prerequisite for this derivation is a closed form representation of the distribution of users over the cell area, which is available only in special cases. The uniform user distribution is such a special case. It is widely used in the analysis of cellular systems and also made here. Furthermore, the cells are assumed to be of circular shape, such that the user position pdf yields

$$p_{\mathbf{r},\varphi}^{(i)}(r, \varphi) = \frac{r}{\pi S_i^2}, \quad 0 < r < S_i, \quad 0 < \varphi < 2\pi. \quad (2.26)$$

Assuming unidirectional antennas, such that the pathloss depends on the distance between BS and user equipment (UE) exclusively, the angular dependence in $p_{\mathbf{r},\varphi}^{(i)}(r, \varphi)$ is not required and integration over φ leads to $p_{\mathbf{r}}^{(i)}(r) = \frac{2r}{S_i^2}$, $0 < r < S_i$. Using this pdf and considering the height h_i of BS i and a pathloss model in a RV transformation, the pdf $f_{\mathbf{a}_{\text{pl}}^{(ii)}}(a_{\text{pl}}^{(ii)})$ of the pathloss is obtained. Slow fading can be considered to be independent of the pathloss, such that according to (2.5), the pdf $f_{\mathbf{a}^{(ii)}}(a^{(ii)})$ of the total signal attenuation in logarithmic scale is obtained by a convolution of the pdf $f_{\mathbf{a}_{\text{pl}}^{(ii)}}(a_{\text{pl}}^{(ii)})$ of the pathloss in logarithmic scale and the pdf $f_{\mathbf{a}_{\text{sf}}}(a^{(ii)})$ of the shadow fading in logarithmic scale and yields

$$f_{\mathbf{a}^{(ii)}}(a^{(ii)}) = \int_{a_{\text{pl},\min}^{(ii)}}^{a_{\text{pl},\max}^{(ii)}} f_{\mathbf{a}_{\text{pl}}^{(ii)}}(a_{\text{pl}}^{(ii)}) \cdot f_{\mathbf{a}_{\text{sf}}}(a^{(ii)} - a_{\text{pl}}^{(ii)}) da_{\text{pl}}^{(ii)}. \quad (2.27)$$

Note that fast fading should not be considered in the total signal attenuation since it is covered by the Scheduler Assumption of Section 2.4.1 and actually treated by the algorithms of the lower plane of the hierarchic concept for the coordination of automatic capacity optimization and scheduling of Section 2.2.

The major challenge in the derivation of the pdf of the SINR consists in obtaining the pdf of the ICI power. In fact, the analytical derivation could not be carried out if the

pdf of the ICI was determined analytically exact. In order to be able to continue the analytical approach, ICI power is, therefore, assumed to be equal to $\bar{P}_{1,i}$ of (2.14) and independent of the position within the cell area. This assumption is clearly a source of inaccuracy, but it is reasonable since $\bar{P}_{1,i}$ is the expected value of the ICI. With this assumption, the SINR $\gamma^{(i)}$ is given by $\gamma^{(i)} = g(a^{(ii)}) = \frac{P_{\text{tx},i}}{10^{\frac{a^{(ii)}}{10}}} \cdot \frac{1}{\bar{P}_{1,i} + P_N}$ and the pdf of the SINR yields

$$\begin{aligned} f_{\gamma^{(i)}}(\gamma^{(i)}) &= f_{\mathbf{a}^{(ii)}}(g^{-1}(\gamma^{(i)})) \cdot \left| \frac{\partial g^{-1}(\gamma^{(i)})}{\partial \gamma^{(i)}} \right| \\ &= f_{\mathbf{a}^{(ii)}}\left(10 \cdot \log_{10}\left(\frac{P_{\text{tx},i}}{P_N + P_{1,i}} \frac{1}{\gamma^{(i)}}\right)\right) \cdot \left| -\frac{10}{\gamma^{(i)} \cdot \ln(10)} \right| \\ &= f_{\mathbf{a}^{(ii)}}\left(10 \cdot \log_{10}\left(\frac{\Gamma_i}{\gamma^{(i)}}\right)\right) \cdot \frac{10}{\gamma^{(i)} \cdot \ln(10)}, \end{aligned} \quad (2.28)$$

with $g^{-1}(\gamma^{(i)})$ the inverse of $g(a^{(ii)})$. Defining $x = 2^{\frac{R_u^{(i)}}{B_u^{(i)}}} - 1$ and using (2.28), the pdf $f_{\mathbf{R}_u^{(i)}}(R_u^{(i)})$ of the achieved user bit rate and the pdf $f_{\mathbf{B}_u^{(i)}}(B_u^{(i)})$ of the bandwidth required by a user can be determined in close analogy to the derivations at the beginning of this section, yielding

$$\begin{aligned} f_{\mathbf{R}_u^{(i)}}(R_u^{(i)}) &= f_{\gamma^{(i)}}(x) \cdot 2^{\frac{R_u^{(i)}}{B_u^{(i)}}} \ln(2) \frac{1}{B_u^{(i)}} \\ &= \frac{5c_2}{S_i^2(x) \ln(10)} \cdot e^{\frac{c_2^2}{4c_3} + c_2(10 \cdot \log_{10}(\frac{\Gamma_i}{x}) - a_0)} \cdot 2^{\frac{R_u^{(i)}}{B_u^{(i)}}} \ln(2) \frac{1}{B_u^{(i)}} \\ &\quad \left(\operatorname{erf}\left(\frac{c_2 + 2c_3(10 \cdot \log_{10}(\frac{\Gamma_i}{x}) - a_{\text{pl,min}})}{2\sqrt{c_3}}\right) \right. \\ &\quad \left. - \operatorname{erf}\left(\frac{c_2 + 2c_3(10 \cdot \log_{10}(\frac{\Gamma_i}{x}) - a_{\text{pl,max}})}{2\sqrt{c_3}}\right) \right) \end{aligned} \quad (2.29)$$

and

$$\begin{aligned} f_{\mathbf{B}_u^{(i)}}(B_u^{(i)}) &= f_{\gamma^{(i)}}(x) \cdot 2^{\frac{R_u^{(i)}}{B_u^{(i)}}} \ln(2) \frac{R_u^{(i)}}{B_u^{(i)2}} \\ &= \frac{5c_2}{S_i^2(x) \ln(10)} \cdot e^{\frac{c_2^2}{4c_3} + c_2(10 \cdot \log_{10}(\frac{\Gamma_i}{x}) - a_0)} \cdot 2^{\frac{R_u^{(i)}}{B_u^{(i)}}} \ln(2) \frac{R_u^{(i)}}{B_u^{(i)2}} \\ &\quad \left(\operatorname{erf}\left(\frac{c_2 + 2c_3(10 \cdot \log_{10}(\frac{\Gamma_i}{x}) - a_{\text{pl,min}})}{2\sqrt{c_3}}\right) \right. \\ &\quad \left. - \operatorname{erf}\left(\frac{c_2 + 2c_3(10 \cdot \log_{10}(\frac{\Gamma_i}{x}) - a_{\text{pl,max}})}{2\sqrt{c_3}}\right) \right), \end{aligned} \quad (2.30)$$

respectively. Full formulae of the derivation of $f_{\mathbf{R}_u^{(i)}}(R_u^{(i)})$ and $f_{\mathbf{B}_u^{(i)}}(B_u^{(i)})$ can be found in Appendix A.1.

Mean and variance of the achieved user bit rate $R_u^{(i)}$ and the bandwidth $B_u^{(i)}$ required by a user are functions of the power ratio Γ_i , as can be seen from (2.29) and (2.30), respectively. Consequently, also mean μ_{R_i} and variance $\sigma_{R_i}^2$ of achieved cell throughput

R_i as well as mean μ_{B_i} and variance $\sigma_{B_i}^2$ of the required cell bandwidth B_i are functions of the power ratio Γ_i . It is important to keep this in mind, since for reasons of readability, the dependence on the power ratio is not explicitly stated in the formulae throughout this thesis.

For the verification of the modeling approach and for the assessment of the effect of assuming location independent ICI, the analytically obtained pdfs of user bit rate $\mathbf{R}_u^{(i)}$ and achieved cell throughput \mathbf{R}_i are compared with empirically obtained pdfs. For the determination of the empirical pdfs, Monte Carlo (MC) simulations in a scenario with seven cells in a regular hexagonal grid, cf. Figure 2.2, are applied. The six outer

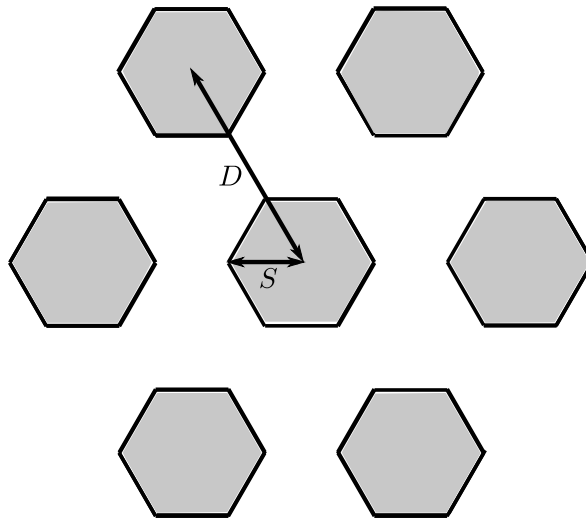


Figure 2.2. Scenario for modeling approach verification.

cells j serve as sources of interference. For the center cell $i, i \neq j$, user positions are created randomly according to user position pdf $p_{\mathbf{r},\varphi}^{(i)}(r, \varphi)$. The assumption of position independent ICI power over the cell area, as it was made for the derivation of (2.28), is not required with the MC simulations such that the user bit rates at the user positions are calculated using the correct ICI power resulting at each user position. The empirical pdfs are determined from the achieved user bit rates that were calculated with the correct ICI power such that the error of the modeling approach resulting from the assumption of position independent ICI power can be assessed by comparing analytical and empirical pdfs. The parameters for the verification can be taken from Table 2.1.

Figure 2.3(a) compares the analytical pdf to the empirical pdf of the achieved user bit rate $\mathbf{R}_u^{(i)}$ of a single user of cell i . Figure 2.3(b) compares the analytical model of the achieved cell throughput \mathbf{R}_i for $N_i = 5$ simultaneously active users to the

Table 2.1. Parameters for model approach verification.

| Parameter | Value |
|---|-------------------------------------|
| Number of cells | 7 |
| Cell radius S | 250 m |
| Reuse distance D | 750 m |
| Height of the BSs | 32 m |
| Height of the UEs | 1.5 m |
| User position probability $p_{r,\varphi}^{(i)}(r, \varphi)$ | uniform |
| Carrier frequency | 1.9 GHz |
| Propagation model | 3GPP Urban Macro |
| Shadow fading variance σ_{sh}^2 | 8 dB |
| Interferer transmit Power $P_{tx,j}$ | 33 dBm |
| Noise PSD | $-167 \frac{\text{dBm}}{\text{Hz}}$ |

empirically obtained pdf of the achieved cell throughput. The figures show that for uniform user distribution, the presented analytical approach with the assumption of location independent ICI leads to only small errors compared to the true pdfs. It can also be seen that even for a small number of users, the assumption of a Gaussian pdf resulting from the CLT leads to a good approximation of the achieved cell throughput.

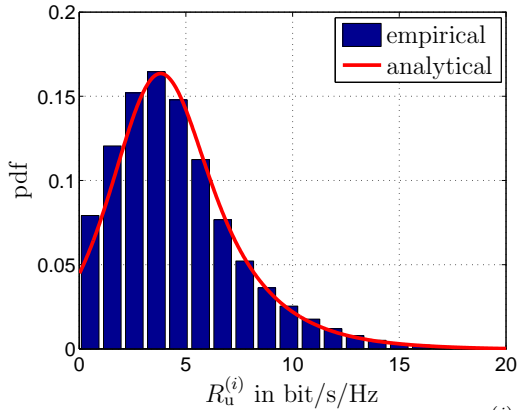
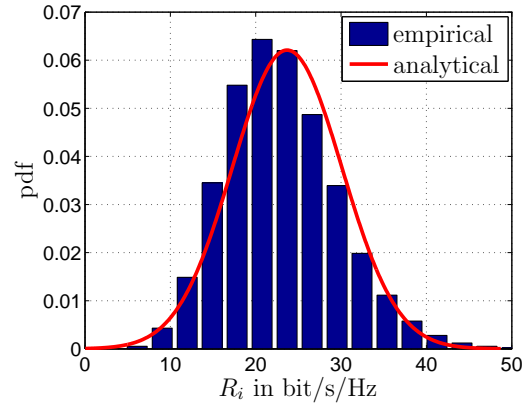
(a) pdf of the achieved user bit rate $R_u^{(i)}$.(b) pdf of the achieved cell throughput R_i for $N_i = 5$ users.

Figure 2.3. Empirical and analytical pdfs of achieved user bit rate $\mathbf{R}_u^{(i)}$ and achieved cell throughput \mathbf{R}_i .

Note that the assumption of location independent ICI within a cell is general not required with the cell-centric network model, but necessary for the specific analytical derivation of the pdf of the SINR of (2.28), as it is exemplarily described in this Section.

2.4.3 PBR-Characteristic

According to (2.29) and (2.30), a relation between user bit rate $R_u^{(i)}$, user bandwidth $B_u^{(i)}$ and power ratio Γ_i exists. As a consequence, also a relation between cell throughput R_i , cell bandwidth B_i and power ratio Γ_i exists. The relations are characteristic to a cell since according to the derivations of Section 2.4.2, cell specific factors such as user distribution, environment and interference situation are regarded by the relation. This section exploits the mentioned relation between R_i , B_i and Γ_i to establish a model called Power-Bandwidth-Rate (PBR)-Characteristic, which links the resource allocations of a cell in terms of transmit power or power ratio Γ_i , respectively, and cell bandwidth B_i with the performance of a cell in terms of cell throughput R_i . The number N_i of users in the cell is assumed to be constant.

Since the PBR-Characteristic relates the resource allocation of a cell with the achieved cell throughput, the derivation is based on the achieved cell throughput \mathbf{R}_i as defined by (2.21). The achieved cell throughput is a RV, according to Section 2.4.2, such that different cell throughputs are achieved with different probabilities. This gives the opportunity to define outage probability and outage capacity at cell level consistently with their definition at link level as it is done in information theory [TV05]. Defining outage probability at cell level as the probability that outage occurs among the users of a cell i , i.e. that at least one user of cell i cannot meet its QoS requirements, outage probability is expressed by the probability that the achieved cell throughput is lower than a given minimum throughput $R_{0,i}$ which is required to fulfill the QoS requirements of all users of cell i . According to this definition and with the error function

$$\operatorname{erf}(x) = \frac{1}{\sqrt{2\pi}} \int_0^x e^{-\frac{y^2}{2}} dy \quad (2.31)$$

and the Standard Normal cdf $\Phi(x) = \frac{1}{2} + \operatorname{erf}(x)$ [PP02], the outage probability $p_{\text{out},i}$ of cell i at cell level is given by

$$\begin{aligned} p_{\text{out},i} &= P(R_i < R_{0,i}) \\ &= \Phi\left(\frac{R_{0,i} - \mu_{R_i}}{\sigma_{R_i}}\right). \end{aligned} \quad (2.32)$$

Outage capacity at cell level is, consequently, defined as the cell throughput R_i that can be supplied by cell i if a certain target cell outage probability \tilde{p}_{out} has to be observed. Thus, with $\Phi^{-1}(\cdot)$ the inverse of the Standard Normal cdf, outage capacity at cell level is defined by

$$\begin{aligned} \tilde{R}_i &= \{R | P(R_i < R) = \tilde{p}_{\text{out}}\} \\ &= \Phi^{-1}(\tilde{p}_{\text{out}}) \sigma_{R_i} + \mu_{R_i}. \end{aligned} \quad (2.33)$$

The definitions of outage probability at cell-level and outage capacity at cell-level are illustrated in Figure 2.4.

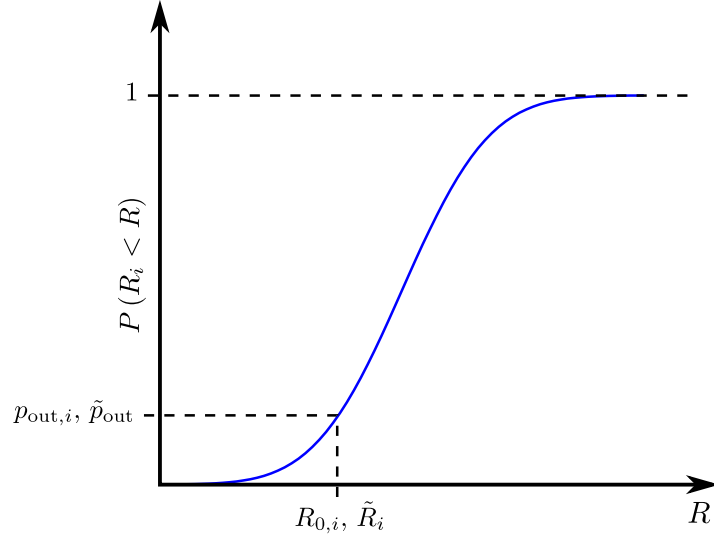


Figure 2.4. Illustration of the definition of outage probability and outage capacity at cell level.

For the further derivation of the PBR-Characteristic, the definition of mean and variance of the achieved user bit rate of (2.25) are used in (2.33) which yields

$$\begin{aligned}
 \tilde{R}_i &= \Phi^{-1}(\tilde{p}_{\text{out}}) \sqrt{\sum_{n=1}^{N_i} \sigma_{R_{u,n}^{(i)}}^2 + \sum_{n=1}^{N_i} \mu_{R_{u,n}^{(i)}}} \\
 &= \Phi^{-1}(\tilde{p}_{\text{out}}) \sqrt{\sum_{n=1}^{N_i} \tilde{B}_{u,n}^{(i)2} \cdot \sigma_{R_u^{(i)}|B_u^{(i)}=1}^2 + \sum_{n=1}^{N_i} \tilde{B}_{u,n}^{(i)} \cdot \mu_{R_u^{(i)}|B_u^{(i)}=1}} \quad (2.34) \\
 &= \Phi^{-1}(\tilde{p}_{\text{out}}) \sqrt{\sum_{n=1}^{N_i} \tilde{B}_{u,n}^{(i)2} \cdot \sigma_{R_u^{(i)}|B_u^{(i)}=1} + \mu_{R_u^{(i)}|B_u^{(i)}=1} \sum_{n=1}^{N_i} \tilde{B}_{u,n}^{(i)}}.
 \end{aligned}$$

Assuming FR scheduling, each user is in average allocated the same bandwidth $\frac{B_i}{N_i}$ and (2.34) can be further simplified to

$$\begin{aligned}
 \tilde{R}_i &= \Phi^{-1}(\tilde{p}_{\text{out}}) \sqrt{N_i \cdot \frac{B_i^2}{N_i^2} \cdot \sigma_{R_u^{(i)}|B_u^{(i)}=1} + N_i \cdot \frac{B_i}{N_i} \cdot \mu_{R_u^{(i)}|B_u^{(i)}=1}} \quad (2.35) \\
 &= \Phi^{-1}(\tilde{p}_{\text{out}}) \cdot \frac{B_i}{\sqrt{N_i}} \cdot \sigma_{R_u^{(i)}|B_u^{(i)}=1} + B_i \cdot \mu_{R_u^{(i)}|B_u^{(i)}=1}.
 \end{aligned}$$

Since $\mu_{R_u^{(i)}|B_u^{(i)}=1}$ and $\sigma_{R_u^{(i)}|B_u^{(i)}=1}$ are functions of Γ_i , according to Section 2.4.2, (2.35) expresses the characteristic relation of transmit power in terms of power ratio Γ_i , cell bandwidth B_i and cell throughput in terms of outage capacity \tilde{R}_i at cell level for a given number of users N_i . Thus, (2.35) is the PBR-Characteristic. Figure 2.5 shows the PBR-Characteristic resulting from (2.35) and based on the derivations of Section 2.4.2 for $N_i = 5$ users and for the parameters of Table 2.1. The figure relates all resource allocations in terms of transmit power or power ratio Γ_i , respectively, and cell bandwidth B_i with performance values in terms of cell throughput or cell

outage capacity \tilde{R}_i , respectively. It can be used, for example, to determine all resource allocations that enable the cell to achieve a certain cell throughput.

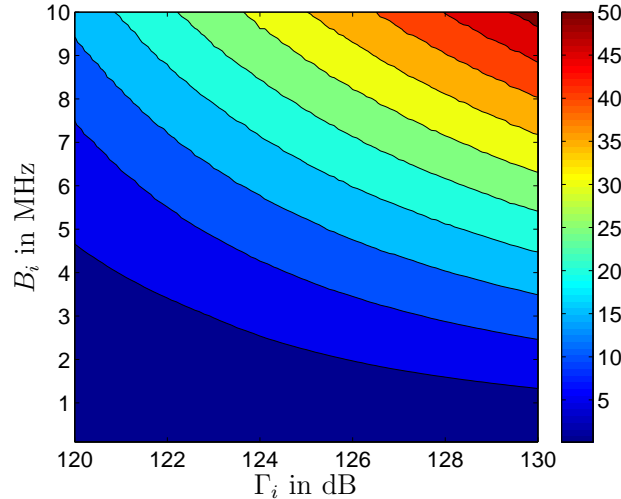


Figure 2.5. Cell throughput in terms of outage capacity \tilde{R}_i at cell level in Mbit/s as a function of power ratio Γ_i and cell bandwidth B_i for $N_i = 5$ users, uniform user distribution and FR scheduling.

2.4.4 PBN-Characteristic

The PBR-Characteristic of Section 2.4.3 is valid in situations where the number of users is fixed and the average user bit rate depends on the resource allocation of the cell. If a fixed average user bit rate is demanded, however, the number of users that can be supported by the cell depends on the resource allocation of the cell. This relation cannot be modeled by the PBR-Characteristic, such that a different characteristic relation, which relates the resource allocation of a cell in terms of transmit power or power ratio Γ_i , respectively, and cell bandwidth B_i with the number of users that can be supported by the cell, is needed. This relation, which is called Power-Bandwidth-Number-of-Users (PBN)-Characteristic, is derived in this section. In contrast to the previous section, the number N_i of users is now variable and the average user bit rate $\bar{R}_u^{(i)}$ is constant.

For the derivation of the PBN-Characteristic, the average user bit rate $\bar{R}_u^{(i)}$ is defined by

$$\bar{R}_u^{(i)} = \frac{\tilde{R}_i}{N_i}. \quad (2.36)$$

Resolving (2.36) for \tilde{R}_i and substituting it in (2.35) yields

$$\begin{aligned} N_i \cdot \bar{R}_u^{(i)} &= \Phi^{-1}(\tilde{p}_{\text{out}}) \cdot \frac{B_i}{\sqrt{N_i}} \cdot \sigma_{R_u^{(i)}|B_u^{(i)}=1} + B_i \cdot \mu_{R_u^{(i)}|B_u^{(i)}=1} \\ N_i^{\frac{3}{2}} \cdot \bar{R}_u^{(i)} &= \Phi^{-1}(\tilde{p}_{\text{out}}) \cdot B_i \cdot \sigma_{R_u^{(i)}|B_u^{(i)}=1} + \sqrt{N_i} \cdot B_i \cdot \mu_{R_u^{(i)}|B_u^{(i)}=1}. \end{aligned} \quad (2.37)$$

Setting $M = \sqrt{N_i}$, (2.37) can be solved for N_i using Cardano's method for solving cubic equations [BSMM08] which yields

$$\begin{aligned} N_i &= (u + v)^2, \\ u &= \sqrt[3]{-q + \sqrt{q^2 + p^3}}, \quad v = \sqrt[3]{-q - \sqrt{q^2 + p^3}}, \\ p &= -\frac{B_i \cdot \mu_{R_u^{(i)}|B_u^{(i)}=1}}{3\bar{R}_u^{(i)}}, \quad q = -\frac{\Phi^{-1}(\tilde{p}_{\text{out}}) \cdot B_i \cdot \sigma_{R_u^{(i)}|B_u^{(i)}=1}}{2\bar{R}_u^{(i)}}. \end{aligned} \quad (2.38)$$

Equation (2.38) gives the relation between the resource allocation of the cell in terms of cell bandwidth and transmit power or power ratio Γ_i , respectively, and the performance of the cell in terms of number of users that can be supported with average user bit rate $\bar{R}_u^{(i)}$. Thus, (2.38) is the PBN-Characteristic. Figure 2.6 shows the PBN-Characteristic resulting from (2.38) and based on the derivations of Section 2.4.2 for an average user bit rate $\bar{R}_u^{(i)}$ of 100 kbit/s and for the parameters of Table 2.1. The figure relates all resource allocations in terms of transmit power or power ratio Γ_i , respectively, and cell bandwidth B_i with performance values in terms of the number of users that can be supported by the cell. It can be used to determine resource allocations that are suited to support a certain number of users with a fixed average user bit rate, for example.

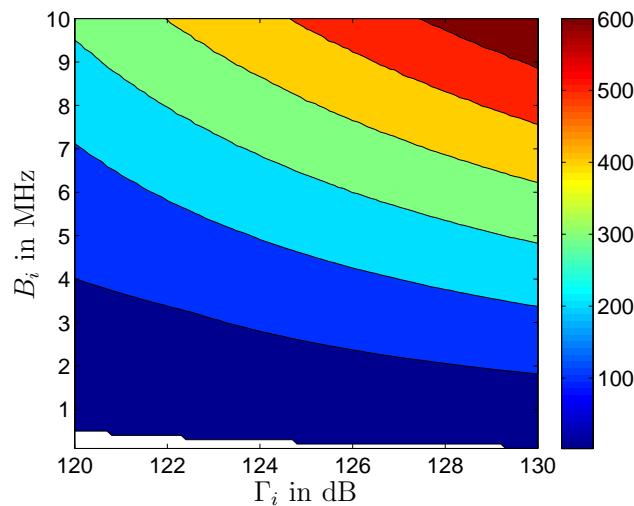


Figure 2.6. Number N_i of users that can be supported by the cell as a function of power ratio Γ_i and cell bandwidth B_i for average user bit rate $\bar{R}_u^{(i)}$ of 100 kbit/s, uniform user distribution and FR scheduling.

2.4.5 Adaptive Fair Resource Scheduling

As addressed in Section 2.3, advanced scheduling strategies for wireless networks are able to maximize the cell throughput while considering fairness constraints and are, thus, attractive for mobile radio networks [VTL02, LCS03]. This section shows how to extend the previous derivations such that advanced scheduling strategies can be considered in the cell-centric network model. PF scheduling [Kel97, LZ06] will be treated exemplarily in this section, which belongs to the group of FR scheduling strategies, according to Section 2.3.

PF scheduling leads to a power gain \mathbf{g}_{pf} , according to Section 2.3. This scheduling power gain scales the SINR multiplicatively. In order to consider scheduling in the derivations of Section 2.4.2, the pdf of the SINR $\gamma_{\text{pf}}^{(i)} = \gamma^{(i)} \cdot g_{\text{pf}}^{(i)}$ after PF scheduling is required. For this purpose, the cdf of $\gamma_{\text{pf}}^{(i)}$ is derived yielding

$$\begin{aligned}
 F_{\gamma_{\text{pf}}^{(i)}}\left(\gamma_{\text{pf}}^{(i)}\right) &= P\left(\gamma^{(i)} \cdot g_{\text{pf}}^{(i)} < \gamma_{\text{pf}}^{(i)}\right) \\
 &= P\left(g_{\text{pf}}^{(i)} < \frac{\gamma_{\text{pf}}^{(i)}}{\gamma^{(i)}}\right) \\
 &= \int_0^{\frac{\gamma_{\text{pf}}^{(i)}}{\gamma^{(i)}}} \int_0^{\infty} f_{\gamma^{(i)}, \mathbf{g}_{\text{pf}}^{(i)}}\left(\gamma^{(i)}, g_{\text{pf}}^{(i)}\right) dg_{\text{pf}}^{(i)} d\gamma^{(i)}.
 \end{aligned} \tag{2.39}$$

In (2.39), the joint pdf $f_{\gamma^{(i)}, \mathbf{g}_{\text{pf}}^{(i)}}\left(\gamma^{(i)}, g_{\text{pf}}^{(i)}\right)$ of SINR and scheduling power gain can be separated into two independent pdfs since fast fading can be considered to be independent of pathloss, slow fading and user distribution, which are the RVs that influence the SINR γ . Thus, (2.39) can be rewritten as

$$\begin{aligned}
 F_{\gamma_{\text{pf}}^{(i)}}\left(\gamma_{\text{pf}}^{(i)}\right) &= \int_0^{\infty} f_{\gamma^{(i)}}\left(\gamma^{(i)}\right) \int_0^{\frac{\gamma_{\text{pf}}^{(i)}}{\gamma^{(i)}}} f_{\mathbf{g}_{\text{pf}}^{(i)}}\left(g_{\text{pf}}^{(i)}\right) dg_{\text{pf}}^{(i)} d\gamma^{(i)} \\
 &= \int_0^{\infty} f_{\gamma^{(i)}}\left(\gamma^{(i)}\right) F_{\mathbf{g}_{\text{pf}}^{(i)}}\left(\frac{\gamma_{\text{pf}}^{(i)}}{\gamma^{(i)}}\right) d\gamma^{(i)}.
 \end{aligned} \tag{2.40}$$

The pdf $f_{\gamma_{\text{pf}}^{(i)}}\left(\gamma_{\text{pf}}^{(i)}\right)$ of the SINR after PF scheduling is given by the derivative of (2.40), such that with the cdf $F_{\mathbf{g}_{\text{pf}}^{(i)}}\left(\mathbf{g}_{\text{pf}}^{(i)}\right)$ of the PF power gain \mathbf{g}_{pf} as given by (2.9), the pdf

of the SINR after PF scheduling is given by

$$\begin{aligned}
f_{\gamma_{\text{pf}}^{(i)}}\left(\gamma_{\text{pf}}^{(i)}\right) &= \frac{\partial F_{\gamma_{\text{pf}}^{(i)}}\left(\gamma_{\text{pf}}^{(i)}\right)}{\partial \gamma_{\text{pf}}^{(i)}} \\
&= \int_0^{\infty} f_{\gamma^{(i)}}\left(\gamma^{(i)}\right) \frac{\partial F_{\mathbf{g}_{\text{pf}}^{(i)}}\left(\frac{\gamma_{\text{pf}}^{(i)}}{\gamma^{(i)}}\right)}{\partial \gamma_{\text{pf}}^{(i)}} d\gamma^{(i)} \\
&= \int_0^{\infty} f_{\gamma^{(i)}}\left(\gamma^{(i)}\right) \frac{N_i}{2\sigma^2\gamma^{(i)}} \cdot e^{-\frac{\gamma_{\text{pf}}^{(i)}}{2\sigma^2\gamma^{(i)}}} \left(1 - e^{-\frac{\gamma_{\text{pf}}^{(i)}}{2\sigma^2\gamma^{(i)}}}\right)^{N_i-1} d\gamma^{(i)}.
\end{aligned} \tag{2.41}$$

Replacing in the derivations of Section 2.4.2 the pdf of the SINR $\gamma^{(i)}$ as given by (2.28), for example, by (2.41) extends the cell-centric network model to consider PF scheduling in the derivation of the pdf $f_{\mathbf{R}_u^{(i)}}\left(R_u^{(i)}\right)$ of achieved user bit rate and in the derivation of the pdf $f_{\mathbf{B}_u^{(i)}}\left(B_u^{(i)}\right)$ of required user bandwidth. The further steps in the derivation of the cell-centric network model concerning the derivation of the pdfs of achieved cell throughput \mathbf{R}_i and required cell bandwidth \mathbf{B}_i are as described in Section 2.4.2.

One aspect in this context, however, requires further discussion. In Section 2.4.2, the assumption of independent users was made, which is valid in the case of independent scheduling. For PF scheduling, however, this cannot be assumed since the users are dependent due to the comparison of their fast fading channel gains, cf. Section 2.3. Therefore, the assumption of independent users has to be considered a simplification in the case of PF scheduling.

In order to verify the approach for considering PF scheduling in the cell-centric network model and in order to investigate the effect of the simplifying assumption concerning the independence of the users, the approach of Section 2.4.2 with the scenario from Figure 2.2 and the parameters from Table 2.1 is applied. The analytical pdfs of achieved user bit rate $\mathbf{R}_u^{(i)}$ and achieved cell throughput \mathbf{R}_i are compared to the respective empirically obtained pdfs in Figures 2.7(a) and 2.7(b). The figures show that the achieved user bit rate is adequately modeled. Concerning the achieved cell throughput, it can be seen that the analytical model is not exact but a good approximation of the true pdf. Comparing Figure 2.7(b) with the achieved cell throughput for channel non-adaptive FR scheduling of Figure 2.3(b) shows that the fit of the analytical curve is less accurate for PF scheduling than for channel non-adaptive FR scheduling as in Section 2.4.2, which is due to the simplifying assumption of independent users.

Since PF scheduling belongs to the group of FR scheduling strategies, (2.35) and (2.38) are also valid for PF scheduling to determine PBR- and PBN-Characteristic, respectively. PBR- and PBN-Characteristic for PF scheduling are shown in Figure 2.8(a) and

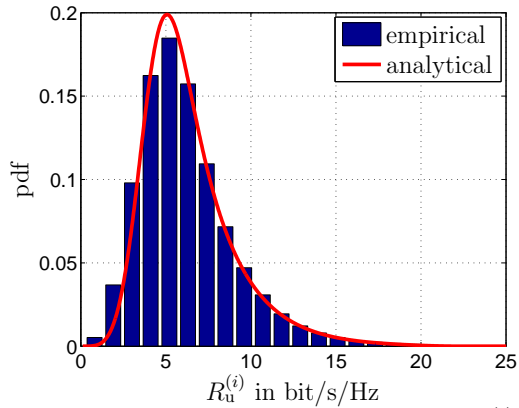
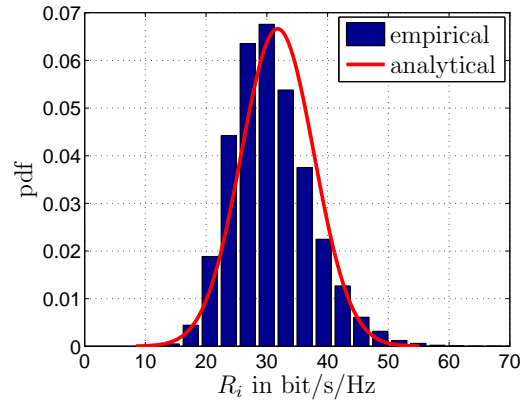
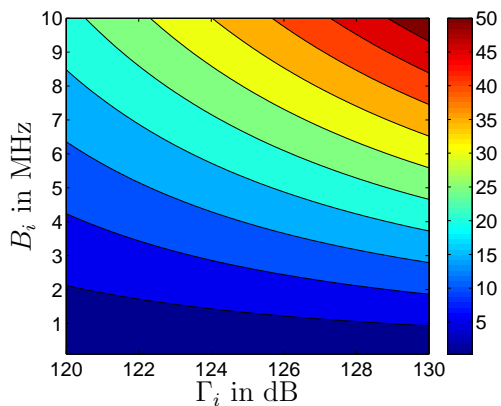
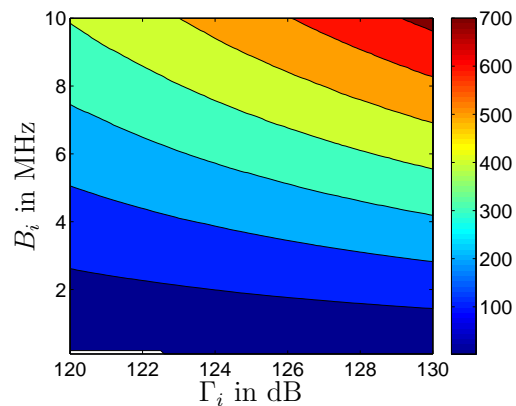
(a) pdf of the achieved user bit rate $R_u^{(i)}$.(b) pdf of the achieved cell throughput R_i for $N_i = 5$ users.

Figure 2.7. Empirical and analytical pdfs of achieved user bit rate $R_u^{(i)}$ and achieved cell throughput R_i for PF scheduling.

Figure 2.8(b) for $N_i = 5$ users and average user bit rate \bar{R}_u of 100 kbit/s, respectively, and for the parameters of Table 2.1. They have the same meaning as for channel non-adaptive FR scheduling and are read the same way. However, due to the scheduling strategy, which exploits the channel variations to maximize the cell throughput, higher performance is achieved compared to channel non-adaptive FR scheduling, cf. Figure 2.5 and 2.6.



(a) Cell throughput.



(b) Number of users.

Figure 2.8. Cell throughput in terms of outage capacity at cell level \tilde{R}_i in Mbit/s and the number N_i of users that can be supported by the cell, both as a function of power ratio Γ_i and cell bandwidth B_i and for uniform user distribution and PF scheduling. The cell throughput is shown for $N_i = 5$ users, the number of users is shown for an average user bit rate \bar{R}_u of 100 kbit/s.

2.4.6 Fair Throughput Scheduling

In systems applying FR scheduling, the bit rate a user achieves depends on the user position, according to Section 2.4.2. Some services, however, require a constant bit rate in order to work properly. FT scheduling is a scheduling strategy that is capable of achieving this [Fer10]. It allocates resources to the users such that fairness among the users of a cell with respect to the user bit rate is achieved. This section presents the proper approach in order to consider FT scheduling strategies in the cell-centric network model.

Assuming FT scheduling, the average user bit rate $\bar{R}_u^{(i)}$ is achieved by each user of a cell. Depending on the user position, however, different user bandwidths are required. The amount of resources that are allocated to a user is the result of the scheduling process. As a consequence, the definitions of PBR- and PBN-Characteristic in connection with FT scheduling is based on the required cell bandwidth as defined in (2.22).

Before continuing with the derivation of PBR- and PBN-Characteristic for FT scheduling, the pdf of the bandwidth $\mathbf{B}_u^{(i)}$ required by a user and the pdf of the required cell bandwidth \mathbf{B}_i , as they were derived in Section 2.4.3, have to be verified. For this verification, the approach of Section 2.4.2 with the scenario from Figure 2.2 and the parameters from Table 2.1 is applied. The analytical pdfs of required user bandwidth $\mathbf{B}_u^{(i)}$ and required cell bandwidth \mathbf{B}_i are compared to empirically obtained pdfs, as shown by Figure 2.9(a) and 2.9(b). The figures show that the cell-centric network

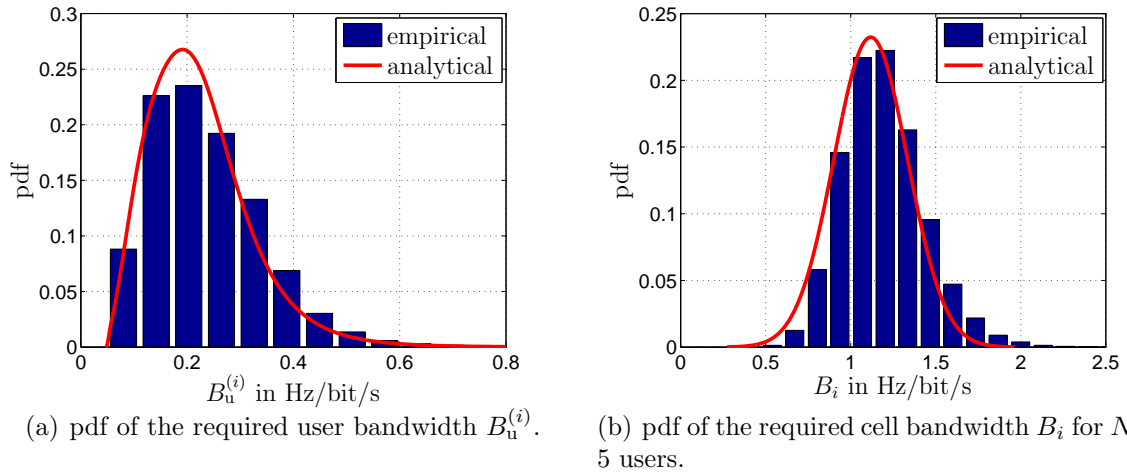


Figure 2.9. Empirical and analytical pdfs of the required user bandwidth $\mathbf{B}_u^{(i)}$ and the required cell bandwidth \mathbf{B}_i for FT scheduling.

model is applicable for FT scheduling. Note that no channel adaptive scheduling strategy is assumed, such that the assumption of independent users is valid.

As in section 2.4.3, outage probability and outage bandwidth can be defined based on the required cell bandwidth \mathbf{B}_i . Using the definition of outage probability $p_{\text{out},i}$ at cell-level from Section 2.4.3 as the probability that outage occurs among the users of cell i , i.e. that at least one user of cell i cannot meet its QoS requirements, outage probability $p_{\text{out},i}$ at cell-level in connection with FT scheduling is defined as the probability that more cell bandwidth is required in order to fulfill the minimum QoS requirements of the users of cell i than a certain minimum bandwidth $B_{0,i}$. Thus, outage probability $p_{\text{out},i}$ of cell i at cell-level in connection with FT scheduling is defined by

$$\begin{aligned} p_{\text{out},i} &= P(B_i > B_{0,i}) \\ &\simeq 1 - \Phi\left(\frac{B_{0,i} - \mu_{B_i}}{\sigma_{B_i}}\right) \end{aligned} \quad (2.42)$$

Outage bandwidth at cell-level in connection with FT scheduling is, consequently, the bandwidth that is required if a certain target cell outage probability \tilde{p}_{out} has to be observed, it is defined by

$$\begin{aligned} \tilde{B}_i &= \{B | P(B_i > B) = \tilde{p}_{\text{out}}\} \\ &\simeq \Phi^{-1}(1 - \tilde{p}_{\text{out}}) \sigma_{B_i} + \mu_{B_i}. \end{aligned} \quad (2.43)$$

The definitions of outage probability at cell-level and outage bandwidth at cell-level for FT scheduling are illustrated in Figure 2.10.

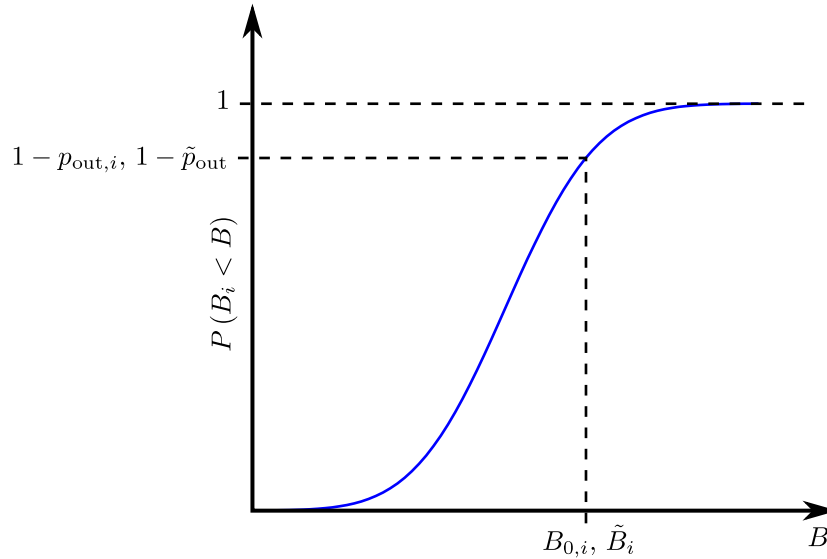


Figure 2.10. Illustration of the definition of outage probability and outage capacity for FT scheduling at cell level.

Using in (2.43) the definition of mean and variance of the bandwidth required by a user of (2.24) yields

$$\begin{aligned}
\tilde{B}_i &= \Phi^{-1}(1 - \tilde{p}_{\text{out}}) \sqrt{\sum_{n=1}^{N_i} \sigma_{B_{u,n}^{(i)}}^2 + \sum_{n=1}^{N_i} \mu_{B_{u,n}^{(i)}}} \\
&= \Phi^{-1}(1 - \tilde{p}_{\text{out}}) \sqrt{\sum_{n=1}^{N_i} \tilde{R}_{u,n}^{(i)2} \cdot \sigma_{B_{u,n}^{(i)}|R_{u,n}^{(i)}=1}^2 + \sum_{n=1}^{N_i} \tilde{R}_{u,n}^{(i)} \cdot \mu_{B_{u,n}^{(i)}|R_{u,n}^{(i)}=1}} \quad (2.44) \\
&= \Phi^{-1}(1 - \tilde{p}_{\text{out}}) \sqrt{\sum_{n=1}^{N_i} \tilde{R}_{u,n}^{(i)2} \cdot \sigma_{B_{u,n}^{(i)}|R_{u,n}^{(i)}=1} + \mu_{B_{u,n}^{(i)}|R_{u,n}^{(i)}=1} \sum_{n=1}^{N_i} \tilde{R}_{u,n}^{(i)}}.
\end{aligned}$$

Note that (2.44) looks similar to (2.34), but since FT scheduling is considered, the user bit rates targets $\tilde{R}_{u,n}^{(i)}$ are now given in place of the user bandwidth targets $\tilde{B}_{u,n}^{(i)}$. Assuming fairness among the users with respect to the achieved user bit rate, the bit rate of each user is equal to bit rate target $\tilde{R}_u^{(i)}$ and (2.44) can be further simplified to

$$\begin{aligned}
\tilde{B}_i &= \Phi^{-1}(1 - \tilde{p}_{\text{out}}) \cdot \sqrt{N_i \cdot \tilde{R}_u^{(i)2} \cdot \sigma_{R_u^{(i)}|B_u^{(i)}=1} + N_i \cdot \tilde{R}_u^{(i)} \cdot \mu_{R_u^{(i)}|B_u^{(i)}=1}} \quad (2.45) \\
&= \Phi^{-1}(1 - \tilde{p}_{\text{out}}) \cdot \sqrt{N_i} \cdot \tilde{R}_u^{(i)} \cdot \sigma_{R_u^{(i)}|B_u^{(i)}=1} + N_i \cdot \tilde{R}_u^{(i)} \cdot \mu_{R_u^{(i)}|B_u^{(i)}=1}.
\end{aligned}$$

Resolving (2.45) for the user bit rate target \tilde{R}_u yields

$$\tilde{R}_u^{(i)} = \frac{\tilde{B}_i}{\Phi^{-1}(1 - \tilde{p}_{\text{out}}) \cdot \sqrt{N_i} \cdot \sigma_{R_u^{(i)}|B_u^{(i)}=1} + N_i \cdot \mu_{R_u^{(i)}|B_u^{(i)}=1}}, \quad (2.46)$$

such that (2.46) relates the resource allocation in terms of transmit power or power ratio Γ_i , respectively and the cell bandwidth B_i with the user bit rate target $\tilde{R}_u^{(i)}$ that can be achieved by each user. It is, thus, the PBR-Characteristic for FT scheduling. Note that the PBR-Characteristic for FT scheduling differs from the PBR-Characteristic for FR scheduling, since with FT scheduling, the PBR-Characteristic gives the user bit rate that can be achieved by each user, while with FR scheduling, the cell throughput that can be achieved is given.

In order to obtain the PBN-Characteristic for FT scheduling, (2.45) is resolved for N_i by setting $M = \sqrt{N_i}$ yielding

$$\begin{aligned}
N_i &= \left(-\frac{p}{2} + \sqrt{\frac{p^2}{4} - q} \right)^2, \\
p &= \frac{\Phi^{-1}(1 - \tilde{p}_{\text{out}}) \cdot \sigma_{R_u^{(i)}|B_u^{(i)}=1}}{\mu_{R_u^{(i)}|B_u^{(i)}=1}}, \quad q = -\frac{\tilde{B}_i}{\tilde{R}_u^{(i)} \cdot \mu_{R_u^{(i)}|B_u^{(i)}=1}}. \quad (2.47)
\end{aligned}$$

The PBN-Characteristic for FT scheduling of (2.47) does not differ qualitatively from the PBN-Characteristic for FR scheduling. In both cases, the number of users that can be supported by the cell under the conditions of the allocated resources is given.

Using (2.46) and (2.47), PBR- and PBN-Characteristic for FT scheduling are plotted in Figure 2.11(a) and Figure 2.11(b) for $N_i = 5$ users and user bit rate \tilde{R}_u of 100 kbit/s, respectively, and for the parameters of Table 2.1. The PBR-Characteristic relates the resource allocation in terms of transmit power or power ratio Γ_i , respectively, and the cell bandwidth B_i with the achievable user bit rate target $\tilde{R}_u^{(i)}$ for a given number of users, the PBN-Characteristic has the same meaning as the PBN-Characteristics from previous sections and is read the same way. Note, however, the difference in the achieved performance, compared to FR scheduling, which is due to the fact that users with low receive signal quality are allocated more bandwidth than users with high receive signal quality in order to achieve fairness in bit rate, which results in a lower overall cell performance.

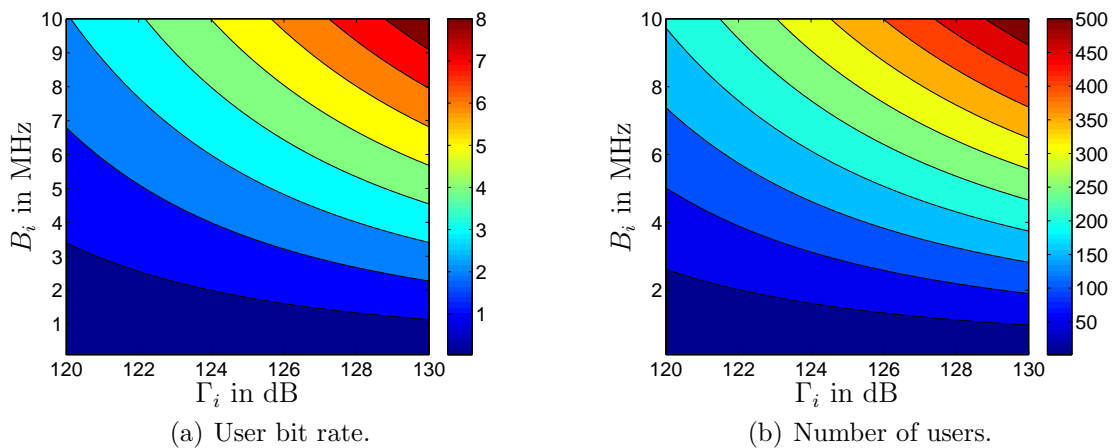


Figure 2.11. Achievable user bit rate target $\tilde{R}_u^{(i)}$ in Mbit/s and the number N_i of users that can be supported by the cell, both as a function of power ratio Γ_i and cell bandwidth B_i for uniform user distribution and FT scheduling. The achievable user bit rate target is shown for $N_i = 5$ users, the number of users is shown for a user bit rate \tilde{R}_u of 100 kbit/s .

2.4.7 Fractional Frequency Reuse

Cellular systems are attractive for terrestrial radio communication since they are able to provide high capacity due to the reuse of frequencies. At the same time, however, ICI increases with decreasing reuse distance, cf. Section 2.3. Thus, the increase of capacity by decreasing the reuse distance leads to increasing ICI in cellular radio networks. Fractional frequency reuse [KN96] has been developed in order to mitigate this effect. This section discusses the application of the cell-centric network model to systems using fractional frequency reuse designs and presents the required extensions of the model.

Fractional frequency reuse counteracts ICI at the cell borders by dividing each cell into several areas. Higher frequency reuse distances are used in areas that are closer to the cell borders while lower frequency reuse distances are applied in the cell center [Hal83, KN96, XW10]. Thus, the overall ICI is lowered. The application of the cell-centric network model to systems using fractional frequency reuse designs is achieved by treating each area of a cell as a separate cell. Throughout this section, a fractional frequency reuse design that uses two areas per cell, inner and outer area, is considered, but the approach is generally valid and can easily be adapted to designs using arbitrary numbers of areas per cell.

For the application of the cell-centric network model to fractional frequency reuse systems, the relative size of the inner area of cell i is termed $\rho_{\text{in},i}$. The relative size of the outer area of cell i is, consequently, given by $1 - \rho_{\text{in},i}$. The relative sizes of inner and outer area are applied to the cdf of the SINR of a single user to divide the users between inner and outer area, according to the idea of fractional frequency reuse to reduce ICI for users that suffer from high ICI. This allows the definition of a SINR threshold

$$\gamma_{\text{th}}^{(i)} = \{ \gamma \mid P(\gamma^{(i)} < \gamma) = 1 - \rho_{\text{in},i} \} \quad (2.48)$$

which determines if a user belongs to inner or outer area. With this threshold, the pdf of the SINR of the inner area can be determined as a conditional pdf [PP02] from the pdf of the SINR of the whole cell according to

$$\begin{aligned} f_{\gamma^{(i,\text{in})}}(\gamma^{(i,\text{in})}) &= f_{\gamma^{(i)}}(\gamma^{(i)} \mid \gamma^{(i)} > \gamma_{\text{th}}^{(i)}) \\ &= \frac{f_{\gamma^{(i)}}(\gamma^{(i)})}{\rho_{\text{in},i}}, \quad \gamma^{(i)} > \gamma_{\text{th}}^{(i)}. \end{aligned} \quad (2.49)$$

The same way, the pdf of the SINR of the outer area can be determined as a conditional pdf from the pdf of the SINR of the whole cell by

$$\begin{aligned} f_{\gamma^{(i,\text{out})}}(\gamma^{(i,\text{out})}) &= f_{\gamma^{(i)}}(\gamma^{(i)} \mid \gamma^{(i)} \leq \gamma_{\text{th}}^{(i)}) \\ &= \frac{f_{\gamma^{(i)}}(\gamma^{(i)})}{1 - \rho_{\text{in},i}}, \quad \gamma^{(i)} \leq \gamma_{\text{th},i}^{(i)}. \end{aligned} \quad (2.50)$$

The derivations from Section 2.4.2 can now be continued with the pdfs of (2.49) and (2.50), respectively, instead of the pdf $f_{\gamma^{(i)}}(\gamma^{(i)})$ of the SINR of the whole cell. Thus, inner and outer area of the cell can be treated as two individual cells in the cell-centric network model and PBR- and PBN-Characteristics can be determined for both areas separately as described in the previous sections. Note that the power ratios $\Gamma_{i,\text{in}}$ and $\Gamma_{i,\text{out}}$ of inner and outer area of cell i , respectively, may have different values, since different frequency reuse factors, different environmental conditions and different user distributions in general hold for inner and outer area.

Above presentation has been chosen because it directly relates to the idea of fractional frequency reuse to improve signal quality in areas that are exposed to high ICI. Alternatively, and more conveniently, the relative sizes of inner and outer area can be applied directly to the cdfs of achieved user bit rate $\mathbf{R}_u^{(i)}$ and required user bandwidth $\mathbf{B}_u^{(i)}$. Following the approach of above, the user bit rate threshold $R_{u,\text{th}}^{(i)}$ and user bandwidth threshold $B_{u,\text{th}}^{(i)}$ to determine if a user belongs to inner or outer area yield

$$\begin{aligned} R_{u,\text{th}}^{(i)} &= \left\{ R \mid P \left(R_u^{(i)} < R \right) = 1 - \rho_{\text{in},i} \right\} \\ B_{u,\text{th}}^{(i)} &= \left\{ B \mid P \left(B_u^{(i)} < B \right) = \rho_{\text{in},i} \right\} \end{aligned} \quad (2.51)$$

and the respective pdfs of the achieved user bit rate of inner and outer area are given by

$$\begin{aligned} f_{\mathbf{R}_u^{(i,\text{in})}} \left(R_u^{(i,\text{in})} \right) &= \frac{f_{\mathbf{R}_u^{(i)}} \left(R_u^{(i)} \right)}{\rho_{\text{in},i}}, \quad R_u^{(i)} > R_{u,\text{th}}^{(i)} \\ f_{\mathbf{R}_u^{(i,\text{out})}} \left(R_u^{(i,\text{out})} \right) &= \frac{f_{\mathbf{R}_u^{(i)}} \left(R_u^{(i)} \right)}{1 - \rho_{\text{in},i}}, \quad R_u^{(i)} \leq R_{u,\text{th}}^{(i)}, \end{aligned} \quad (2.52)$$

the pdfs of the bandwidth required by a user for inner and outer area yield

$$\begin{aligned} f_{\mathbf{B}_u^{(i,\text{in})}} \left(B_u^{(i,\text{in})} \right) &= \frac{f_{\mathbf{B}_u^{(i)}} \left(B_u^{(i)} \right)}{\rho_{\text{in},i}}, \quad B_u^{(i)} \leq B_{u,\text{th}}^{(i)} \\ f_{\mathbf{B}_u^{(i,\text{out})}} \left(B_u^{(i,\text{out})} \right) &= \frac{f_{\mathbf{B}_u^{(i)}} \left(B_u^{(i)} \right)}{1 - \rho_{\text{in},i}}, \quad B_u^{(i)} > B_{u,\text{th}}^{(i)}. \end{aligned} \quad (2.53)$$

With (2.52) and (2.53), the calculations to obtain the pdfs of achieved user bit rate and required user bandwidth do not have to be carried out for inner and outer area individually, as they would have to if the threshold for dividing the users between inner and outer area of (2.48) was applied to the pdf of the SINR, but only once for the whole cell.

2.4.8 Sources of Inaccuracies

The cell-centric network model is a complex model that combines several factors which influence the relation between resource allocation and cell performance. It reduces the number of variables and enables efficient treatment of a cellular network compared to user-centric models. However, the cell-level focus with the abstraction from individual users requires some far-reaching assumptions. This section recalls the leading assumptions and discusses if and how the assumptions may cause inaccuracies.

Section 2.4.2 makes the assumption in the derivation of the pdf of the SINR $\gamma_n^{(i)}$ that ICI is independent of the position within a cell. This assumption is necessary in order

to be able to continue the analytical derivation of the model but it is also simplifying and introduces inaccuracy. The inaccuracy introduced by this assumption depends on the distance of the considered cell to the source of interference. For the evaluation of the introduced inaccuracy, the scenario from Figure 2.2 with the parameters from Table 2.2 is applied. The average ICI power $\bar{P}_{1,i}$ is assumed to be independent of the

Table 2.2. Parameters for the investigation of the error introduced by the assumption of position independent ICI power.

| Parameter | Value |
|--|-------------------------------------|
| Number of cells | 7 |
| Number of users N_i | 5 |
| Height of the BSs | 32 m |
| Height of the UEs | 1.5 m |
| User position probability $p_{\mathbf{r},\varphi}^{(i)}(r, \varphi)$ | uniform |
| Carrier frequency | 1.9 GHz |
| Propagation model | 3GPP Urban Macro |
| Shadow fading variance σ_{sh}^2 | 8 dB |
| Transmit Power $P_{\text{tx},j}$ | 33 dBm |
| Noise PSD | -167 $\frac{\text{dBm}}{\text{Hz}}$ |
| Scheduling strategy | FT |
| User bit rate target $\tilde{R}_u^{(i)}$ | 100 kbit/s |
| Cell outage probability p_{cell} | 0.05 |

position and equal to the true value of the ICI power at the center of a cell. With $B_i^{(\text{emp})}$ the bandwidth that is required by the center cell obtained empirically using the MC approach of Section 2.4.2 and with $B_i^{(\text{ana})}$ the bandwidth that is required by the center cell obtained analytically using (2.45), the relative error e_{B_i} of the required cell bandwidth introduced by the assumption of position independent ICI power can be determined according to

$$e_{B_i} = \frac{B_i^{(\text{ana})}}{B_i^{(\text{emp})}} - 1. \quad (2.54)$$

Figure 2.12 shows the relative error e_{B_i} as a function of reuse distance D for different relations r between the reuse distance D and cell radius S , both as illustrated in Figure 2.2, defined by

$$r = \left(\frac{D}{\sqrt{3} \cdot S} \right)^2. \quad (2.55)$$

The Figure shows that using the analytic approach with the assumption of position independent ICI power, the required cell bandwidth is under estimated. The reason is that the average ICI power $\bar{P}_{1,i}$ is assumed to be equal to the true ICI power at the cell center, independent of the position. Since in the cell center, ICI is weaker than at the cell border, the required cell bandwidth is under estimated. Furthermore, it can be seen

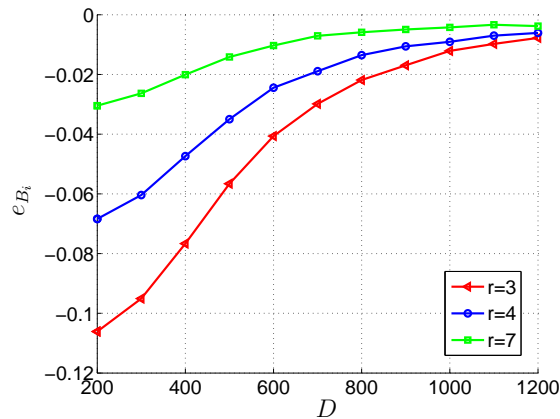


Figure 2.12. Relative error e_{B_i} of the bandwidth required by a cell due to the assumption of position independent ICI power as a function of reuse distance D .

from Figure 2.12 that if the distance between the interfering cells and the considered cell is large compared to the size of the cell, the introduced error is small. In practice, however, interferers are more likely to be located closely, since high system capacity requirements demand low reuse distances D , such that the assumption of position independent ICI power may lead to significant errors. Note that with FT scheduling, the users at the cell borders require more bandwidth than users in the cell center. At the same time, the assumption of position independent ICI power is most inaccurate for the users at the cell border. As a consequence, the error introduced by the assumption of position independent ICI power has more impact with FT scheduling than with FR scheduling, such that this analysis can be considered a worst case analysis.

Note, however, that the mostly analytical derivations of the previous sections are intended to introduce the cell-centric network model and to describe the intentions and the functioning of the model. For practical implementation, an approach based on measurements, which is presented in Section 2.5, is recommended. In this practical approach, ICI is contained in the measurements, such that the true ICI is considered. The assumption of position independent ICI is, thus, not required with the practical approach, such that the discussed inaccuracies are not relevant in practice.

The second central assumption is the independence of the individual users. In the previous sections, it has become clear that this property in principle exists. Depending on the scheduling strategy, however, the property may be lost. Especially channel adaptive scheduling approaches can be expected to establish some degree of dependence between the users of a cell. In these cases, the assumption of independent users has to be considered a simplification which potentially introduces inaccuracies to the cell-centric network model. In Section 2.4.5, it could be shown that for the case of PF scheduling

and uniform user distribution, the inaccuracies are of minor effect. This, however, cannot be generalized. Instead, the effect of this assumption has to be investigated separately for each scheduling strategy that destroys the property of independence among the users. This also holds for the approach for practical implementation of the model, as it will be presented in Section 2.5. Section 2.4.5 shows with Figures 2.7(a) and 2.7(b) how the effect of a scheduling strategy can be assessed, for example.

2.5 Implementation Aspects

Section 2.4 introduces the cell-centric network model using the theoretical approach. This approach is used since it enables a full description and easy understanding of the model. On the other hand, however, it requires an analytical description of the user distribution and establishes assumptions that impose barriers for practical implementation. This section presents approaches that focus specifically on the practical implementation of the cell-centric network model and do not require an analytical description of the user distribution. In particular, Section 2.5.1 presents an approach for the determination of the achieved cell throughput and the required cell bandwidth based on measurements. Section 2.5.2 discusses the determination of the average ICI power based on measurements.

2.5.1 Measurement Based Determination of Achieved Cell Throughput and Required Cell Bandwidth

The theoretic derivation of the cell-centric network model from Section 2.4 is based on an analytical description of the distribution of the users over the cell area. In practice, however, the true distribution will be hardly known and an analytical description is in general not possible. This section presets an alternative approach for the determination of achieved cell throughput and required cell bandwidth, that is not based on an analytical description of the user distribution and is, therefore, applicable in practice.

Recalling the derivations from Section 2.4.2, it becomes clear that the distribution of the users over the cell area in terms of position pdf $p_{\mathbf{r},\varphi}^{(i)}(r, \varphi)$ is required to obtain mean and variance of the achieved user bit rate $\mathbf{R}_u^{(i)}$ and the required user bandwidth $\mathbf{B}_u^{(i)}$, respectively, which are required to determine the achieved cell throughput \mathbf{R}_i and the required cell bandwidth \mathbf{B}_i , respectively, cf. (2.21), (2.22) and (2.23). An approach to become independent of the analytical user position pdf $p_{\mathbf{r},\varphi}^{(i)}(r, \varphi)$, is the approximation

of the mean values and variances of achieved user bit rate and required user bandwidth from SINR measurements taken by the users of the cell.

For this purpose, a set $\mathbb{S}_u^{(i)} = \{\gamma_k^{(i)'}\}$ of K SINR measurements $\gamma_k^{(i)'}$ of the users of cell i is collected at cell i . Since the SINR values have to be related to the transmit power of the cell and the overall interference situation, the value $\Gamma_{0,k}^{(i)'}$ of the power ratio at the time of measurement is determined by the BS of cell i and stored with the measurements. Using (2.2) and considering $\Gamma_{0,k}^{(i)'}$ and the current value Γ_i of the power ratio, the set can be transformed into a set $\mathbb{R}_u^{(i)} = \{R_{u,k}^{(i)'}\}$ of achieved user throughput values and a set $\mathbb{B}_u^{(i)} = \{B_{u,k}^{(i)'}\}$ of required user bandwidth values that are valid for the current interference situation according to

$$R_{u,k}^{(i)'} = 1 \cdot \log_2 \left(1 + \frac{\gamma_k^{(i)'}}{\Gamma_{0,k}^{(i)'}} \cdot \Gamma_i \right), \quad B_{u,k}^{(i)'} = \frac{1}{\log_2 \left(1 + \frac{\gamma_k^{(i)'}}{\Gamma_{0,k}^{(i)'}} \cdot \Gamma_i \right)}. \quad (2.56)$$

With sufficient measurements in set $\mathbb{S}_u^{(i)}$, which implies $K \gg N_i$, the distribution of the users over the cell area is well approximated by the set of measurements, and mean and variance of the achieved user bit rate $\mathbf{R}_u^{(i)}$ and the bandwidth $\mathbf{B}_u^{(i)}$ required by a user can be estimated based on the set of measurements. Since one Hertz of user bandwidth is considered in the determination of $\mathbb{R}_u^{(i)}$ and one bit/s is considered in the determination of $\mathbb{B}_u^{(i)}$, according to (2.56), estimates of mean $\mu_{B_u^{(i)}|R_u^{(i)}=1}$ and variance $\sigma_{B_u^{(i)}|R_u^{(i)}=1}^2$ of the user bandwidth required to achieve a user bit rate of one bit per second as well as mean $\mu_{R_u^{(i)}|B_u^{(i)}=1}$ and variance $\sigma_{R_u^{(i)}|B_u^{(i)}=1}^2$ of the user bit rate achieved for one hertz of user bandwidth, as they are used in (2.24) and (2.25), can be obtained by [KK98, PP02]

$$\begin{aligned} \hat{\mu}_{\{R_u^{(i)}, B_u^{(i)}\}} &= \frac{1}{K} \sum_{k=1}^K \{R_{u,k}^{(i)'}, B_{u,k}^{(i)'}\} \\ &= \hat{\mu}_{\{R_u^{(i)}|B_u^{(i)}=1, B_u^{(i)}|R_u^{(i)}=1\}} \\ \hat{\sigma}_{\{R_u^{(i)}, B_u^{(i)}\}}^2 &= \frac{1}{K-1} \sum_{k=1}^K \left(\{R_{u,k}^{(i)'}, B_{u,k}^{(i)'}\} - \hat{\mu}_{\{R_u^{(i)}, B_u^{(i)}\}} \right)^2 \cdot \\ &= \hat{\sigma}_{\{R_u^{(i)}|B_u^{(i)}=1, B_u^{(i)}|R_u^{(i)}=1\}}^2 \end{aligned} \quad (2.57)$$

The estimates from (2.57) can be used to determine the pdf of the achieved cell throughput \mathbf{R}_i and the pdf of the required cell bandwidth \mathbf{B}_i using (2.21) and (2.22) together with (2.24) and (2.25).

With (2.57), the proposed measurement based approach provides a way to use the cell-centric network model without an analytical description of the distribution of users over the cell area, which is an important prerequisite for the practical implementation and

application of the cell-centric network model. Note that furthermore, this approach regards the exact strength of the interference at each location of measurement in the cell, since the approach is based on SINR measurements at the locations of the mobile terminals. The assumption of location independent ICI is, thus, not required with the measurement based approach. Instead, the interference situation is considered in detail. The same way, the effect of the environment of the users on signal propagation is inherently considered in detail. Thus, the accuracy of the measurement based approach depends exclusively on the number K of measurements that are considered.

Note that the measurements should not be measurements of the instantaneous SINR but average values, such that fast fading is not considered. The reason is that fast fading is considered by the Scheduler Assumption of Section 2.4.1 and treated in the lower plane of the hierarchic concept for the coordination of automatic capacity optimization and scheduling of Section 2.2. Furthermore, the scheduling gain is considered this way if the effective average SINR, which includes the scheduling gain, is determined based on the user bandwidth and the achieved user bit rate.

2.5.2 Measurement Based Determination of the Average ICI Power

In the theoretic derivation of the cell-centric network model from Section 2.4, the average ICI power $\bar{P}_{I,i}$ is determined based on an analytical description of the distribution of the users over the cell area, cf. (2.14). Again, the true distribution will be hardly known in practice and an analytical description is in general not possible. This Section presents approaches for the estimation of the average ICI power that do not require an analytical description of the user distribution.

The easiest approach for the estimation of the average ICI power is to take measurements from a single location in the cell, preferably from the location of the BS. In this approach, changes in the interference are reflected by changes in the average ICI power, while at the same time, the measurements are obtainable with little effort concerning hardware and signaling. Thus, the approach can be implemented easily and at low cost. The drawback of this approach, however, is its inaccuracy, since the distribution of the interference over the cell area is not regarded. As a consequence, detected changes in the average ICI power can be of no relevance if no users are affected, while significant changes in the interference perceived by the users may not be detected by observing the average ICI power if it is measured at a single location. The same considerations apply concerning the height at which the measurements are taken. Measurements taken at

the height of the antenna, for example, enable to monitor ICI from several BSs. On the other hand, many users might not receive ICI from that many BSs, such that the collection of the measurements from a location close to the ground might be more adequate.

In order to alleviate this problem, the average ICI power $\bar{P}_{1,i}$ can be estimated as the average of interference measurements collected from the users. If the number of interference measurements is sufficiently large, the distribution of the users and the interference over the cell area is approximated and the average of the interference measurements approaches (2.14). Thus, the approach assures that the overall interference situation is regarded by the average ICI power. Depending on the mobile radio technology, suited measurement could be standardized, such that no additional signaling is needed. Otherwise, additional signaling effort would be caused since the interference measurements have to be transmitted from the UEs to the BSs. Even if the SINR measurements, which are collected for the approach of Section 2.5.1, are used to obtain interference measurements, additional signaling is involved since additional information, such as the total signal attenuation, for example, is required to determine the interference strength from SINR measurements.

Furthermore, mixtures between the two proposed approaches are possible. For example, interference measurements could be collected from several fixed locations in the cell. Depending on the number of measurement locations and their positions with respect to the user distribution, a trade-off between signaling effort and accuracy is made.

2.6 Areas of Application

This section introduces the application of the model and the use of PBR- and PBN-Characteristics in different areas of operation and management of cellular networks. The strength of the cell-centric network model is the abstraction from individual users since this greatly reduces the modeling effort. A consequence of this abstraction, however, is that individual users cannot be regarded by the model. The decision which user will not be served in case that the resources allocated to a cell are insufficient, for example, is not possible with the cell-centric network model. Note, however, that at the same time, user distribution, environment and interference situation are considered. The model, thus, provides a low complexity view of the network without neglecting the different QoS-requirements of the users, which makes the model and PBR- and

PBN-Characteristics attractive for all tasks that focus on the cells and their resource allocations.

In this context, an important application of the cell-centric network model and PBR- and PBN- Characteristics is the evaluation of the state of the cells of the network from the point of view of cell performance. This can be done by using (2.32) or (2.42), respectively, to determine the cell outage probability $p_{\text{out},i}$ of a cell i for the current resource allocation in terms of cell bandwidth B_i and cell transmit power or power ratio Γ_i and for the current operating conditions. Doing this with every cell allows to determine the operating state of the network and allows to locate areas where action has to be taken and to decide which optimization action has to be taken. Section 3.1 relies on this approach in order to establish self-organizing behavior of the proposed automatic capacity optimization approaches for SONs.

Additionally, not only the current resource allocation of a cell can be used in the cell-centric network model in order to determine the state of the cell. Also possible future resource allocations can be verified with respect to the performance of a cell in terms of cell throughput R_i or the number N_i of users that can be supported by the cell they are expected to lead to, or with respect to the outage probability $p_{\text{out},i}$ they are expected to lead to, for example. This way, PBR- and PBN-Characteristic can be used for finding resource allocations for the cells that lead to good performance of the network. PBR- and PBN-Characteristics are, therefore, also relevant in the optimization of cellular radio networks. Chapter 3 applies the cell-centric network model and PBR- and PBN-Characteristics for capacity optimization in cellular radio networks.

Chapter 3

Automatic Capacity Optimization

3.1 Introduction and Self-organizing Approach

Communication networks are set in a dynamically evolving environment where new users appear and existing users vanish. The behavior of the users concerning type of the requested services and usage of the services vary over time and lead to further dynamics. This is especially true for cellular mobile radio networks, in which due to the mobility of the UEs, significant variations in the distributions of the users amplify the addressed effects.

For reliable and efficient operation of cellular mobile radio networks and for the maximization of the network capacity, dynamic approaches, which allocate at all times and all places only as many resources to each of the cells of the network as currently required, are therefore needed. This section proposes approaches for automatic capacity optimization of cellular radio networks that aim for this goal. The approaches allocate resources to the cells such that the capacity of the network is maximized. The focus on the allocation of resources to the cells, instead of the users, allows to consider large areas of a network, or even complete networks, with relatively low complexity. The proposed approaches are, therefore, applicable in the upper plane of the hierarchic concept for coordination of automatic capacity optimization and scheduling of Section 2.2. The resources that are considered in the automatic capacity optimization approach of this chapter are cell bandwidth and cell transmit power, according to Section 1.2.

The cell-centric network model of Chapter 2 provides a model of a cellular radio network regarding the key factors that determine how many resources a cell needs, which makes the cell-centric network model well suited for automatic capacity optimization. As a consequence, the automatic capacity optimization approaches of this chapter use PBR- and PBN-Characteristics to define mathematical optimization problems that optimize cellular radio networks by means of adjusting the resource allocation of the cells. Such optimization problems can be solved automatically, and using the cell-centric network model for identifying the need for optimization action, as proposed in Section 2.6, an autonomous and self-organizing approach is established.

Furthermore, the coordination of the bandwidth allocations of different cells is an important aspect in order to control ICI and a key aspect for the implementation of

automatic capacity optimization approaches for SONs, according to Section 2.2. Coordination was neglected in the discussion of the cell-centric network model but has to be considered in the allocation of resources. Section 3.2 discusses this aspect and extends the current modeling to consider the coordination of the bandwidth allocations of the cells. Section 3.3 introduces the capacity optimization goals aimed for in this chapter and Section 3.4 discusses the resource allocation techniques considered for the automatic capacity optimization approaches with regard to establishing optimization problems for resource allocation. Section 3.5 investigates how the different resource allocation techniques achieve the concentration of capacity at locations of high capacity demand. Section 3.6 finally combines optimization goals and resource allocation techniques to obtain specific optimization problems for automatic capacity optimization. Parts of this work have been originally published by the author in [HKG09a,HKG09b].

Note that the cell bandwidth values that result from the automatic capacity optimization discussed in this chapter refer to the bandwidth that should be allocated to each of the cells in order to optimize the network capacity. In multi-carrier transmission schemes, however, bandwidth can be allocated only in discrete parts of one or several subcarriers. In this thesis, the allocation of specific frequencies or subcarriers to the cells is not considered and has to be carried out separately. Different approaches for the allocation of subcarriers can be found in the literature, such as in [AvK⁺01,HKG08] and references therein, for example.

Throughout this chapter, the transmit power allocation is usually represented by the power ratios Γ_i , since it simplifies expressions and links directly to the equations of the cell-centric network model, which are defined in dependence of the power ratio Γ_i . Furthermore, the power ratio Γ_i depends on the cell bandwidths and on the transmit powers, such that Γ_i is usually denoted as a function of either of them or both.

3.2 Coordination of Bandwidth Allocations

In the allocation of resources to the cells, the aspect of coordination of the bandwidth allocations of different cells is of great importance. With the hierarchic concept of Section 2.2, furthermore, the coordination of the bandwidth allocations determines if state of the art scheduling based approaches or new automatic capacity optimization approaches for SONs are considered. This section discusses the coordination of the bandwidth allocations and extends the modeling approach of this thesis to consider the coordination of bandwidth allocations.

In this thesis, the bandwidth allocation of two cells is referred to as being coordinated if the cells use orthogonal sets of frequencies. Using coordinated bandwidth allocations, ICI can be controlled. Regarding ICI and the interference relation between different cells, cellular radio networks can be described by a so-called interference coupling gain matrices \mathbf{G} that is defined using the average channel gain g_{ij} of (2.13) by

$$[\mathbf{G}]_{i,j} = g_{ij}. \quad (3.1)$$

Thus, matrix \mathbf{G} express how strong the influence of interference is between the cells. Applying a threshold T_{coup} to matrix \mathbf{G} , it can be used to identify cells that potentially interfere strongly, such that their bandwidth allocations need to be coordinated in order to mitigate ICI. Using \mathbf{G} and threshold T_{coup} , the binary coordination matrix \mathbf{C} , that identifies cell pairs that have to coordinate their bandwidth allocations, is defined according to

$$[\mathbf{C}]_{i,j} = \begin{cases} 1 & \text{if } [\mathbf{G}]_{i,j} > T_{\text{coup}} \\ 0 & \text{else} \end{cases}. \quad (3.2)$$

The effective interference coupling that exists between the cells considering the coordination of the bandwidth allocations is determined from coupling gain matrix \mathbf{G} and coordination matrix \mathbf{C} . With $\mathbf{1}_{N_c \times N_c}$ a matrix of dimension $N_c \times N_c$ with ones in every element, the effective interference coupling is given by matrix

$$[\mathbf{E}]_{i,j} = [\mathbf{G}]_{i,j} \cdot \left(\mathbf{1}_{N_c \times N_c} - [\mathbf{C}]_{i,j} \right). \quad (3.3)$$

For the approaches of this chapter, it is convenient to use the Neighborhood Group (NG) concept. In this concept, two cells i and j are defined to be neighbors if their interference coupling gain is above threshold T_{coup} , such that they have to coordinate their bandwidth allocations in order to mitigate ICI. With this definition, coordination matrix \mathbf{C} expresses the neighbor relations of all cells of a network. The NG is defined as a set $\{i_1, i_2, \dots\}$ of cells that are all mutual neighbors such that set \mathbb{G} of all NGs is defined by

$$\mathbb{G} = \left\{ \{i_1, i_2, \dots\} \mid [\mathbf{C}]_{i_l, i_m} = 1 \right\}, \quad l, m = 1, 2, \dots. \quad (3.4)$$

In the special case of a regular hexagonal scenario [ZK01], an alternate definition of the set \mathbb{G} of all NGs is possible. With reuse distance D and with $d(i_l, i_m)$ the distance between the BSs of cell i_l and cell i_m , the set \mathbb{G} of all NGs is defined by

$$\mathbb{G} = \left\{ \{i_1, i_2, \dots\} \mid d(i_l, i_m) < D \right\}, \quad l, m = 1, 2, \dots. \quad (3.5)$$

In any case, set \mathbb{G} can be expressed by the binary NG matrix \mathbf{N} , in which each row represents one NG and each column represents a cell of the network. The elements of the matrix are equal to one if the cell represented by the column is contained in the

NG represented by the row and zero otherwise. With N_{ng} the number of NGs, \mathbf{N} has dimensions $N_{\text{ng}} \times N_c$.

Note that the NG concept is also valid considering cells with more than one sector. In this case, each sector has to be considered separately and the NGs are formed by sectors with mutual neighbor relations.

3.3 Optimization Goals

The optimization of cellular radio networks can have different goals, as stated in Section 1.2. This section introduces specific capacity optimization goals since the focus of thesis is on capacity optimization, according to Section 1.2. In particular, Section 3.3.1 presents the optimization goal of the network throughput, Section 3.3.2 presents the optimization goal of the total number of users that can be supported by the network.

3.3.1 Network Throughput

With the cell throughput as it is given by (2.35) and as it can be determined by multiplying (2.46) with the number N_i of users of the cell, respectively, and with $\mathbf{b} = (B_1, B_2, \dots, B_{N_c})^T$ the vector of the cell bandwidths B_i and $\mathbf{\Gamma} = (\Gamma_1, \Gamma_2, \dots, \Gamma_{N_c})^T$ the vector of the power ratios Γ_i , the total network throughput is given by the sum of the cell throughputs of all cells according to

$$R_{\text{nw}}(\mathbf{b}, \mathbf{\Gamma}) = \sum_{i=1}^{N_c} \tilde{R}_i(\mathbf{b}, \mathbf{\Gamma}). \quad (3.6)$$

According to the cell-centric network model and to the definitions of the PBR-Characteristic, the cell throughput is a function of the cell bandwidths B_i and the transmit powers $P_{\text{tx},i}$. The network throughput is, thus, a function of the cell bandwidths and the transmit powers, too.

Using (3.6) as objective function without further constraints in a maximization problem favors cells that can exploit resources more efficiently than other cells. While this leads to high network throughput, low service quality may result in some cells. In order to assure minimum QoS requirements, a constraint concerning the average user bit rate $\bar{R}_u^{(i)}$ of (2.36) achieved by the cells according to

$$\bar{R}_u^{(i)}(\mathbf{b}, \mathbf{\Gamma}) \geq R_{u,\text{min}} \quad (3.7)$$

has to be introduced, which is also a function of the cell bandwidths and the transmit powers.

3.3.2 Total Number of Users

The capacity of a communication network can also be expressed in terms of the number of users that can be supported with a certain QoS. At first thought, the maximization of the number of users may seem irrelevant for the operation of a cellular mobile radio network since in practical operation of a cellular mobile radio network, the number of users in each cell is given externally by the distribution of the users. This may be true in conditions of low to medium load, in situations with high load, however, this optimization goal becomes relevant in order to avoid or limit the amount of users that cannot be supported.

The number of users that can be supported by a cell can be determined from the cell-centric network model using (2.38) and (2.47), respectively. The total number of users that can be supported by the whole network is given by the sum of the numbers of users of the cells according to

$$N_{\text{nw}}(\mathbf{b}, \mathbf{\Gamma}) = \sum_i^{N_c} N_i(\mathbf{b}, \mathbf{\Gamma}). \quad (3.8)$$

Also the total number of users that can be supported by the network is a function of the cell bandwidths and the transmit powers.

Using (3.8) without further constraints in a maximization problem leads to solutions that, again, favor cells which are able to support its users more efficiently than others. This causes a mismatch between the distribution of the users and the configuration of the network. In order to obtain a resource allocation tailored to the user distribution, a constraint that forces the solution to observe the user distribution is required. With $\rho_{\text{rel},i}$ the amount of users that request service from cell i relative to the total number of users, the constraint is given by

$$N_i(\mathbf{b}, \mathbf{\Gamma}) = \rho_{\text{rel},i} \cdot N_{\text{nw}}(\mathbf{b}, \mathbf{\Gamma}). \quad (3.9)$$

Note that no constraint concerning the observation of minimum QoS requirements is formulated explicitly. Instead, the minimum QoS requirement is considered implicitly by setting the average user bit rate $\bar{R}_u^{(i)}$ in (2.38) and the user bit rate target $\tilde{R}_u^{(i)}$ in (2.47) equal to the minimum QoS requirement $R_{u,\text{min}}$.

3.4 Resource Allocation Techniques

This section discusses the allocation of the resources cell bandwidth and transmit power for capacity optimization of cellular radio networks. Each of the resources has

its specific effects in capacity optimization and its individual feasibility requirements. Section 3.4.1 treats the allocation of cell bandwidth and all related aspects. The allocation of transmit power to the cells with its related aspects is treated in Section 3.4.2. Section 3.4.3 discusses different approaches for a joint allocation of transmit power and cell bandwidth.

3.4.1 Cell Bandwidth Allocation

This section treats the allocation of bandwidth to the cells. It is assumed that the transmit powers of the cells are given and fixed. The capacity optimization of the network is achieved exclusively by adjusting the cell bandwidths.

Cell bandwidth allocation is well suited for capacity optimization of a cellular radio network since more cell bandwidth enables a cell to provide more capacity. With coordinated bandwidth allocations, any bandwidth allocation to a cell has effect on the bandwidth allocations of nearby cells, due to the application of the frequency reuse concept, which requires to observe the reuse distance. Feasibility requirements in the allocation of cell bandwidth consider this and require that the cell bandwidth allocations are achievable with the total available system bandwidth at any place and any time. In this context, the coupling gain threshold T_{coup} and the frequency reuse distance D , respectively, play an important role since they significantly affect the flexibility in cell bandwidth allocation.

In order to be able to reliably express and observe feasibility requirements of the cell bandwidth allocations, the NG concept of Section 3.2 is used. Within each NG, no frequency can be reused, according to the definition of NGs of Section 3.2. Thus, the sum of the allocated cell bandwidths in each NG must not exceed the total system bandwidth B_{sys} such that every cell bandwidth allocation has to observe the constraint

$$\sum_{i \in \{i_1, i_2, \dots\}} B_i \leq B_{\text{sys}} \quad \forall \{i_1, i_2, \dots\} \in \mathbb{G}. \quad (3.10)$$

Using the NG matrix \mathbf{N} of Section 3.2, the constraint of (3.10) can be conveniently expressed by

$$\mathbf{N}\mathbf{b} \leq B_{\text{sys}}. \quad (3.11)$$

Since ICI increases with the cell bandwidth, according to (2.14), the power ratio decreases for larger cell bandwidths. As a consequence, there exists a relation between power ratio Γ_i and cell bandwidth B_i . The plot of this relation will in the following be

called a trace. Plotting traces of the cell bandwidth allocation leads to the light grey lines as shown in Figure 3.1. The traces relate the power ratio values and the corresponding cell bandwidth allocations. Figure 3.1 shows the traces of the cell bandwidth allocation for the scenario from Figure 2.2 with the parameters of Table 2.1 and for transmit powers $P_{\text{tx},i}$ of the center cell between 27 dBm and 39 dBm in steps of 3 dBm. It can be seen that the larger the transmit power of cell i , the more on the right is the trace. Consequently, the larger the transmit power of interfering cells, expressed by the average ICI power $\bar{P}_{\text{I},i}$ of cell i , the more on the left would be a trace. Note that the traces are plotted over a PBR-Characteristic and a PBN-Characteristic. The cell throughput values of the PBR-Characteristic and the values of number of users from the PBN-Characteristic that are below the traces are the performance achieved by the cell for the respective cell bandwidth allocation.

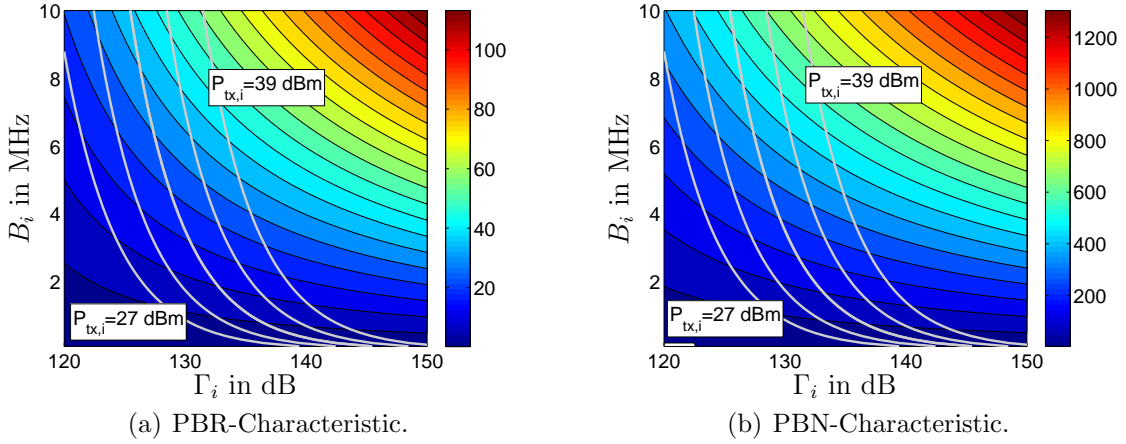


Figure 3.1. Relation between cell bandwidth B_i and the corresponding power ratio Γ_i plotted as light grey lines over a PBR-Characteristic and a PBN-Characteristic assuming PF scheduling. The different curves are valid for different cell transmit power strengths.

It is interesting to point out that the traces of Figure 3.1 fully illustrate the behavior of the cell bandwidth allocation. In particular the bandwidth allocations of other cells do not influence the traces since ICI strength is independent of the bandwidth of the interfering cells, according to (2.14).

3.4.2 Transmit Power Allocation

Also the transmit power can be used to adjust the capacity of a cell since according to (2.2), the receiver SINR $\gamma_n^{(i)}$ influences the capacity of a radio link. This section focuses on the capacity optimization of a cellular radio network by the allocation of

transmit power to the cells. Two different approaches are proposed. One directly allocates transmit power to the cells. The second approach first allocates power ratio values, which are subsequently used to determine the corresponding transmit powers of the cells. The cell bandwidth allocation is assumed to be given and fixed.

The separate consideration of transmit power by itself, however, is not meaningful in the allocation of transmit power. Instead, ICI has to be taken into account and the relation of transmit power to interference power has to be regarded. In the cell-centric network model, the power ratio Γ_i is an adequate figure of merit for this purpose. It takes at cell-level the meaning of the receiver SINR $\gamma_n^{(i)}$ concerning a single user. Thus, the cell transmit power allocation requires a constraint concerning the minimum acceptable power ratio $\Gamma_{\min,i}$ for each cell. Furthermore, the transmit power has to be limited to the maximum transmit power P_{\max} . With $\mathbf{\Gamma}_{\min} = (\Gamma_{\min,1}, \Gamma_{\min,2}, \dots, \Gamma_{N_c})^T$ the vector of the minimum power ratios $\Gamma_{\min,i}$ and with $\mathbf{p} = (P_{\text{tx},1}, P_{\text{tx},2}, \dots, P_{\text{tx},N_c})^T$ the vector of transmit power $P_{\text{tx},i}$ and using the definition of the power ratio of (2.10), the constraints required for transmit power allocation are given by

$$\begin{aligned} \mathbf{\Gamma}(\mathbf{b}, \mathbf{p}) &\geq \mathbf{\Gamma}_{\min} \\ \mathbf{p} &\leq P_{\max}. \end{aligned} \quad (3.12)$$

As an alternative to the immediate allocation of transmit power, it is also possible to allocate power ratios to the cells. The transmit powers can subsequently be determined from the power ratios. With $\mathbf{n} = (P_N, P_N, P_N, \dots)^T$ the $N_c \times 1$ vector of the receiver noise power, \mathbf{I}_{N_c} the identity matrix of size N_c with ones on its diagonal and zeros elsewhere and using (2.10) with the matrix formulation $\bar{\mathbf{P}}_{\mathbf{I}} = \text{diag}(\beta) \mathbf{E} \mathbf{p}$ of (2.14) and resolving it for \mathbf{p} , the transmit powers are determined by

$$\mathbf{p}(\mathbf{b}, \mathbf{\Gamma}) = (\mathbf{I}_{N_c} - \text{diag}(\mathbf{\Gamma}) \text{diag}(\beta) \mathbf{E})^{-1} \text{diag}(\mathbf{n}) \mathbf{\Gamma}. \quad (3.13)$$

Allocating power ratio values and determining the transmit powers in a second step is in particular attractive since it allows to exploit certain mathematical properties, as it will be shown below.

In the allocation of power ratios, however, the interdependencies between the cells are not considered immediately. Instead, ICI is taken into account only in the following step, the determination of transmit powers from the power ratio values. Infeasible power ratio allocations, however, result in negative transmit powers, which are not meaningful in practice. Therefore, the feasibility of the power ratio allocation has to be considered and assured in the allocation of power ratios.

For this purpose, a transmit power vector \mathbf{p} is called feasible if all its elements are non-negative. With spectral radius $\rho(\mathbf{X})$ of a square matrix \mathbf{X} , which is defined as the largest magnitude of the eigenvalues λ_l of \mathbf{X} according to [Var10]

$$\rho(\mathbf{X}) = \max_l \{|\lambda_l|\} , \quad (3.14)$$

this holds true for an expression of the structure of (3.13) if the vectors and matrices of the expression are non-negative and if

$$\rho(\text{diag}(\mathbf{\Gamma}) \text{diag}(\beta) \mathbf{E}) < 1 \quad (3.15)$$

holds [Var10,SWB06,SWB09]. Equation (3.15) and a maximum power constraint based on (3.13) are, thus, the constraints required in the allocation of power ratios.

Plotting the traces of transmit power allocation and power ratio allocation over a PBR- or a PBN-Characteristic results in straight horizontal lines that run in parallel to the Γ_i -axis. Due to the feasibility requirement of (3.15), the traces stop at certain power ratios, depending on the cell bandwidth of cell i and on the transmit powers of the interfering cells. Interestingly, the endpoints of the traces of transmit power allocation and power ratio allocation are given by the traces of cell bandwidth allocation of Figure 3.1 since the points on the traces of cell bandwidth allocation represent the maximum Γ_i that is achievable for the cell bandwidth B_i with respect to the resource allocations of the interfering cells. Thus, the traces of the cell bandwidth allocation mark the feasible region for transmit power allocation and power ratio allocation.

3.4.3 Joint Power and Bandwidth Allocation

The generalization of transmit power allocation and cell bandwidth allocation is the joint allocation of both, cell bandwidth and transmit power. This is in principle achievable by combining the constraints of Section 3.4.1 and Section 3.4.2 in a single optimization problem with both, cell bandwidths \mathbf{b} and transmit powers \mathbf{p} or power ratios $\mathbf{\Gamma}$, respectively, as optimization variables. In the scope of algorithm development, however, the simple combination of the two previous allocation techniques result in very complex optimization problems, that may be impossible to transform into exact and efficient algorithms. As a consequence, this section proposes two alternative approaches that both allocate transmit power and cell bandwidth jointly but at the same time allow efficient algorithm development, as it will be shown in Section 4.2.5.

The idea behind the approaches is to avoid implementation complexity by keeping certain parameters constant. The first approach requires the definition of a fixed power

ratio $\tilde{\Gamma}_i$ for each cell. Power ratio $\tilde{\Gamma}_i$ is considered as a target that has to be achieved by the resource allocation, such that this power ratio target is considered as a constraint to the resource allocation yielding

$$\Gamma_i = \tilde{\Gamma}_i. \quad (3.16)$$

The joint resource allocation is carried out by allocating cell bandwidths to the cells. Due to the fixed power ratios, the cell bandwidths B_i implicitly result in a certain transmit power allocation which is determined using (3.13). Due to the variable cell bandwidths, however, the feasibility of the fixed power ratio targets has to be observed in the optimization problem and the constraint of (3.15) has to be regarded. Furthermore, the total system bandwidth has to be observed using the constraint of (3.11) and the transmit power has to yield a maximum value, which can be assured by introducing a maximum power constraint based on (3.13).

Plotting the traces of the joint resource allocation with fixed power ratios Γ_i over a PBR- or a PBN-Characteristic results in straight vertical lines running in parallel to the B_i -axis. As for transmit power and power ratio allocation, the feasibility constraint of (3.15) terminates the traces, such that as before, the endpoints of the traces of the joint resource allocation with fixed power ratios $\tilde{\Gamma}_i$ are given by the traces of the cell bandwidth allocation as in Figure 3.1, for example.

The second approach for the joint allocation of cell bandwidth and transmit power assumes a constant transmit power per subcarrier or, more general, a constant transmit power spectral density (PSD)

$$\rho_{\text{tx},i} = \frac{P_{\text{tx},i}}{B_i}. \quad (3.17)$$

Joint resource allocation is carried out by assuming a fixed PSD target $\tilde{\rho}_{\text{tx},i}$ and allocating cell bandwidths. The transmit power allocation results from the cell bandwidth allocation according to

$$P_{\text{tx},i} = \tilde{\rho}_{\text{tx},i} \cdot B_i. \quad (3.18)$$

The allocation is feasible if the constraint on the allocated cell bandwidths of (3.11) is observed and if the required transmit power resulting from (3.18) does not exceed the maximum transmit power P_{max} yielding

$$P_{\text{tx},i} \leq P_{\text{max}}. \quad (3.19)$$

Note that the system modeling has to be modified with this approach. Since the transmit power is no longer independent of the cell bandwidth when specifying PSDs instead of transmit powers, ICI experienced in a cell is no longer independent of the

bandwidth allocation of other cells. Substituting (2.14) in (2.10) and considering (3.17) resolved for $P_{\text{tx},i}$ in the both equations yields

$$\Gamma_i = \frac{\rho_{\text{tx},i} \cdot B_i}{\sum_{i \neq j} \rho_{\text{tx},j} \cdot B_j \cdot \beta_i \cdot g_{ij} + P_{\text{N}}} \quad (3.20)$$

and with the definition of β_i from (2.12)

$$\Gamma_i = \frac{\rho_{\text{tx},i}}{\sum_{i \neq j} \rho_{\text{tx},j} \cdot \frac{B_j}{B_{\text{sys}}} \cdot g_{ij} + \frac{P_{\text{N}}}{B_i}} \quad (3.21)$$

follows. It can be seen from (3.21) that all transmit powers in (2.10) turn into their PSDs in (3.21). This also holds for the average interference power $\bar{P}_{\text{I},i}$, which turns into PSD $\bar{\rho}_{\text{I},i} = \sum_{i \neq j} \rho_{\text{tx},j} \cdot \beta_j \cdot g_{ij}$, considering (2.12). Note that $\bar{\rho}_{\text{I},i}$ is defined using the relative cell bandwidth β_j of the interfering cell. As a consequence, the specification of PSDs instead of transmit powers requires to generally work with PSDs instead of transmit powers in the cell-centric network model. Furthermore, the relative cell bandwidth of the interfering cell has to be used instead of the relative cell bandwidth of the considered cell in the determination of ICI power, according to (3.21).

3.5 Principles of Operation of Capacity Optimization

For the further discussion and for the interpretation of performance results, a deeper understanding of how the different resource allocation techniques achieve to shift capacity and to concentrate capacity at locations of higher capacity demands is fundamental. This section discusses the principles of operation of capacity optimization of each of the resource allocation techniques and draws conclusions concerning the importance of coordination of the bandwidth allocations for each of the resource allocation techniques.

The allocation of resources changes the capacity of a cellular network by two different effects. One is controlling and adjusting interference, which enables to increase user SINR in cells with high capacity demand and to decrease user SINR in cells with low capacity demand. User throughput changes with user SINR, such that this mechanism is capable of shifting and concentrating capacity. It comes into effect especially in the allocation of transmit power and works with coordinated bandwidth allocation as well as with uncoordinated bandwidth allocations.

For the allocation of cell bandwidth, which assumes a fixed transmit power allocation, this mechanism does not apply since ICI increases with allocated cell bandwidth, according to (2.14). Thus, a cell that uses more bandwidth to be able to provide more capacity has to accept higher ICI. In the case of cell bandwidth allocation, capacity can, therefore, be shifted only if a lightly loaded cell leaves bandwidth to a heavily loaded cell. This is the second mechanism that is capable of shifting and concentrating capacity and it requires the coordination of the bandwidth allocations, otherwise a leaving of cell bandwidth by one cell to another cell is not possible. As a consequence, the allocation of cell bandwidth is applicable for network throughput maximization in inhomogeneous capacity demand scenarios only with coordinated bandwidth allocations.

Similar considerations apply for the joint resource allocation techniques. Assuming fixed transmit PSD, ICI in a cell depends on the cell bandwidth of the interfering cells, according to Section 3.4.3, and the first mechanism comes into effect, leading to more cell bandwidth and higher user SINR in cells with high capacity demand. Joint resource allocation with fixed PSD, therefore, works with coordinated as well as with uncoordinated bandwidth allocations. Concerning the joint resource allocation with fixed power ratios, a situation similar to the situation of the allocation of cell bandwidth applies since due to the fixed power ratios, capacity can be shifted only by shifting cell bandwidth from lightly loaded cells to heavily loaded cells, with requires coordinated bandwidth allocations. As a consequence, also the joint resource allocation technique with fixed power ratios in connection with uncoordinated bandwidth allocations is not applicable for network throughput maximization.

Another important aspect concerning the principles of operation of the different resource allocation techniques is that the resource allocation techniques that work with the adaptation of transmit power or user SINR, respectively, are resource allocation techniques that affect larger areas in the concentration of capacity at a certain location. More illustratively, it can be said that they draw capacity from a larger area to concentrate it at one point. In contrast to that, resource allocation techniques that rely on the shifting of cell bandwidth only influence the neighbors, according to the definition of neighbored cells from Section 3.2, of a cell. These resource allocation techniques are, consequently, limited to a few closely located cells to draw capacity from and affect only a small area of the network.

3.6 Optimization Problems

In Section 3.3, optimization goals with the respective objective functions and required constraints are discussed. Section 3.4 introduces different resource allocation techniques to achieve the optimization goals and discusses feasibility requirements and resulting constraints. This section combines optimization goals and resource allocation techniques to obtain specific optimization problems for the capacity optimization of cellular radio networks.

The optimization problems are built by combining the objective function and its constraint from the optimization goals of Section 3.3 with the constraints of the resource allocation techniques of Section 3.4. The general definition of objective functions and constraints as functions of the cell bandwidth and the transmit powers are adapted for each optimization problem to reflect only the relevant dependencies. Tables 3.1 and 3.2 list the optimization problems, detailed discussion of the optimization goals and the resource allocation techniques can be found in Sections 3.3 and 3.4.

Furthermore, each of the optimization problems can in principle be carried out with or without coordination of the bandwidth allocations such that either state of the art scheduling based approaches or new automatic capacity optimization approaches for SONs are considered, cf. Section 2.2. According to the considerations on the principles of operation of the different resource allocation techniques of Section 3.5, however, the network throughput optimization approaches that allocate cell bandwidth and the network throughput optimizing approach with fixed power ratios Γ_i are not applicable with uncoordinated bandwidth allocations.

Table 3.1. Optimization problems for capacity optimization, part 1.

| Resource allocation technique | Optimization goal | |
|-------------------------------|---|--|
| | Network throughput | Number of users |
| Cell bandwidth allocation | $\begin{aligned} \mathbf{b}^* &= \arg \max_{\mathbf{b}} \{R_{\text{nw}}(\mathbf{b}, \mathbf{\Gamma}(\mathbf{b}))\} \\ \text{s.t. } &\bar{R}_{\text{u}}^{(i)}(\mathbf{b}, \mathbf{\Gamma}(\mathbf{b})) \geq R_{\text{u},\text{min}} \\ &\mathbf{N}\mathbf{b} \leq B_{\text{sys}} \end{aligned} \quad (3.22)$ | $\begin{aligned} \mathbf{b}^* &= \arg \max_{\mathbf{b}} \{N_{\text{nw}}(\mathbf{b}, \mathbf{\Gamma}(\mathbf{b}))\} \\ \text{s.t. } &N_i(\mathbf{b}, \mathbf{\Gamma}(\mathbf{b})) = \rho_{\text{rel},i} \cdot N_{\text{nw}}(\mathbf{b}, \mathbf{\Gamma}(\mathbf{b})) \\ &\mathbf{N}\mathbf{b} \leq B_{\text{sys}} \end{aligned} \quad (3.23)$ |
| Transmit power allocation | $\begin{aligned} \mathbf{\Gamma}^* &= \arg \max_{\mathbf{\Gamma}} \{R_{\text{nw}}(\mathbf{\Gamma})\} \\ \text{s.t. } &\bar{R}_{\text{u}}^{(i)}(\mathbf{\Gamma}) \geq R_{\text{u},\text{min}} \\ &\rho(\text{diag}(\mathbf{\Gamma}) \text{diag}(\beta) \mathbf{E}) < 1 \\ &\mathbf{p}(\mathbf{b}, \mathbf{\Gamma}) \leq P_{\text{max}} \end{aligned} \quad (3.24)$ $\mathbf{p}^* = (\mathbf{I}_{N_c} - \text{diag}(\mathbf{\Gamma}^*) \text{diag}(\beta) \mathbf{E})^{-1} \text{diag}(\mathbf{n}) \mathbf{\Gamma}^*$ | $\begin{aligned} \mathbf{\Gamma}^* &= \arg \max_{\mathbf{\Gamma}} \{N_{\text{nw}}(\mathbf{\Gamma})\} \\ \text{s.t. } &N_i(\mathbf{\Gamma}) = \rho_{\text{rel},i} \cdot N_{\text{nw}}(\mathbf{\Gamma}) \\ &\rho(\text{diag}(\mathbf{\Gamma}) \text{diag}(\beta) \mathbf{E}) < 1 \\ &\mathbf{p}(\mathbf{b}, \mathbf{\Gamma}) \leq P_{\text{max}} \end{aligned} \quad (3.25)$ $\mathbf{p}^* = (\mathbf{I}_{N_c} - \text{diag}(\mathbf{\Gamma}^*) \text{diag}(\beta) \mathbf{E})^{-1} \text{diag}(\mathbf{n}) \mathbf{\Gamma}^*$ |

Table 3.2. Optimization problems for capacity optimization, part 2.

| Resource allocation technique | Optimization goal | |
|---|---|---|
| | Network throughput | Number of users |
| Joint resource allocation with fixed power ratios Γ_i | $ \begin{aligned} \mathbf{b}^* &= \arg \max_{\mathbf{b}} \{R_{\text{nw}}(\mathbf{b})\} \\ \text{s.t. } \bar{R}_{\text{u}}^{(i)}(\mathbf{b}) &\geq R_{\text{u},\min} \\ \mathbf{N}\mathbf{b} &\leq B_{\text{sys}} \\ \rho \left(\text{diag}(\tilde{\mathbf{\Gamma}}) \text{diag}(\beta) \mathbf{E} \right) &< 1 \\ \mathbf{p}(\mathbf{b}, \tilde{\mathbf{\Gamma}}) &\leq P_{\max} \end{aligned} \tag{3.26} $ $ \mathbf{p}^* = \left(\mathbf{I}_{N_c} - \text{diag}(\tilde{\mathbf{\Gamma}}) \text{diag}(\beta^*) \mathbf{E} \right)^{-1} \text{diag}(\mathbf{n}) \tilde{\mathbf{\Gamma}} $ | $ \begin{aligned} \mathbf{b}^* &= \arg \max_{\mathbf{b}} \{N_{\text{nw}}(\mathbf{b})\} \\ \text{s.t. } N_i(\mathbf{b}) &= \rho_{\text{rel},i} \cdot N_{\text{nw}}(\mathbf{b}) \\ \mathbf{N}\mathbf{b} &\leq B_{\text{sys}} \\ \rho \left(\text{diag}(\tilde{\mathbf{\Gamma}}) \text{diag}(\beta) \mathbf{E} \right) &< 1 \\ \mathbf{p}(\mathbf{b}, \tilde{\mathbf{\Gamma}}) &\leq P_{\max} \end{aligned} \tag{3.27} $ $ \mathbf{p}^* = \left(\mathbf{I}_{N_c} - \text{diag}(\tilde{\mathbf{\Gamma}}) \text{diag}(\beta^*) \mathbf{E} \right)^{-1} \text{diag}(\mathbf{n}) \tilde{\mathbf{\Gamma}} $ |
| Joint resource allocation with fixed transmit PSDs $\rho_{\text{tx},i}$ | $ \begin{aligned} \mathbf{b}^* &= \arg \max_{\mathbf{b}} \{R_{\text{nw}}(\mathbf{b}, \mathbf{\Gamma}(\mathbf{b}))\} \\ \text{s.t. } \bar{R}_{\text{u}}^{(i)}(\mathbf{b}, \mathbf{\Gamma}(\mathbf{b})) &\geq R_{\text{u},\min} \\ \mathbf{N}\mathbf{b} &\leq B_{\text{sys}} \\ \tilde{\rho}_{\text{tx},i} \cdot B_i &\leq P_{\max} \end{aligned} \tag{3.28} $ $ P_{\text{tx},i}^* = \tilde{\rho}_{\text{tx},i} \cdot B_i^* $ | $ \begin{aligned} \mathbf{b}^* &= \arg \max_{\mathbf{b}} \{N_{\text{nw}}(\mathbf{b}, \mathbf{\Gamma}(\mathbf{b}))\} \\ \text{s.t. } N_i(\mathbf{b}, \mathbf{\Gamma}(\mathbf{b})) &= \rho_{\text{rel},i} \cdot N_{\text{nw}}(\mathbf{b}, \mathbf{\Gamma}(\mathbf{b})) \\ \mathbf{N}\mathbf{b} &\leq B_{\text{sys}} \\ \tilde{\rho}_{\text{tx},i} \cdot B_i &\leq P_{\max} \end{aligned} $ $ P_{\text{tx},i}^* = \tilde{\rho}_{\text{tx},i} \cdot B_i^* \tag{3.29} $ |

Chapter 4

Algorithms for Automatic Capacity Optimization

4.1 Introduction

An important aspect in the field of mathematical optimization is the solution of the optimization problems. Also in the scope of this thesis, algorithms that solve the optimization problems for capacity optimization derived in Chapter 3 have to be developed.

Different types of algorithms concerning the implementation of the algorithms exist. Central algorithms are carried out by a single instance and need to have all data available at that instance. Central approaches are, therefore, of interest for simulation, for example. In practical cases, however, a central solving approach may be prohibitive due to reasons of complexity or robustness or due to the structure or architecture of the considered system. In these cases, a distributed implementation, in which the solution of the problem is not found by a single instance but by several instances jointly, is of interest. Also for cellular radio networks, which are highly distributed systems, a distributed implementation of self-organizing functionality is very attractive.

This chapter focuses on both of the above addressed aspects of algorithm development. Section 4.2 presents central solving approaches that are relevant for simulation and analysis. Section 4.3 derives distributed implementations that do not require a central instance and that are relevant for practical implementation. Section 4.4 proposes a concept that makes the application of both, central and distributed solving approaches, possible and increases the robustness of networks using self-organizing functionality.

4.2 Central Algorithms

4.2.1 Introduction

Central solving approaches for optimization problems in cellular radio networks are relevant especially for analysis purposes since they can be used conveniently in simulations

and to provide performance references. Depending on the properties of optimization problems, different approaches for the solution of mathematical optimization problems exist. For continue valued problems, such as those of Section 3.6, convex optimization is very attractive since for convex optimization problems, the optimum solution can be identified reliably and efficiently [BV08].

In order to solve the optimization problems established in Chapter 3 with convex solving techniques, the problems have to be convex in a mathematical sense. To this end, each of the optimization problems is discussed in this section with respect to convexity. Where necessary, reformulations to equivalent optimization problems or convex approximations of the optimization problems are introduced. For this purpose, Section 4.2.2 introduces convex optimization and the mathematical properties of convex optimization problems. Concerning the discussion of the optimization problems, reasoning and reformulations are similar for the optimization goals of network throughput maximization and maximization of the number of users that can be supported, but different for the different resource allocation techniques. The remainder of this section is, therefore, structured according to the resource allocation techniques, such that Section 4.2.3 treats the cell bandwidth allocation, Section 4.2.4 discusses the transmit power allocation and Section 4.2.5 considers the joint allocation of cell bandwidth and transmit power. Note that in some cases in the discussion, a purely mathematical proof of convexity is very complicated due to the complex derivation and the non-linearities of the cell-centric network model. In these cases, more illustrative descriptions are employed to show convexity. The discussions of this section are made using the example of FR scheduling but the results are applicable also to other scheduling strategies.

4.2.2 Convex Optimization

This section introduces convex optimization and presents the corresponding mathematical properties. In particular, the mathematical properties that are required are convexity of the objective function and convexity of the domain of the optimization problem, which is the set of valid solutions defined by the constraints [BV08].

Concerning a function $f(x)$, it is said to be convex if

$$f(\theta x_1 + (1 - \theta)x_2) \leq \theta f(x_1) + (1 - \theta)f(x_2), \quad 0 \leq \theta \leq 1, \quad (4.1)$$

holds [BV08], which includes linear relations. If $f(x)$ is twice differentiable, the equivalent second order condition is given by [BV08]

$$\nabla^2 f(x) \geq 0. \quad (4.2)$$

Concerning a set \mathbb{C} , convexity requires that all points on a line between any two points $x_1, x_2 \in \mathbb{C}$ have to be part of set \mathbb{C} , as expressed by

$$\theta x_1 + (1 - \theta) x_2 \in \mathbb{C}, \quad 0 \leq \theta \leq 1. \quad (4.3)$$

Since the domain of the optimization problem is a set defined by the constraints of the optimization problem, the set is convex if all inequality constraints of the optimization problem are convex functions. Thus, the inequality constraints of a convex optimization problem have to fulfill (4.1). Equality constraints have to be affine sets, which means that all points on a line through two points $x_1, x_2 \in \mathbb{C}$ have to be part of set \mathbb{C} yielding [BV08]

$$\theta x_1 + (1 - \theta) x_2 \in \mathbb{C}, \quad \theta \in \mathbb{R}. \quad (4.4)$$

Optimization problems fulfilling these requirements and having inequality constraints that are bounded above can be minimized using convex optimization techniques. If maximization is desired, the negative objective function can be minimized. Note, however, that in this case, the negative objective function has to be convex, which means that the objective function is said to be concave. For the exact definition of concavity, the inequality signs in (4.1) and (4.2) have to be reversed. Figure 4.1 shows an illustration of a convex and a concave function.

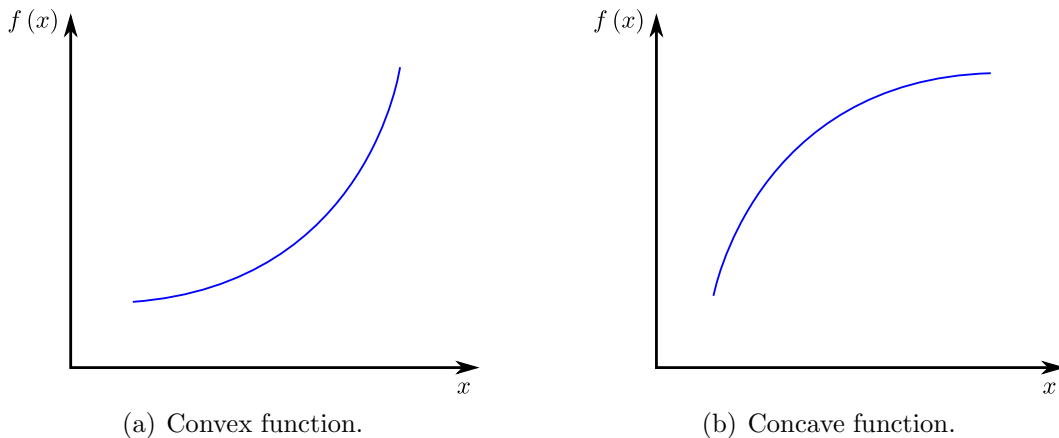


Figure 4.1. Illustration of a convex and a concave function.

Another important property in the context of convex optimization is log-convexity. A function is called log-convex if the logarithm of the function is convex [BV08]. Log-convexity is of great relevance since it provides a convenient way in the transformation of optimization problems to equivalent convex optimization problems and since it increases the number of relations and functions that can be used in convex problems.

4.2.3 Cell Bandwidth Allocation

This section discusses the convexity of the cell bandwidth allocation capacity optimization problems of (3.22) and (3.23). Concerning the constraint on the NG sum bandwidth in the allocation of cell bandwidth of (3.11), the discussion is easy since it is linear and, thus, convex, according to Section 4.2.2. Concerning the other constraint and the objective function, the discussion is more complex since the average ICI power $\bar{P}_{1,i}$ depends on the cell bandwidth B_i , according to (2.14), such that the relation between cell bandwidth B_i and cell throughput \tilde{R}_i from (2.35) as well as the relation between cell bandwidth B_i and number N_i of users that can be supported by a cell from (2.38) are non-linear.

For the discussion of convexity, it is pointed out that network throughput and total number of users are linear combinations of cell throughput and the number of users that can be supported by a cell, respectively. Thus, network throughput and total number of users are convex functions if cell throughput and number of users supported by a cell are convex functions [BV08]. The detailed mathematical proof of convexity of cell throughput and the number of users that can be supported by a cell, however, is complicated due to the complex derivation and construction of the corresponding relations. As a consequence, a more illustrative approach is taken to identify convexity. For this, the following considerations are made. As stated above, the relation between cell bandwidth B_i and cell throughput \tilde{R}_i is linear. With increasing cell bandwidth, however, ICI increases, according to (2.14), which decreases the cell throughput. The decrease in cell throughput monotonically grows with higher ICI power and, therefore, with increasing cell bandwidth. As a consequence, the relation between cell bandwidth B_i and cell throughput \tilde{R}_i is bent downwards, such that the second derivative of the cell throughput with respect to the cell bandwidth is smaller than zero, which fulfills the definition of a concave function.

Thus, the network throughput is a concave function of the cell bandwidth since it is the sum of several concave functions of the cell bandwidth. For the same reason, the first constraint of (3.22), which assures that minimum QoS levels are observed, is concave, too. Multiplying with minus one and moving the minimum user bit rate $R_{u,\min}$ to the left side yields

$$R_{u,\min} - \bar{R}_u^{(i)}(\mathbf{b}, \mathbf{\Gamma}(\mathbf{b})) \leq 0, \quad (4.5)$$

which is a convex constraint as required according to Section 4.2.2. The cell bandwidth allocating network throughput maximization as stated (3.22) can, therefore, be solved using convex optimization techniques.

In order to verify above reasoning, Figure 4.2(a) shows the traces of cell bandwidth allocation from Figure 3.1(a) as a representation of the relation between cell bandwidth and cell throughput for a single cell and for the parameters of Table 2.1 and for different transmit powers $P_{\text{tx},i}$ of the center cell between 27 dBm and 39 dBm in steps of 3 dBm. In this representation, the curves are called BR-Characteristics. The figure is obtained by relating the cell bandwidth values with the cell throughput values that are lying below the traces in Figure 3.1(a). It can be seen that the cell throughput is a concave function of the cell bandwidth.

The considerations concerning the increasing ICI for increasing cell bandwidth also apply for the number of users that can be supported by a cell. The relation between number of users that can be supported and allocated cell bandwidth additionally has a component that increases more than proportionally since the cell bandwidth required to support a certain number of users increases in one of the summands of (2.45) only with the square root of the number of users, which is less than proportional. This effect bends the relation between cell bandwidth and number of users to give it a convex form, while the ICI power depending of the cell bandwidth bends the relation into a concave form. The concave effect is stronger the more power is allocated to interfering cells and the larger the average channel gain g_{ij} is. The determination which effect prevails depends on the exact parameters. Due to the square root relation and assuming target cell probabilities \tilde{p}_{out} with practical relevance, however, the convex influence is very small such that the concave effect can be expected to prevail.

Figure 4.2(b) shows the BN-Characteristics obtained from the traces of cell bandwidth allocation over the PBN-Characteristic of Figure 3.1(b) and, thus, for the scenario from Figure 2.2 with the parameters of Table 2.1 and for different transmit powers $P_{\text{tx},i}$ of the center cell between 27 dBm and 39 dBm in steps of 3 dBm. It can be seen that in the considered cases, the concave effect clearly prevails, making convex optimization techniques suitable for the cell bandwidth allocating maximization of the total number of users.

4.2.4 Transmit Power Allocation

The transmit power allocating capacity optimization problems of (3.24) and (3.25) cannot be directly shown to be a convex optimization problem due to the feasibility constraint of the power ratio allocation of (3.15) and the maximum power constraint based on (3.13). In order to be able to apply convex techniques, the problem has to be transformed to an equivalent problem. This section presents the derivation of a convex equivalent of the optimization problem.

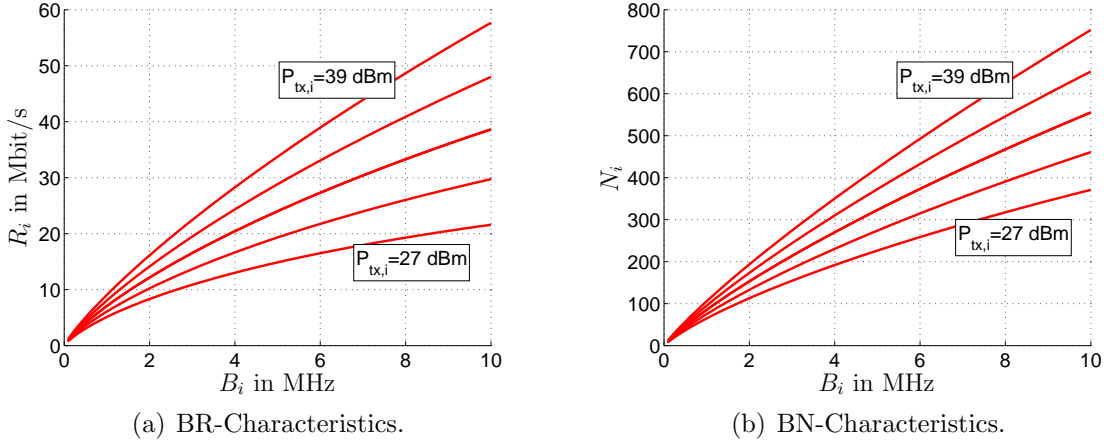


Figure 4.2. BR- and BN-Characteristics for PF scheduling, obtained from the traces of the cell bandwidth allocation of Figure 3.1.

For the equivalent problem, it is considered that the spectral radius $\rho(\mathbf{X}(\omega))$ of a matrix $\mathbf{X}(\omega)$ is log-convex if the elements of $\mathbf{X}(\omega)$ are log-convex functions in ω , according to [SWB06, SWB09]. With this in mind, the modified power ratio $\check{\Gamma}_i$ is introduced and defined by

$$\check{\Gamma}_i = \ln(\Gamma_i). \quad (4.6)$$

Rewriting the power ratio feasibility constraint of (3.15) using the modified power ratio yields

$$\rho\left(\text{diag}\left(e^{\check{\Gamma}}\right) \text{diag}(\beta) \mathbf{E}\right) < 1 \quad (4.7)$$

which is log-convex since $e^{\check{\Gamma}}$ is a log-convex function in $\check{\Gamma}$. Furthermore, it can be shown that the transmit power as defined in (3.13) is also log-convex under these conditions [SWB06, SWB09]. Thus, the modified power ratio conveniently enables the convex formulation (4.7) of the power ratio feasibility constraint and a convex formulation of the maximum power constraint of (3.12).

The introduction of the modified power ratio requires the reformulation of the transmit power allocating capacity optimization problems of (3.24) and (3.25) such that the modified power ratio $\check{\Gamma}_i$ is the optimization variable. For the discussion of convexity of objective function and QoS constraint of the transformed network throughput maximization problem, a strictly mathematical way of showing convexity is not easily available due to the complex construction of the cell-centric network model. A different approach is, therefore, taken. For this, (2.11) is used with (4.6) resolved for the modified power ratio $\check{\Gamma}_i$ in (2.2), which yields

$$R_{u,n}^{(i)} = B_{u,n}^{(i)} \cdot \log_2\left(1 + \psi_n^{(i)} \cdot e^{\check{\Gamma}_i}\right) \quad (4.8)$$

Considering (2.11), it can be seen from (4.8) that a linear relation between user bit rate $R_{u,n}^{(i)}$ and modified power ratio $\check{\Gamma}_i$ results for large SINR values. Large parts of the users of a cell have high SINR, and since in the cell-centric network model, all users of a cell are considered jointly, the relation between modified power ratio $\check{\Gamma}_i$ and network throughput can be approximated to be linear. The same considerations apply in the context of the number of users that can be supported, such that also the relation between modified power ratio and total number of users that can be supported can be approximated to be linear.

For the verification of above reasoning, Figure 4.3 shows PR- and PN-Characteristics for the scenario from Figure 2.2 with the parameters of Table 2.1 and for different cell bandwidths B_i of the center cell between 2 MHz and 10 MHz in steps of 2 MHz. It can be seen that the figure confirms the proposed linear approximations. Note that feasibility requirements are not regarded in Figure 4.3, some part of the curves for larger values of $\check{\Gamma}_i$ may, therefore, be infeasible, depending on the resource allocations of the remaining cells.

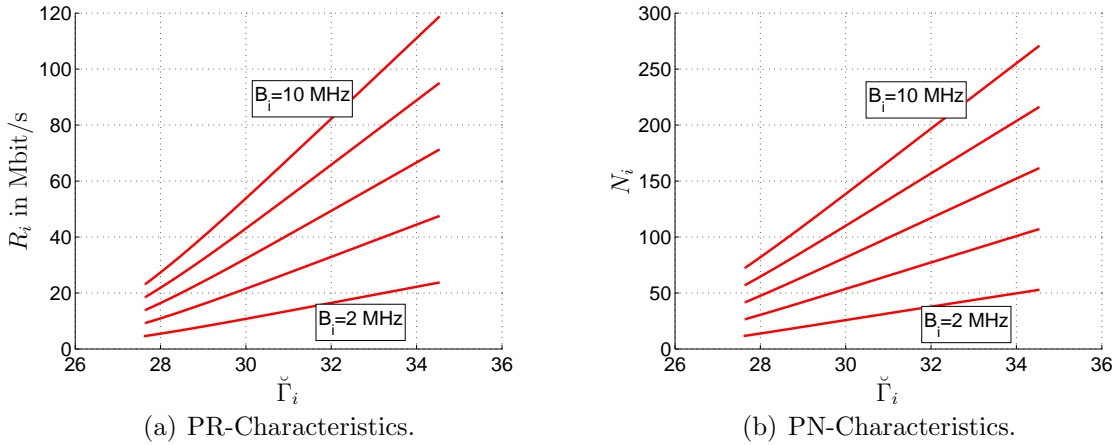


Figure 4.3. PR- and PN-Characteristics for PF scheduling.

As a consequence from above discussion, the objective functions and the remaining constraints of both, the network throughput optimization and the optimization of the number of users that can be supported, can be approximated by a convex problem formulation. To this end, a linear approximation of the cell throughput around $(\check{\Gamma}_{\text{ref},i}, R_{\text{ref},i})$ with slope Δ_{R_i}

$$R'_i(\check{\Gamma}_i) = R_{\text{ref},i} + \Delta_{R_i} \cdot (\check{\Gamma}_i - \check{\Gamma}_{\text{ref},i}) \quad (4.9)$$

and a linear approximation of the number of users that can be supported by a cell

around $(\check{\Gamma}_{\text{ref},i}, N_{\text{ref},i})$ with slope Δ_{N_i}

$$N'_i(\check{\Gamma}_i) = N_{\text{ref},i} + \Delta_{N_i} \cdot (\check{\Gamma}_i - \check{\Gamma}_{\text{ref},i}) \quad (4.10)$$

are defined. Using (4.9) and (4.10) in the optimization problems for maximum network throughput and maximum number of users that can be supported, respectively, yields the convex approximations of (3.24) and (3.25)

$$\begin{aligned} \check{\mathbf{\Gamma}}^* &= \arg \max_{\check{\mathbf{\Gamma}}} \left\{ \sum_{i=1}^{N_c} R'_i(\check{\Gamma}_i) \right\} \\ \text{s.t.} \quad &\frac{R'_j(\check{\Gamma}_j)}{N_j} \geq R_{\text{u,min}} \\ &\ln \left(\rho \left(\text{diag}(\mathbf{e}^{\check{\mathbf{\Gamma}}}) \text{diag}(\beta) \mathbf{E} \right) \right) < 0 \\ &\ln \left(\mathbf{p}(\mathbf{b}, \mathbf{e}^{\check{\mathbf{\Gamma}}}) \right) \leq \ln(P_{\text{max}}), \end{aligned} \quad (4.11)$$

and

$$\begin{aligned} \check{\mathbf{\Gamma}}^* &= \arg \max_{\check{\mathbf{\Gamma}}} \left\{ \sum_{i=1}^{N_c} N'_i(\check{\Gamma}_i) \right\} \\ \text{s.t.} \quad &N'_j(\check{\Gamma}_j) = N_{\text{rel},j} \cdot \sum_i N'_i(\check{\Gamma}_i) \\ &\ln \left(\rho \left(\text{diag}(\mathbf{e}^{\check{\mathbf{\Gamma}}}) \text{diag}(\beta) \mathbf{E} \right) \right) < 0 \\ &\ln \left(\mathbf{p}(\mathbf{b}, \mathbf{e}^{\check{\mathbf{\Gamma}}}) \right) \leq \ln(P_{\text{max}}), \end{aligned} \quad (4.12)$$

respectively. The optimum transmit powers are obtained from the optimum modified power ratios $\check{\mathbf{\Gamma}}^*$ according to

$$\mathbf{p}^* = \left(\mathbf{I}_{N_c} - \text{diag}(\mathbf{e}^{\check{\mathbf{\Gamma}}^*}) \text{diag}(\beta) \mathbf{E} \right)^{-1} \text{diag}(\mathbf{n}) \mathbf{e}^{\check{\mathbf{\Gamma}}^*}. \quad (4.13)$$

4.2.5 Joint Power and Bandwidth Allocation

This section discusses the convexity of the joint allocation of cell bandwidth and transmit power. Two different approaches for this are proposed in Section 3.4.3. The approach for the joint resource allocation of (3.26) and (3.27), which assume fixed power ratios, lead to optimization problems that are very similar to the power allocating optimization problems of (3.24) and (3.25), respectively. The difference is, however, that the joint allocation is achieved by means of a cell bandwidth allocation, according to Section 3.4.3. As a consequence, the objective function of the joint resource allocation is a function of the cell bandwidth, according to (3.26) and (3.27), which prohibits to use the approach for convex reformulation taken in Section 4.2.4 since it would destroy the concave shape of the objective functions.

In order to be able to solve the joint resource allocation optimization problems efficiently, a different approach is, therefore, taken. This approach assumes that the fixed power ratio targets $\tilde{\Gamma}_i$ are feasible and result in transmit powers \mathbf{p} that observe the maximum transmit power limit P_{\max} at all times. With this assumption, the power ratio feasibility constraint and the maximum transmit power constraint can be neglected in the optimization problems of (3.26) and (3.27) such that they can be rewritten to

$$\begin{aligned} \mathbf{b}^* &= \arg \max_{\mathbf{b}} \{R_{\text{nw}}(\mathbf{b})\} \\ \text{s.t. } &\bar{R}_{\text{u}}^{(i)}(\mathbf{b}) \geq R_{\text{u},\min} \\ &\mathbf{N}\mathbf{b} \leq B_{\text{sys}} \end{aligned} \quad (4.14)$$

and

$$\begin{aligned} \mathbf{b}^* &= \arg \max_{\mathbf{b}} \{N_{\text{nw}}(\mathbf{b})\} \\ \text{s.t. } &N_i(\mathbf{b}) = N_{\text{rel},i} \cdot N_{\text{nw}}(\mathbf{b}) \\ &\mathbf{N}\mathbf{b} \leq B_{\text{sys}}, \end{aligned} \quad (4.15)$$

respectively.

The optimization of the network throughput of (4.14) is a linear optimization problem, as can be seen considering (2.35) and (2.46). Concerning the optimization of the number of users that can be supported from (4.15), a non-linear effect is contained due to the multiplication of the standard deviation with the term $\frac{1}{\sqrt{N_i}}$ and $\sqrt{N_i}$, respectively, according to (2.37) and (2.46). Due to the square root relation and assuming values with practical relevance for the target cell outage probability \tilde{p}_{out} in these expressions, however, the non-linear part is negligible compared to the linear part, such that a linear approximation is possible. This can also be seen in the BN-Characteristics for fixed Γ_i and for the scenario from Figure 2.2 with the parameters of Table 2.1 and for power ratio targets $\tilde{\Gamma}_i$ of the center cell between 110 dB and 130 dB in steps of 5 dB as shown in Figure 4.4 for PF and FT scheduling. As a consequence, also the optimization of the number of users that can be supported can be approximated by a linear optimization problem.

An important prerequisite for this approach, however, is the proper choice of the power ratio targets $\tilde{\Gamma}_i$. Feasible power ratio targets whose corresponding transmit powers observe the maximum transmit power can be obtained by assuming maximum transmit power and the total system bandwidth for each cell. The corresponding power ratios are determined using (2.10) and the lowest achieved power ratio is selected as target power ratio $\tilde{\Gamma}_i$ for all cells. This selection constitutes a lower bound for feasible power ratio targets and assures a feasible transmit power allocation. Alternatively, a general approach that determines the power ratio targets in an iterative way is possible. The steps of this iterative algorithm consist in choosing initial targets, solving the optimization problems of (4.14) or (4.15), respectively, and choosing new power ratio targets if feasibility or maximum power constraint are violated.

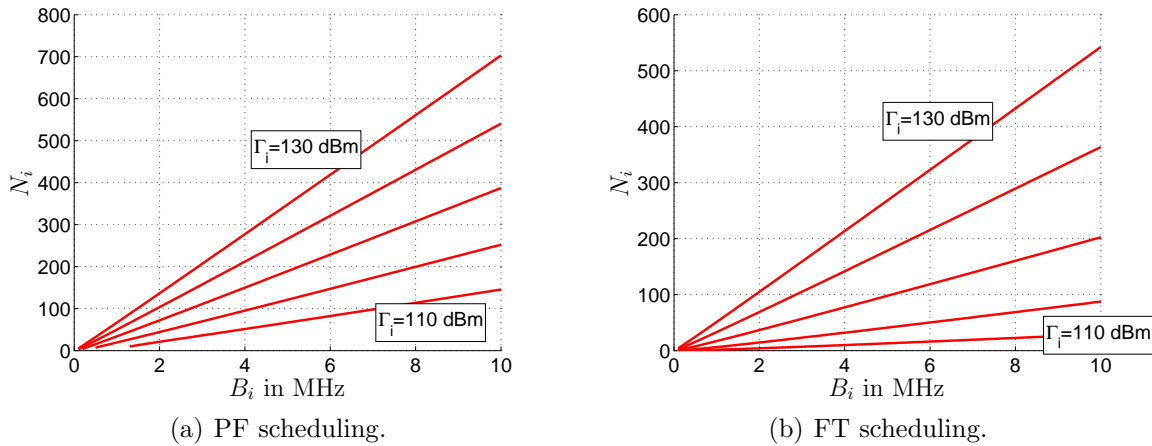


Figure 4.4. BN-Characteristics for constant power ratio and for PF scheduling and FT scheduling.

The presented approach for joint power and bandwidth allocation is very attractive since the linear optimization problems arising from the approach of this section can be solved very efficiently, as can be concluded regarding complexity considerations of linear optimization problems [Van01] and the structure of the optimization problems arising in the scope of this thesis. Additionally, solving algorithms for linear optimization problems can be implemented in a distributed way, as will be shown below. The constant power ratios furthermore allow to define and to implicitly observe minimum signal quality for all users.

For the joint resource allocation approaches of (3.28) and (3.29), which assume a fixed PSD $\tilde{\rho}_{\text{tx},i}$, convex formulations could not be established. Convex solving techniques can still be used for the solution of the optimization problems, the identified solutions, however, in general depend on the initial starting point and are in general suboptimum. The approach is still attractive, since the allocated cell bandwidth is considered in the transmit power allocation, leading to larger power ratio values for cells that require more resources, which is reasonable with respect to capacity optimization goals.

4.3 Distributed Algorithms

4.3.1 Introduction and General Approach

Cellular radio networks are highly distributed systems due to their cellular structure. Current technical evolution and current standards, such as LTE and System Architecture Evolution (SAE) [3GP11b], for example, account for this fact in the system design

and aim for mostly distributed systems with possibly flat hierarchy that need as little central entities as possible. Also self-organizing functionality has to consider the trend toward distributed implementations.

In the development of distributed implementations, the pursued optimization goals of network throughput maximization and maximization of the number of users have to be evaluated in a practical context. As addressed in Section 3.3.2, the number of users as well as the relative distribution of the users is given in practice. In this context, the goal of maximizing the number of users while observing the relative user distribution, as it is defined in Section 3.3.2, is achieved by accepting the new users and adjusting the resource allocation accordingly to serve the new users. This is possible as long as the corresponding optimization problem is feasible and assuming that users enter the system one by one or in small groups. Once all resources are allocated, every additional user will make the problem infeasible and cannot be served.

As a consequence, Section 4.3 focuses on the development of distributed algorithms that solve the problem of maximizing the network throughput. The optimization problems of Tables 3.1 and 3.2 are considered, but their reformulations of Section 4.2 are used for all derivations. The basis for all further discussion of this section is made in Section 4.3.2 with an introduction to linear network throughput optimization. Section 4.3.3 introduces an algorithm for the distributed implementation of linear optimization problems using the cell-centric network model. This algorithm can be used to solve any arising linear optimization problem, such as the joint resource allocation problems from Section 4.2.5, for example. The algorithms can also be extended by an iterative approach to solve nonlinear optimization problems, as proposed in Section 4.3.4. Section 4.3.5 presents a distributed algorithm for transmit power allocation, such that the capacity optimization approaches can be implemented in a fully distributed way.

4.3.2 General Linear Network Throughput Optimization

In this section, a general linear formulation of the cell bandwidth allocating network throughput optimization problem is derived. This derivation is relevant for the cell bandwidth allocating capacity optimization problems of (3.22) and (3.23) and the joint resource allocating approaches from table 3.2 since they are based on the allocation of cell bandwidth.

An optimization problem with affine objective function and affine constraints is called a linear optimization problem or short a linear program (LP). If the only inequality

constraints of a LP are nonnegativity constraints of the optimization variables, it is called a standard form LP. With $\mathbf{x}, \mathbf{c} \in \mathbb{R}^l$, $\mathbf{b} \in \mathbb{R}^m$ and $\mathbf{A} \in \mathbb{R}^{m \times l}$, the standard form LP is defined by [BV08]

$$\begin{aligned} \mathbf{x}^* &= \arg \max_{\mathbf{x}} \mathbf{c}^T \mathbf{x} \\ \text{s.t. } &\mathbf{A} \mathbf{x} = \mathbf{b} \\ &\mathbf{x} \geq \mathbf{0}. \end{aligned} \quad (4.16)$$

Every general LP can be transformed into standard form by introducing so-called slack variables [BV08].

Regarding the considerations of Section 4.2.5 and selecting the target power ratios $\tilde{\Gamma}_i$ accordingly, the joint resource allocation problem with fixed power ratios of (4.14) is a LP. The following discussion is, therefore, made exemplarily for the optimization problem of (4.14). With ϵ_i the cell spectral efficiency given by

$$\epsilon_i = \frac{\tilde{R}_i}{B_i}, \quad (4.17)$$

which can be obtained from the PBR-Characteristic and expresses how much throughput cell i can provide for target power ratio $\tilde{\Gamma}_i$ and for one Hertz of cell bandwidth, the optimization problem of (4.14) is rewritten as

$$\begin{aligned} \mathbf{b}^* &= \arg \max_{\mathbf{b}} \sum_{i=1}^{N_c} \epsilon_i B_i \\ \text{s.t. } &\frac{\epsilon_i}{N_i} B_i \geq R_{u,\min} \\ &\mathbf{N} \mathbf{b} \leq B_{\text{sys}}. \end{aligned} \quad (4.18)$$

The minimum cell bandwidth $B_{\min,i} = R_{u,\min} \frac{N_i}{\epsilon_i}$ required by cell i to observe the minimum QoS requirements of the users can be allocated to each cell prior to the network throughput optimization. The first constraint of (4.18) can then be neglected if the already allocated minimum cell bandwidths are considered in the second constraint. With $\mathbf{b}_{\min} = (B_{\min,1}, B_{\min,2}, \dots, B_{\min,N_c})^T$ the vector of the minimum cell bandwidths $B_{\min,i}$ and with $\mathbf{b}_{\text{ng},\min} = (B_{\text{ng},\min,1}, B_{\text{ng},\min,2}, \dots, B_{\text{ng},\min,N_{\text{ng}}})^T$ the vector of the sums $B_{\text{ng},\min,k}$ of the minimum bandwidths $B_{\min,i}$ required by the cells of NG k given by

$$\mathbf{b}_{\text{ng},\min} = \mathbf{N} \mathbf{b}_{\min}, \quad (4.19)$$

the optimization problem of (4.18) can be simplified to

$$\begin{aligned} \mathbf{b}^* &= \arg \max_{\mathbf{b}} \sum_{i=1}^{N_c} \epsilon_i B_i \\ \text{s.t. } &\mathbf{N} \mathbf{b} \leq B_{\text{sys}} - \mathbf{b}_{\text{ng},\min}. \end{aligned} \quad (4.20)$$

The optimization problem of (4.18) or (4.20), respectively, can also be used in iterative solving strategies for non-linear optimization problems since it can be obtained from linearization. It is, therefore, also of relevance for nonlinear cell bandwidth allocation problems and generally for other non-linear allocation problems that are based on cell bandwidth allocation, as it will be shown in Section 4.3.4.

each iteration the non-basic variable that has the largest positive coefficient in the objective function and will result in the largest increase of the optimization objective. If no variable with positive coefficient in the objective function is found, the optimum solution is reached. Otherwise, the variable with the largest positive coefficient is moved to the set of basic variables. The variable that is moved from the set of basic variables to the set of non-basic variables is the variable that constraints the maximum value of the new basic variable most, considering the values of the other basic variables. In all equations of the dictionary including the objective function, the new basic variable is then substituted by a function of the non-basic variables. Thus, the dictionary changes with every iteration [Van01].

The choices of the variables that move between the sets of basic and non-basic variables are usually referred to as row choice and column choice. The term column choice refers to the choice of the non-basic variable that moves to the set of basic variables, since the non-basic variables stand in the columns of the dictionary. Row choice consequently denominates the choice of the basic variable that moves to the set of non-basic variables, since basic variables stand in the rows of the dictionary. The idea of the distributed implementation of the full tabloid simplex method is that the column choice can be distributed over several nodes carrying out the column choice locally in only a part of the dictionary and broadcasting the results to all nodes, which allows each node to determine if it found the non-basic variable with the largest coefficient. The node that found the non-basic variable with the largest coefficient carries out the row choice and broadcasts the chosen basic variable to all other nodes. Finally, all nodes update their partial dictionary such that the next iteration can begin. [Yar01, Yv09].

This distributed approach can be applied to a cellular radio network. For reasons of simplicity, it is assumed that each BS serves as a node for the distributed execution of the simplex algorithm. The local column choice of each node is in this case carried out only across the sectors of the BS and the largest ϵ_i is broadcast. Each node compares the incoming broadcasts with the maximum ϵ_i of its own sectors, the node that finds to have the maximum ϵ_i in one of its sectors has won the column choice and makes the row choice. For this purpose, the node has to know about the minimum bandwidth requirements of all sectors that are neighbors to the sector with the largest ϵ_i , according to the definition of neighbored cells from Section 3.2. Note that the required local knowledge is limited to the neighbors of the sector with the largest ϵ_i , since rows of the dictionary that represent NGs to which the sector with the largest ϵ_i does not belong are not eligible as row choice since they do not affect the bandwidth allocation to the sector with the maximum ϵ_i . The row choice is signaled to all nodes, the nodes adjust their part of the dictionary and the next iteration begins.

As it can be seen from this description, the distributed implementation of the simplex algorithm in a cellular radio network requires signaling between the nodes. Note that concerning the information about other sectors of other nodes, which is required by each node to be able to make the row choice, only local information is required. For the row choice, however, the broadcast of information to all nodes is required. In this context, setting the number of optimization nodes equal to the number of BSs causes much signaling traffic overhead and is not practical. Instead, it is desirable to have a clearly lower number of optimization nodes, since this will reduce signaling traffic significantly. Each node then represents several BSs, collects the required data from these BSs and their sectors and carries out the necessary operations.

General investigations on efficiency and on the optimum number of optimization nodes, i.e. the tradeoff between signaling and computational complexity, are carried out in [HS94, Yar01]. The investigations show that the distributed implementation of the simplex algorithms is capable of achieving good performance also for several tens or even more than one hundred optimization nodes. Setting the number of BSs that are represented by each optimization node to several tens, large parts of a cellular radio network of hundreds of BSs can be optimized with the distributed implementation of the simplex algorithm.

4.3.4 Sequential Linear Programming

Efficient solving techniques also exist for non-linear convex optimization problems, such as interior point methods, for example. The barrier method [BV08] is an example of an interior point method. Compared to the simplex algorithm, interior point methods can be more efficient than the worst case performance of the simplex algorithm. Especially for large problems, interior point methods are computationally attractive [Van01, BV08] and are, therefore, relevant algorithms for the central implementation of the optimization problems of Section 4.2. The distributed implementation of interior point methods, however, is usually not as easily possible as for the simplex method, cf. Section 4.3.3. Consequently, alternative approaches for solving non-linear convex optimization problems are of interest in the scope of this thesis. This section proposes Sequential Linear Programming (SLP) for the solution of non-linear convex optimization problems for automatic capacity optimization of cellular radio networks.

SLP is an iterative approach that exploits the advantages of LPs and their solving techniques for the solution of non-linear optimization problems. The idea of SLP is to linearize the objective function and the constraints around a reference point and

to solve the resulting LP. This solution is used to determine a new reference point, around which the non-linear problem is linearized again and the resulting LP is solved to once again determine the next reference point. The algorithm finishes if the solutions of the LP obtained from the linearizations converge. Thus, the algorithm iteratively approaches a local optimum. If the optimization problem is convex, SLP approaches the global optimum.

In this thesis, the non-linear network throughput optimization problems based on the allocation of cell bandwidth of (3.22), (3.23) and (3.26) to (3.29) are considered for the application of SLP. The problems are linearized by assuming that the power ratios resulting from the bandwidth allocation $\mathbf{b}^{(l-1)}$ of iteration $l-1$ are constant for iteration l . The resulting LP is solved using the simplex algorithm, obtaining the optimum cell bandwidth allocation $\mathbf{b}^{*(l)}$ of iteration l . The cell bandwidth allocation $\mathbf{b}^{(l)}$ of iteration l is determined from the cell bandwidth allocation $\mathbf{b}^{(l-1)}$ of the previous iteration and the optimum cell bandwidth allocation $\mathbf{b}^{*(l)}$ of the current iteration according to

$$\mathbf{b}^{(l)} = (1 - \rho_{\text{slp}}) \mathbf{b}^{(l-1)} + \rho_{\text{slp}} \cdot \mathbf{b}^{*(l)}, \quad 0 \leq \rho_{\text{slp}} \leq 1. \quad (4.22)$$

Parameter ρ_{slp} plays an important role for the algorithm and has to be chosen carefully. It has two opposite effects on the performance of the algorithm. The smaller ρ_{slp} is chosen, the slower the algorithm converges. On the other hand, the accuracy of the result increases with smaller ρ_{slp} . As a consequence, a compromise between speed and quality of the result has to be found. Figure 4.5 shows exemplary performance results of SLP applied to a cellular network with 21 cells and the remaining parameters from Table 2.1 and for different values of ρ_{slp} . The relation between speed of convergence and ρ_{slp} is shown in Figure 4.5(a), the inverse relation between ρ_{slp} and accuracy of the solution is shown in Figure 4.5(b), which shows the MSE in terms of the difference between two consecutive iterations.

4.3.5 Distributed Power Allocation

The capacity optimization problems of (3.24) to (3.27) require a second step that determines the optimum cell transmit powers using (3.13) and based on the optimum power ratios from the previously solved optimization problem, cf. Section 3.4.2. This section presents for this second step a distributed approach, such that the automatic capacity optimization can be implemented fully distributed.

Much research has been carried out in the field of transmit power allocation to single users, for example in [Zan92a, Zan92b, FM93, GZ94, JK00]. Using the cell-centric network model, these approaches can be applied to the allocation of transmit power to the

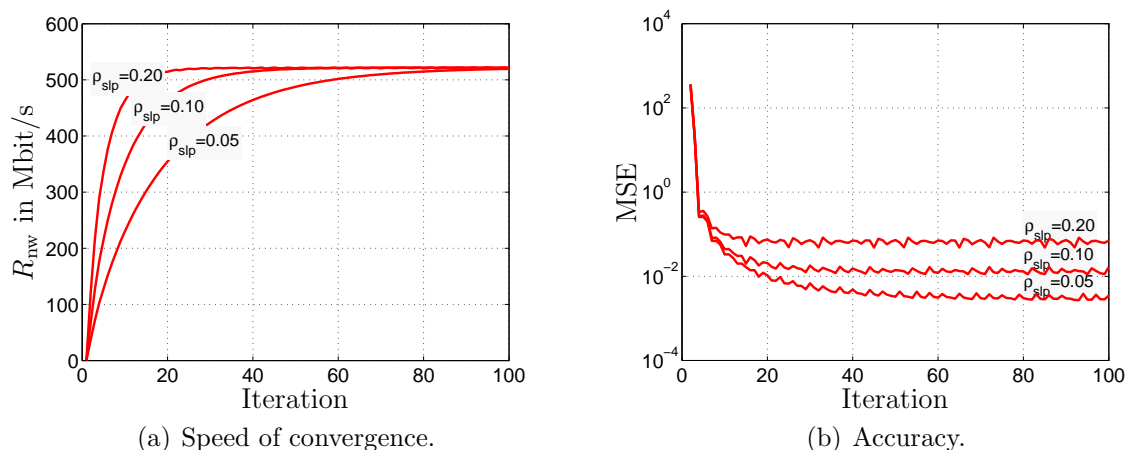


Figure 4.5. Exemplary performance results of SLP applied to a cellular network with 21 cells. The relations between speed of convergence and ρ_{slp} as well as the relation between accuracy of the solution in terms of MSE between consecutive iterations and ρ_{slp} are shown.

cells of a cellular radio network. In this section, the Distributed Power Control (DPC) algorithm suggested by [FM93] in the formulation of [JK00,ZK01] is applied to solve the determination of the transmit power allocation from the power ratios as it is required in (3.24) to (3.27).

The algorithm proposed by [FM93] is an iterative algorithm that requires only local knowledge about channel gains for the determination of the transmit powers. With $\mathbf{M}, \mathbf{N} \in \mathbb{R}^{N_c \times N_c}$ and $\check{\mathbf{\Gamma}} = \mathbf{\Gamma}^*$ for (3.24) and (3.25) and $\check{\mathbf{\Gamma}} = \tilde{\mathbf{\Gamma}}$ for (3.26) and (3.27), respectively, and according to the formulation of [JK00] observing the nomenclature used in this thesis, an iterative approach that solves (3.13) is given by

$$\mathbf{p}^{(l+1)} = \mathbf{M}^{-1} \mathbf{N} \mathbf{p}^{(l)} + \mathbf{M}^{-1} \text{diag}(\mathbf{n}) \check{\mathbf{\Gamma}}. \quad (4.23)$$

It can be shown that the algorithm of (4.23) converges if \mathbf{M} and \mathbf{N} are chosen such that for the spectral radius $\rho(\mathbf{M}^{-1} \mathbf{N}) < 1$ holds [ZK01].

In accordance with [ZK01] and in order to apply this approach to the cell-centric model and to solve (3.13), the definitions $\mathbf{M} = \mathbf{I}_{N_c}$ and $\mathbf{N} = \text{diag}(\check{\mathbf{\Gamma}}) \text{diag}(\beta) \mathbf{E}$ are chosen. With this definitions and due to the constraints of the optimization problem carried out previously, the requirement $\rho(\mathbf{M}^{-1} \mathbf{N}) < 1$ is fulfilled, cf. (3.24) to (3.27). Regarding the matrix formulation of (2.14) given by $\bar{\mathbf{P}}_I = \text{diag}(\beta) \mathbf{E} \mathbf{p}$, (4.23) can be rewritten to

$$\mathbf{p}^{(l+1)} = \mathbf{I}_{N_c} \text{diag}(\check{\mathbf{\Gamma}}) \bar{\mathbf{P}}_I^{(l)} + \mathbf{I}_{N_c} \text{diag}(\mathbf{n}) \check{\mathbf{\Gamma}} \quad (4.24)$$

Considering a single row of the linear system of equation of (4.24) and resolving (2.10) for $\bar{P}_{1,i}$, (4.24) can be further simplified according to

$$\begin{aligned} P_{\text{tx},i}^{(l+1)} &= \check{\Gamma}_i \bar{P}_{1,i}^{(l)} + P_N \check{\Gamma}_i \\ &= \check{\Gamma}_i \left(\frac{P_{\text{tx},i}^{(l)}}{\Gamma_i} - P_N \right) + P_N \check{\Gamma}_i \\ &= \frac{\check{\Gamma}_i}{\Gamma_i} P_{\text{tx},i}^{(l)}. \end{aligned} \quad (4.25)$$

It can be seen from (4.25) that the presented distributed power allocation algorithm requires at each cell i only measurements of the power ratio Γ_i . Thus, the optimum transmit power of each cell can be achieved in a distributed way and without any coordination between the cells and using only local measurements. Note that due to the constraints of the previously solved optimization problem, the maximum power constraint is observed by the transmit power allocation obtained with this algorithm, cf. (3.24) to (3.27). General investigations on convergence speed and extensions of the presented approach to increase convergence speed can be found in [JK00, ZK01].

4.4 Local Approach

Cellular radio networks are set in a heterogeneous environment. As a consequence, in some areas covered by the network, such as urban areas or areas containing large roads, for example, large capacity demand inhomogeneities will be present while in other areas, such as rural areas, for example, only little dynamics will happen. This section presents a concept that allows the separate treatment of local areas with automatic capacity optimization approaches for SONs.

Based on the observations of different capacity demand inhomogeneities in different areas, the network can be divided into areas in that automatic capacity optimization will provide high gains and into areas in which automatic capacity optimization will have little effect, compared to a static resource allocation. The areas of high effect of automatic capacity optimization are in general limited by areas of low effect of automatic capacity optimization.

A concept of great practical relevance for automatic capacity optimization approaches for SONs can be derived from these considerations. This concept envisions static resource allocations for all areas for that low performance gain from automatic capacity optimization is expected. Thus, rural areas with little population or areas covered with forests, for example, will be served with static resource allocations. As a consequence, the areas in which automatic capacity optimization is expected to achieve high gains,

such as cities and areas with large traffic infrastructure, for example, are islands isolated from each other by areas with static resource allocations. Within each of these islands, any of the algorithms of this chapter can be applied. Since the islands are expected to be small compared to the total network, even the application of central algorithms may be of relevance. Furthermore, the separation of the islands that apply automatic capacity optimization approaches for SONs by areas with static allocations increases the robustness of SONs since it assures that possible problems resulting from the automatic capacity optimization are limited to a local extent.

Chapter 5

Performance Analysis

5.1 Introduction

In order to validate the developed automatic capacity optimization approaches and in order to gain insight into their behavior and performance, simulations are carried out. In this thesis, two different simulation approaches are employed. Section 5.2 carries out a functional analysis that uses simple and unambiguous scenarios in order to obtain insight into the general behavior of the proposed approaches and in order to achieve a deeper understanding of the functioning of the resource allocation techniques in connection with capacity optimization in inhomogeneous scenarios. Additionally, Section 5.3 carries out a real-world analysis that uses measurement data to construct a complex real-world scenario that is used to assess the performance gain of the capacity optimization approaches that can be expected in real-world application.

Throughout this chapter, the assumption of uncoordinated bandwidth allocations treats the state of the art scheduling based approaches for the adaptation of the network to changing capacity demands, as discussed in Section 2.2. Assuming coordinated bandwidth allocations, the proposed automatic capacity optimization approaches for SONs are considered, according to the hierarchic concept for coordination of automatic capacity optimization and scheduling of Section 2.2. As a consequence, the comparison of state of the art scheduling based approaches and automatic capacity optimization approaches for SONs is carried out by comparing the performance achieved with uncoordinated bandwidth allocations to the performance achieved with coordinated bandwidth allocations.

5.2 Functional Analysis

For the functional analysis and for the investigation of the general behavior of the capacity optimization approaches, a simple and clear simulation approach with appropriate scenarios that enables proper and unambiguous interpretation of the simulation results is required. Section 5.2.1 proposes a simulation approach and suited scenarios that allow to relate scenario properties with the behavior of the different approaches

and, thus, enable clear and unambiguous interpretation of the results. The evaluation of the approaches and resource allocation techniques of Chapter 3 is carried out using this simulation approach and the simulation results are presented with focus on different aspects: Section 5.2.2 compares state of the art scheduling based approaches with the new automatic capacity optimization approaches for SONs, Section 5.2.3 discusses the effect of different scheduling strategies on the performance of the capacity optimization approaches, Section 5.2.4 investigates the performance of the different capacity optimization approaches with respect to the distribution of the inhomogeneous capacity demand and in Section 5.2.5, the QoS performance of the different capacity optimization approaches is evaluated.

5.2.1 Simulation Approach and Scenarios

The crucial point in connection with resource allocating capacity optimization is the ability of the capacity optimization approaches to adjust the resource allocation of the network to inhomogeneous user distributions and inhomogeneous capacity demands. This depends strongly on the capabilities of the resource allocation techniques to match the resource allocation to the capacity demand distribution. This section proposes a simulation approach and suited scenarios to assess and investigate the performance of capacity optimization approaches in cellular networks with inhomogeneous capacity demand distribution and to assess the abilities of the different resource allocation techniques to match the different inhomogeneous capacity demand distributions.

In order to consider inhomogeneous capacity demand distributions, so-called hotspot (HS) scenarios are used. In HS scenarios, areas with increased capacity demand, so-called hotspots, exist, such that the cells in HSs, which are called HS cells, experience higher capacity demand than the other cells. The increased capacity demand in the HS cells is assumed to result from an increased number of users that request service. This way, an inhomogeneous user distribution is regarded. The strength of a HS can be measured in terms of the number N_{hs} of users of the HS cells and the number N_0 of users of the non-HS cells. For this purpose, the HS strength ρ_{hs} defined by

$$\rho_{\text{hs}} = \frac{N_{\text{hs}}}{N_0} \quad (5.1)$$

is introduced. Note that for the maximization of the number of users, the specification of ρ_{hs} is sufficient since the actual number of users in HS cells and non-HS cells result from the optimization. In network throughput maximization, however, the cell throughputs result from the optimizations, such that the total number of users in the scenario has to be specified additionally.

In practice, different situations concerning the distribution and the size of the HSs arise and require different capabilities of the capacity optimization approaches. Large HSs consisting of clustered HS cells require algorithms that are able to shift capacity over a distance of several cells towards the HS cells. For the optimization of a scenario with several small and distributed HSs, however, the algorithms should draw capacity from cells within a short distance from the HSs, such that only few cells that are located close to the HS cells are affected.

As a consequence of these considerations, the three different scenarios of Figure 5.1 have been identified as relevant for simulations. The Single HS Scenario of Figure 5.1(a) contains only a single HS cell. It is suited to generally investigate the capability of a resource allocation technique to cope with inhomogeneous capacity demand distributions and its ability to shift capacity to a HS. The Cluster HS Scenario of Figure 5.1(b) models a bigger HS that expands over several neighbored cells. It allows to show the ability of a resource allocation technique to shift capacity over the distance of several cells. The third scenario is the Multi HS scenario of Figure 5.1(c) with several small and distributed hotspots. With this scenario, the ability of a resource allocation technique to concentrate capacity from neighbored cells can be evaluated. The scenarios of Figure 5.1 can be considered as basic scenarios and, therefore, as building blocks of complex scenarios, such that complex scenarios can be broken down into a weighted combination of the basic scenarios of Figure 5.1.

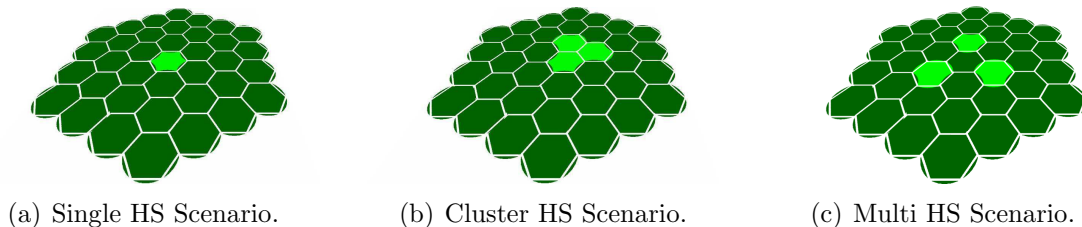


Figure 5.1. Simulation scenarios for functional analysis.

Behavior and performance results of all capacity optimization approaches are studied for each of the scenarios of Figure 5.1 separately and the ability and properties of each capacity optimization approach and the respective resource allocation techniques concerning the shift of capacity over large and short distances is evaluated independently. Considering a complex scenario that contains several of the basic scenarios and assuming that the basic scenarios are spatially separated, conclusions concerning the performance of a capacity optimization approach and the respective resource allocation technique in the complex scenario can be drawn based on the results obtained for the basic scenarios and considering the construction of the complex scenario from the basic scenarios.

The size of the scenarios used in the simulations is 39 cells. A wrap-around technique [ZK01] which wraps the scenarios around a torus is applied, such that each cell appears as if it was placed in the middle of the scenarios, which avoids border effects. The simulation parameters are summarized in Table 5.1, they are typical for LTE-based cellular radio networks in an urban environment. The total number of users is chosen

Table 5.1. Simulation parameters for functional analysis.

| Parameter | Value |
|---|-------------------------------------|
| Cell radius S_i | 250 m |
| Number N_C of cells | 39 |
| Reuse distance D for coord. bandwidth allocations | $3S_i$ |
| Height of the BSs | 32 m |
| Height of the UEs | 1.5 m |
| Capacity demand distribution | HS scenarios |
| User position probability $p_{\mathbf{r},\varphi}^{(i)}(r, \varphi)$ over the cell area | uniform |
| Carrier frequency | 1.9 GHz |
| Propagation model | 3GPP Urban Macro |
| Shadow fading variance σ_{sh}^2 | 8 dB |
| Noise PSD | $-167 \frac{\text{dBm}}{\text{Hz}}$ |
| System bandwidth B_{sys} | 10 MHz |
| Minimum user bit rate $R_{\text{u,min}}$ | $100 \frac{\text{kbit}}{\text{s}}$ |
| Target cell outage probability \tilde{p}_{out} | 0.05 |
| Scheduling strategies | PF, FT |
| Total number of users for throughput max. (uncoord., FT) | 780 |
| Total number of users for throughput max. (all others) | 1950 |
| Minimum power ratio with transmit power allocation | 100 dB |
| Maximum power ratio with transmit power allocation | 150 dB |
| Target power ratio $\tilde{\Gamma}_i$ for coord. bandwidth allocations | 127 dB |
| Target power ratio $\tilde{\Gamma}_i$ for uncoord. bandwidth allocations | 115 dB |
| Maximum transmit power P_{max} | 46 dBm |

such that the capacity optimization problems of Chapter 3 are feasible in the scenarios of Figure 5.1 and with the parameters of Table 5.1. The simulation results of this chapter are presented such that they can be compared also for different total numbers of users. The target power ratios $\tilde{\Gamma}_i$ are chosen using the non-iterative approach presented in Section 4.2.5.

According to the reuse distance D for coordinated bandwidth allocations as given by Table 5.1, the HS in the Cluster HS scenario consists of three HS cells, since this corresponds to a NG, according to Section 3.2. This way, the Cluster HS scenario represents a challenging user distribution for the capacity optimization approaches since the cells of the HS cannot reuse any resources. Concerning the Multi HS scenario,

also 3 HS cells exist for reasons of comparability. The distance between the HS cells is equal to the reuse distance D , such that also in the Multi HS scenario, a challenging user distribution exists, since the HS cells interfere with each other.

The PBR- and PBN-Characteristics required by the capacity optimization approaches are determined from measurements collected in a homogeneous scenario and using the approaches for practical implementation proposed in Section 2.5. The simulations are done such that the HS strength ρ_{hs} is varied and the capacity optimization is carried out for the different HS strengths. Performance results are shown in terms of the spectrum efficiency of the network as a function of ρ_{hs} . For the maximization of the number of users, the spectrum efficiency $\epsilon_{N_{\text{nw}}}$ of the network in bits/s/Hz/cell given by

$$\epsilon_{N_{\text{nw}}} = \frac{N_{\text{nw}}(\mathbf{b}, \mathbf{\Gamma}) \cdot \bar{R}_{\text{u}}^{(i)}}{B_{\text{sys}} \cdot N_{\text{c}}} \quad (5.2)$$

is used. For network throughput maximization, the spectrum efficiency $\epsilon_{R_{\text{nw}}}$ of the network in bits/s/Hz/cell given by

$$\epsilon_{R_{\text{nw}}} = \frac{R_{\text{nw}}(\mathbf{b}, \mathbf{\Gamma})}{B_{\text{sys}} \cdot N_{\text{c}}} \quad (5.3)$$

is used. All capacity optimization approaches from Chapter 3 are considered and used with coordinated bandwidth allocations as well as uncoordinated bandwidth allocations, if applicable according to the considerations of Section 3.5. The central algorithms from Section 4.2 are used to solve the capacity optimization problems. For all scenarios, the performance of a static homogeneous resource allocation [ZK01] with reuse distance D is determined as reference. In the static scenario, the cell bandwidth $B_i = \frac{B_{\text{sys}}}{3}$ and the transmit power $P_{\text{tx},i} = P_{\text{max}}$ is allocated to each cell.

According to the definition of the cell-centric network model of Chapter 2, the resource allocations obtained using the cell-centric network model observe the minimum QoS requirement $R_{\text{u},\text{min}}$ of the users. Also the solving algorithms of chapter 4 observe the minimum QoS requirement of the users. Prerequisite to both, however, is that the SINR measurements collected for the determination of PBR- and PBN-Characteristics, as proposed in Section 2.5, represent the interference situation of the users of the cell. The interference situation of the users, however, depends on the resource allocations of the cells, such that the adaptation of the resource allocations of the cells in order to optimize the network may change the interference situation of the users. The measurements may then no longer represent the actual interference situation of the users, such that the cell-centric network model can get inaccurate and the minimum QoS provided by the cells can be affected. As a consequence, the performance of the cells with respect to

the QoS of the users has to be evaluated in order to assess the influence of the network adaptation on the QoS of the users.

The evaluation of the QoS of the users requires the consideration of individual users. In order to verify the capacity optimization results especially with respect to the user QoS requirements, MC simulations are carried out. For this purpose, realizations of the user distributions are generated for each cell according to the user position probability $p_{\mathbf{r},\varphi}^{(i)}(r, \varphi)$ and the number N_i of users of the cell. Considering the propagation model and the scheduling strategy, the user bit rate $R_{\mathbf{u},\text{mc},n}^{(i)}$ achievable for each of the users is determined given the resource allocation resulting from the previously carried out capacity optimization. The MC simulations are, thus, carried out at user level, considering each user individually and determining the QoS of each user. This way, violations of minimum QoS requirements can be identified and the reliability of the proposed capacity optimization approaches with respect to assuring minimum QoS requirements can be assessed.

The minimum QoS of the users of a cell is determined according to the definition of cell outage probability $p_{\text{out},i}$ in the cell-centric network model of (2.32) and (2.42). With these definitions, the minimum QoS requirement is observed if a fraction of at most \tilde{p}_{out} of the users achieve bit rates that are below the minimum user bit rate $R_{\mathbf{u},\text{min}}$. Thus, the \tilde{p}_{out} -percentile $R_{\mathbf{u},\text{mc},\tilde{p}_{\text{out}}}^{(i)}$ of the user bit rates $R_{\mathbf{u},\text{mc},n}^{(i)}$ obtained in the MC simulations as given by

$$R_{\mathbf{u},\text{mc},\tilde{p}_{\text{out}}}^{(i)} = \{R_{\mathbf{u},\text{mc}} \mid P(R_{\mathbf{u},\text{mc}}^{(i)} < R_{\mathbf{u},\text{mc}}) = \tilde{p}_{\text{out}}\} \quad (5.4)$$

is evaluated for each cell in order to verify the different capacity optimization approaches with respect to the QoS of the users.

Throughout this chapter, the expression of observing minimum QoS requirements of the users denotes that the \tilde{p}_{out} -percentile $R_{\mathbf{u},\text{mc},\tilde{p}_{\text{out}}}^{(i)}$ of the user bit rate is equal to or larger than the minimum user bit rate $R_{\mathbf{u},\text{min}}$. For the actual evaluation of the QoS performance, the average $\bar{R}_{\mathbf{u},\text{mc},\tilde{p}_{\text{out}}}^{(i)}$ of the \tilde{p}_{out} -percentile $R_{\mathbf{u},\text{mc},\tilde{p}_{\text{out}}}^{(i)}$ of the user bit rate over all cells, defined by

$$\bar{R}_{\mathbf{u},\text{mc},\tilde{p}_{\text{out}}}^{(i)} = \frac{1}{N_c} \sum_{i=1}^{N_c} R_{\mathbf{u},\text{mc},\tilde{p}_{\text{out}}}^{(i)}, \quad (5.5)$$

is used to assess the QoS performance considering the whole network. The worst case QoS performance in the network is evaluated using the minimum $\check{R}_{\mathbf{u},\text{mc},\tilde{p}_{\text{out}}}^{(i)}$ of the \tilde{p}_{out} -percentile $R_{\mathbf{u},\text{mc},\tilde{p}_{\text{out}}}^{(i)}$ of the user bit rate over all cells, as given by

$$\check{R}_{\mathbf{u},\text{mc},\tilde{p}_{\text{out}}}^{(i)} = \min_i \left\{ R_{\mathbf{u},\text{mc},\tilde{p}_{\text{out}}}^{(i)} \right\}. \quad (5.6)$$

5.2.2 Comparison of Capacity Optimization Approaches

This section evaluates the performance of the different capacity optimization approaches in order to generally investigate their behavior in scenarios with inhomogeneous capacity demand. The Single HS scenario is applied for this purpose since it provides a simple capacity demand distribution that allows a clear interpretation of the results. The simulation results are, furthermore, applied to compare state of the art scheduling based approaches with automatic capacity optimization approaches for SONS. The analysis is carried out separately for the different optimization goals. First, the maximization of the total number of users that can be supported is investigated. Subsequently, the approaches for the maximization of the network throughput are evaluated.

Note that for sake of simplicity and clearness of presentation, only results for PF scheduling are shown in this section. The findings for FT scheduling, however, do not differ qualitatively. Section 5.2.3 contains the corresponding performance results for FT scheduling.

Maximum Total Number of Users

In the maximization of the number of users in HS scenarios, the applied optimization problems in general always have a solution since the total number of users in the scenario reduces if the constraints are not observed. The spectral efficiency $\epsilon_{N_{\text{nw}}}$ can, therefore, be determined for every hotspot strength ρ_{hs} , such that the performance of the different capacity optimization approaches for the maximization of the number of users is evaluated using the spectral efficiency $\epsilon_{N_{\text{nw}}}$ of (5.2) of the network.

Figure 5.2 shows the spectral efficiency $\epsilon_{N_{\text{nw}}}$ of the network achieved by the different capacity optimization approaches for the maximization of the number of users of Chapter 3 for different HS strengths ρ_{hs} in the Single HS scenario. PF scheduling is assumed and coordinated as well as uncoordinated bandwidth allocations are considered. The different resource allocation techniques are identified by different markers, performance results obtained with coordinated bandwidth allocations are visualized by solid red lines, results obtained with uncoordinated bandwidth allocations are illustrated by dashed blue lines. A static homogeneous resource allocation as described in Section 5.2.1 is considered as reference, it is represented by the solid green line.

The figure shows that for a HS strength of one, i.e. for a homogeneous capacity demand distribution, state of the art scheduling based approaches clearly outperform automatic

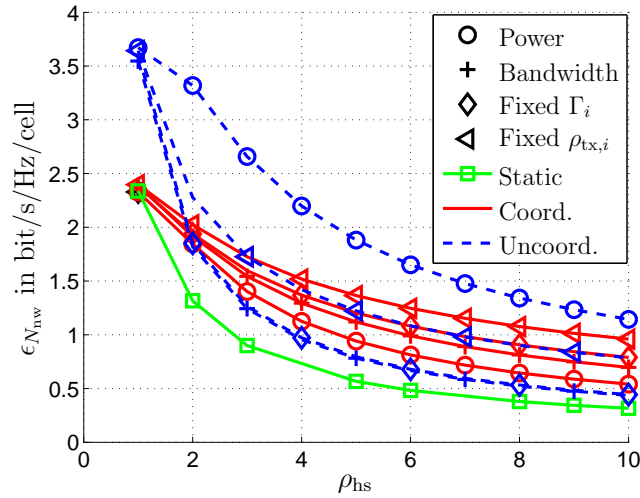


Figure 5.2. Performance results of the maximization of the number of users in the Single HS scenario and for PF scheduling.

capacity optimization approaches for SONs. This result is expected since coordination of the bandwidth allocations leads to lower frequency reuse. Furthermore, users at the cell border, which are influenced most by ICI, do not effect the overall cell performance too much, since PF scheduling is assumed. The effect of uncoordinated bandwidth allocations in terms of uncontrolled ICI is, therefore, acceptable in the homogeneous scenario and compensated by the higher frequency reuse achievable with uncoordinated bandwidth allocations. Among the different resource allocation techniques, small differences can be observed for the homogeneous capacity demand distribution, which result from different initializations, such as the choice of the target power ratios in the case of the joint resource allocation with fixed power ratios, for example.

With increasing inhomogeneity of the capacity demand, as indicated by increasing HS strength ρ_{hs} , the advantage of coordination of the bandwidth allocations, which is the lower and controlled ICI, increases. This is true especially from the point of view of the HS cell, which is capable of accommodating more users due to the lower ICI. The decreased frequency reuse due to the coordination of the bandwidth allocations is of less importance in this context, since non-HS cells have lower capacity demands and, thus, can afford to use less resources in favor of the heavily loaded HS cells. As a consequence, the main disadvantage of the coordination of the bandwidth allocations in homogeneous scenarios loses weight with increasing inhomogeneity of the capacity demand, such that the performance differences between coordinated and uncoordinated bandwidth allocations quickly reduce and automatic capacity optimization approaches for SONs outperform the state of the art scheduling based approaches already in scenarios with low to moderate HS strengths, as can be seen from Figure 5.2.

This explanation does not hold for transmit power allocation, which shows very high performance for uncoordinated bandwidth allocations, according to Figure 5.2. The reason for this behavior is the very large range allowed for the power ratio, cf. Table 5.1. As a consequence of this large range, power ratio differences of more than 30 dB may arise even between neighbored cells. Furthermore, the lower border of the power ratio range has been set to a very low value since otherwise, the power allocating capacity optimization problems quickly become infeasible, even for small HS strengths. The range as given in Table 5.1 has been chosen despite these critical points in order to be able to consider transmit power allocation in the functional analysis. For practical application, however, the chosen range is not suited, since the large power ratio differences that arise due to the large range for power ratio Γ_i may lead to very low SINR $\gamma_n^{(i)}$ at the receivers, according to (2.11), which may be problematic for physical layer transmission techniques. Furthermore, the lower border of the power ratio range of 100 dB is extremely low since in the considered scenarios with the parameters of Table 5.1, the pathloss between BS and a UE at the cell border may easily exceed 120 dB, such that a power ratio of 100 dB, for example, results in a very low SINR $\gamma_n^{(i)}$ at the receiver, according to (2.11).

To summarize the findings for the maximization of the number of users that can be supported by the network, it should be mentioned that automatic capacity optimization approaches for SON outperform state of the art scheduling based approaches for low to medium HS strengths. Transmit power allocation may lead to large transmit power differences even between neighbored cells, which can be problematic for transmission techniques, such that transmit power allocation is not suited for practical implementation.

Maximum Network Throughput

With network throughput optimization, the definition of a fixed total number of users in the scenario is required additionally to the specification of the hotspot strength, according to Section 5.2.1. Since the total number of users in the scenario is fixed, there exists a maximum hotspot strength or maximum level of inhomogeneity of the capacity demand, respectively, beyond that the optimization problems applied for throughput optimization are infeasible. The maximum hotspot strength or the maximum capacity demand inhomogeneity, respectively, depends on the resource allocation technique, such that additionally to the spectral efficiency $\epsilon_{R_{nw}}$ of the network, the maximum HS strength that can be handled by a capacity optimization approach can be used to evaluate the performance of the capacity optimization approaches for network throughput maximization.

Figure 5.3 shows the performance results of the capacity optimization approaches for the maximization of the network throughput of Chapter 3 in the Single HS scenario. PF scheduling is assumed and the static homogeneous resource allocation has been included as reference in the figure. The figure shows the spectral efficiency $\epsilon_{R_{nw}}$ of the network achieved by the capacity optimization approaches for different HS strengths ρ_{hs} . Furthermore, the end points of the curves give the maximum HS strength that can be handled. Line styles, colors and markers are chosen as for the previous discussion of the performance of the maximization of the total number of users. Note that cell bandwidth allocation and joint resource allocation with fixed power ratio are not considered with uncoordinated bandwidth allocations since these resource allocation techniques are not capable of maximizing the network throughput using uncoordinated bandwidth allocations, as discussed in Section 3.5.

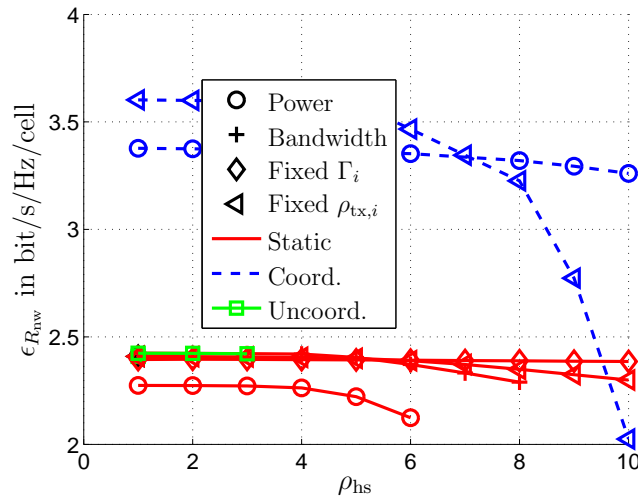


Figure 5.3. Performance results of the network throughput maximization in the Single HS scenario and for PF scheduling.

Evaluating Figure 5.3 with respect to the maximum HS strength, it can be seen how the different resource allocation techniques can cope with different degrees of capacity demand inhomogeneity. The static resource allocation can handle HS strengths of up to 3, transmit power allocation with coordinated bandwidth allocations can handle HS strengths of up to 6, coordinated cell bandwidth allocation can handle HS strengths of up to 8 and the joint resource allocation approaches with coordinated bandwidth allocations can handle HS strengths of at least 10. Thus, all resource allocation techniques outperform the static resource allocation with respect to the ability to cope with inhomogeneous capacity demand distributions. The joint resource allocation approaches are, furthermore, capable of adapting the network to the inhomogeneous capacity demand distribution without sacrificing much network capacity.

Comparing uncoordinated and coordinated bandwidth allocations or state of the art scheduling based approaches and automatic capacity optimization approaches for SONs, respectively, Figure 5.3 again shows that approaches with uncoordinated bandwidth allocations outperform approaches with coordinated bandwidth allocations for homogeneous capacity demand distributions. Furthermore, even for medium to high HS strengths, approaches with uncoordinated bandwidth allocations outperform approaches with coordinated bandwidth allocations. The reason for this difference, compared to the maximization of the total number of users, is that apart from areas close to a HS cell, the scenario mostly contains a homogeneous capacity demand distribution, according to Figure 5.1(a). While the approaches with coordinated bandwidth allocations achieve high performance gains in the areas with inhomogeneous capacity demand, the approaches with uncoordinated bandwidth allocations perform better in the areas with homogeneous capacity demands. Since the scenario mostly consists of areas with homogeneous capacity demand, the locally achieved significant gains of the automatic capacity optimization approaches for SONs appear in the overall network performance only for very strong HS strengths ρ_{hs} , as can be seen from Figure 5.3.

As in the evaluation of the maximization of the total number of users, transmit power allocation performs very well for uncoordinated bandwidth allocations. The reason for this high performance is, as for the maximization of the total number of users, the large range of values and the low values allowed for Γ_i , which may result in large transmit power differences among the cells and in low SINR $\gamma_n^{(i)}$ of the users. As a consequence, also for network throughput maximization, transmit power allocation is not suited for practical application.

To summarize the investigations on the maximization of the network throughput, it should to be mentioned that the capacity optimization approaches are capable of adapting a cellular radio network even to strong inhomogeneities in the capacity demand. Considering the maximum HS strength and the capacity in terms of spectral efficiency $\epsilon_{R_{\text{nw}}}$ of the network, it is found that especially the joint resource allocation techniques with coordinated bandwidth allocations perform very well since they are able to cope with high inhomogeneity in the capacity demand without significantly sacrificing network capacity. Furthermore, it was reasoned that with network throughput maximization, gains are achieved especially locally in areas of high inhomogeneity in the capacity demand. As for the maximization of the total number of users, transmit power allocation is not suited for practical application

5.2.3 The Effect of Scheduling

The scheduling strategy decides how the radio resources of a cell are distributed to the users of the cell. According to Section 1.2, scheduling has great effect on the capacity of a cell and, therefore, also on the performance of the capacity optimization approaches. This section presents the results of the performance analysis of the different capacity optimization approaches for FT scheduling. The results are compared to the results for PF scheduling presented in Section 5.2.2 and interpreted with respect to the effect of the different scheduling strategies on the capacity optimization approaches.

The general difference between PF scheduling and FT scheduling is the metric that is used to express fairness. While PF scheduling distributes the resources fair among all users, according to Section 2.3, FT scheduling assures a fair distribution of the cell throughput, such that all users achieve the same user bit rate. As a consequence, users with worse reception conditions are allocated more resources with FT scheduling, such that users with bad reception conditions have a larger share of the resources of the cell and, therefore, more impact on the overall cell performance than with PF scheduling.

The effect of FT scheduling of shifting more influence to users with bad reception conditions leads in particular to more influence of ICI, since cell edge users are most affected by ICI and, at the same time, are the users with usually bad reception conditions. In this context, coordinated bandwidth allocations are expected to gain importance, since they allow to control ICI to a certain extent. In order to verify this expectation, Figure 5.4 shows the performance results of the capacity optimization approaches for the maximization of the total number of users and for network throughput optimization, respectively, both in the Single HS Scenario and for FT scheduling. The legend of Figure 5.4(a) also holds for Figure 5.4(b) and line styles, colors and markers are as in Section 5.2.2. Again, the static homogeneous resource allocation has been included as reference in the figures.

Figure 5.4 shows that assuming FT scheduling, the automatic capacity optimization approaches for SONs generally outperform the state of the art scheduling based approaches, even for the homogeneous capacity demand distribution. The reason behind this observation is the increased effect of ICI, compared to PF scheduling, which is effectively mitigated by the automatic capacity optimization approaches for SONs. Concerning the network throughput maximization, the performance differences of the approaches in terms of the maximum HS strength that can be handled are clearly visible. Note that compared to Figure 5.3, the spectral efficiency as well as the maximum HS strengths that are achieved are lower than for PF scheduling, which is also due to the increased influence of ICI.

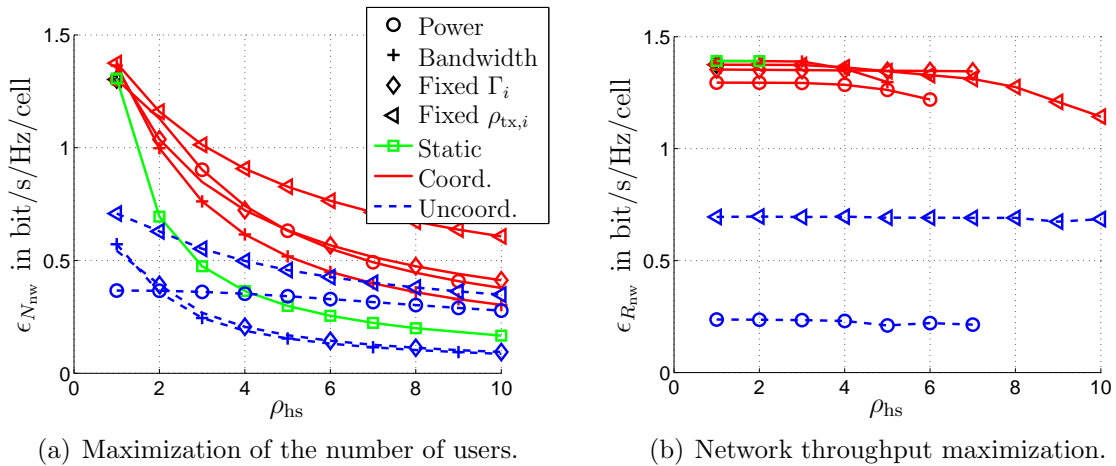


Figure 5.4. Performance results of the maximization of the number of users and of the network throughput maximization in the Single HS Scenario and for FT scheduling

The comparison of Figure 5.4(a) and Figure 5.4(b) with Figure 5.2 and Figure 5.3, respectively, furthermore allows to assess the importance of ICIC in connection with users with bad reception conditions. It shows that the more influence users with bad reception conditions have, the more importance gains ICIC and, consequently, the automatic capacity optimization approaches for SONS. The influence of users with bad reception conditions increases with throughput fairness and depends on the distribution of the users over the cell area. As a consequence, automatic capacity optimization approaches for SONS are of higher importance in areas where many users experience bad reception conditions, such as areas with many users at the cell borders or in strongly attenuated environments, such as indoor environments, for example.

5.2.4 Influence of the HS Distribution

Also the location of the HS cells relative to each other is of relevance for the performance of the capacity optimization approaches. This section evaluates the different capacity optimization approaches in the Cluster HS Scenario and in the Multi HS Scenario of Figure 5.1 in order to investigate behavior and performance of the approaches for different distributions of the HS cells.

Note that with uncoordinated bandwidth allocations, the HS scenarios differ only with respect to the density of the HSs but have no fundamental differences. For coordinated bandwidth allocations, however, the clustering of the HS cells in the Cluster HS Scenario and the distribution of the HSs in the Multi HS Scenario do exhibit fundamental differences since the HS cells belong to the same NG, as in the case of the

Cluster HS Scenario, or to different NGs, as in the case of the Multi HS Scenario. As a consequence, the HS distribution is for the capacity optimization approaches using coordinated bandwidth allocations of significant influence, but for the capacity optimization approaches using uncoordinated bandwidth allocations only of minor effect. Therefore, only coordinated bandwidth allocations are considered in this section.

Figure 5.5 shows the performance results of the capacity optimization approaches for the maximization of the number of users in the Cluster HS Scenario and in the Multi HS Scenario with coordinated bandwidth allocations and for FT scheduling. The figure shows significant performance differences depending on scenario and resource allocation technique. In particular, transmit power allocation significantly outperforms all other resource allocation techniques in the Cluster HS scenario, while in the Multi HS scenario, transmit power allocation performs clearly worse than the other resource allocation techniques.

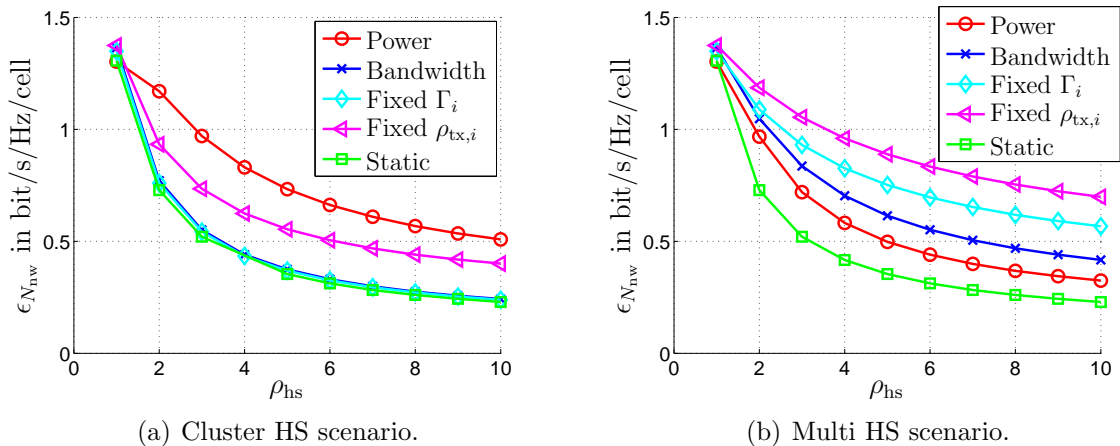


Figure 5.5. Performance results of the maximization of the number of users in the Cluster HS Scenario and in the Multi HS Scenario with coordinated bandwidth allocations and for FT scheduling.

An explanation for these observations can be found considering the principles of operation of the different resource allocation techniques as discussed in Section 3.5. It is reasoned there that transmit power allocation shifts capacity over larger distances even from cells that are located further away. Cell bandwidth allocation, on the other hand, draws capacity only from neighbored cells in the sense of neighborhood as defined in Section 3.2. Putting these considerations in the context of coordinated bandwidth allocations, it becomes clear that depending on the resource allocation technique and on the HS scenario, the HS cells may be mutually dependent and may compete with each other in the adaptation to the inhomogeneous capacity demand situation, causing performance degradation.

More specifically, for cell bandwidth allocation in the Cluster HS scenario, this means that every HS cell competes with the other HS cells for more cell bandwidth, such that the HS cells limit each other in obtaining more resources to fulfill the increased capacity demand. As a consequence, the HS cells in the Cluster HS Scenario are mutually dependent and compete with each other in the adaptation to the inhomogeneous capacity demand, which leads to performance degradation. In fact, the HS cluster appears for cell bandwidth allocation as a homogeneous scenario, such that cell bandwidth allocation performs in the Cluster HS scenario the same as the static resource allocation, as can be seen from Figure 5.5(a).

For transmit power allocation, the situation is different. Since, due to coordination of the bandwidth allocations, the resource allocations of the HS cells are orthogonal in the Cluster HS scenario, capacity can be accumulated at each HS cell using transmit power allocation without competing with any of the other HS cells. The HS cells in the Cluster HS Scenario are, thus, independent from the point of view of transmit power allocation, such that no HS cell limits another HS cell in adapting to the higher capacity demand. As a consequence, transmit power allocation clearly outperforms all other resource allocation techniques in the Cluster HS Scenario, as can be seen from Figure 5.5(a).

Similar considerations can be made for the Multi HS scenario. For cell bandwidth allocation, the HS cells are now independent and do not compete with each other for resources since they are no longer neighbors. Cell bandwidth allocation is, therefore, capable of achieving good performance in the Multi HS Scenario. From the point of view of transmit power allocation, however, the HS cells are now dependent since they interfere with each other. Consequently, the HS cells compete with each other for more transmit power and limit each other in achieving high cell capacity, which leads to the performance degradation of transmit power allocation in the Multi HS scenario as shown in Figure 5.5(b).

Special consideration is required for the joint resource allocation approaches. According to Section 3.4.3, the joint approaches are based on cell bandwidth allocation but additionally contain mechanisms to adapt transmit power. Thus, the joint approaches show similar performance as the cell bandwidth allocation but may very likely outperform the cell bandwidth allocation. This becomes especially clear regarding the joint resource allocation technique with fixed PSD $\rho_{\text{tx},i}$, which allocates more cell bandwidth as well as more transmit power to cells with higher capacity demand. As a consequence, it is capable of exploiting to a certain extent the advantage of transmit power allocation in the Cluster HS Scenario as well as the advantages of cell bandwidth allocation

in the Multi HS Scenario, which results in a performance advantage compared to cell bandwidth allocation, as can be seen from Figure 5.5.

Figure 5.6(b) shows the performance of the different capacity optimization approaches for network throughput maximization in the Cluster HS scenario and in the Multi HS Scenario with coordinated bandwidth allocations and for FT scheduling. Using the

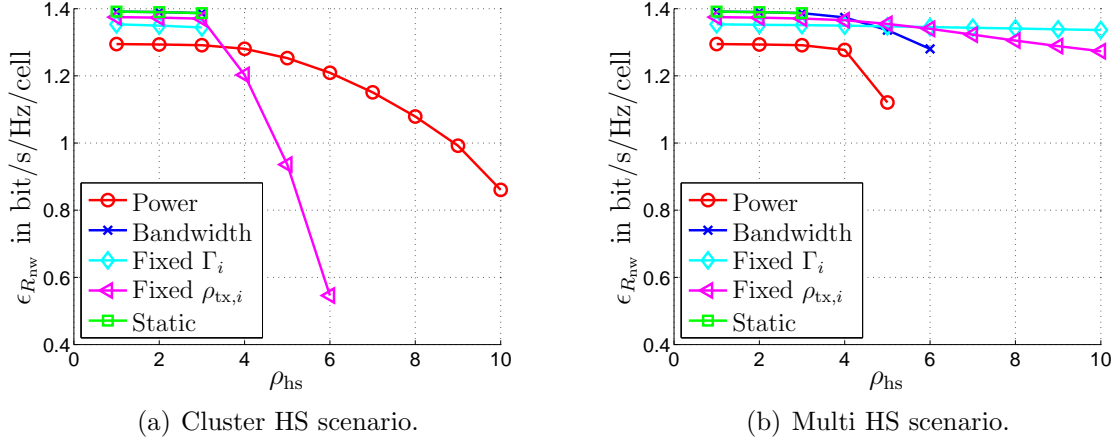


Figure 5.6. Performance results of the network throughput maximization in the Cluster HS Scenario and in the Multi HS Scenario with coordinated bandwidth allocations and for FT scheduling.

maximum HS strength that can be handled by the different resource allocation techniques to compare the different capacity optimization approaches for the maximization of the network throughput with each other, it can be seen from the figure that, as before, transmit power allocation outperforms all other resource allocation techniques in the Cluster HS Scenario in terms of the maximum HS strength. For higher HS strengths, transmit power allocation outperforms the other resource allocation techniques also in terms of network capacity or spectrum efficiency $\epsilon_{R_{nw}}$, respectively. In the Multi HS Scenario, cell bandwidth allocation and the joint allocation techniques show superior performance. Among these approaches, the joint resource allocation with fixed power ratio Γ_i performs best for high HS strengths.

To summarize, in this section it is shown that transmit power allocation performs best with clustered HS cells, while cell bandwidth allocation and joint resource allocation performs best in scenarios with distributed HS cells. Note that for sake of simplicity and clearness of presentation, only results for FT scheduling are shown in this section. The findings for PF scheduling, however, do not differ qualitatively and lead to the same results, as can be seen from the corresponding performance results for PF scheduling from Appendix A.2.1.

5.2.5 QoS Performance Evaluation

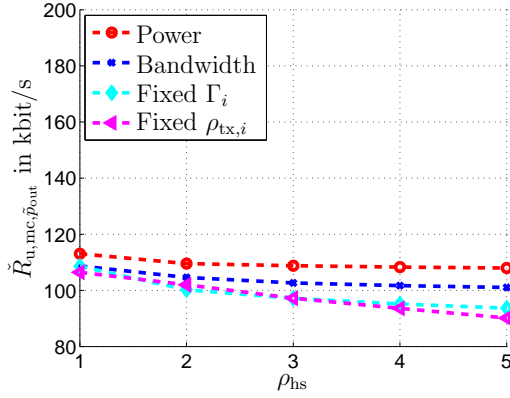
For the evaluation of the QoS performance, MC simulations, as described in Section 5.2.1, are used. This section presents and interprets the relevant simulation results. First, the QoS performance of the maximization of the total number of users is evaluated, followed by the evaluation of the QoS performance of the network throughput maximization.

Maximum Total Number of Users

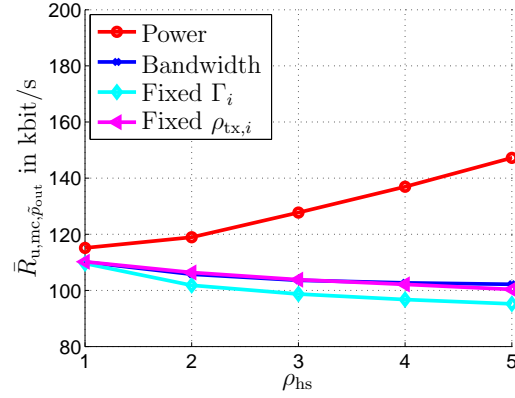
The results of the MC simulations of the QoS performance of the maximization of the total number of users in the Single HS Scenario and for PF scheduling are shown in Figure 5.7 in terms of the minimum $\check{R}_{u,mc,\tilde{p}_{out}}$ of the p_{out} -percentile of the user bit rates achieved in the cells on the left side of the figure and the average $\bar{R}_{u,mc,\tilde{p}_{out}}$ of the p_{out} -percentiles of the user bit rates over all cells on the right side of the figure. The upper plots show the performance with uncoordinated bandwidth allocations, the lower plots show the performance with coordinated bandwidth allocations.

According to Figure 5.7, the minimum user bit rate $R_{u,min}$ as set in Table 5.1 is in general assured. Two exceptions, however, apply. The first exception is the joint resource allocation with fixed power ratios Γ_i and with uncoordinated bandwidth allocations. It delivers a user QoS that falls with increasing hotspot strength ρ_{hs} below the minimum requirement, as can be observed in Figure 5.7(a). The decrease in user QoS, however, is exponentially decaying, which points to a constant offset rather than a general violation of the minimum QoS requirement. The performance of the joint resource allocation with fixed power ratios Γ_i can, therefore, be corrected by considering a weighting factor with the minimum QoS requirement which compensates the offset.

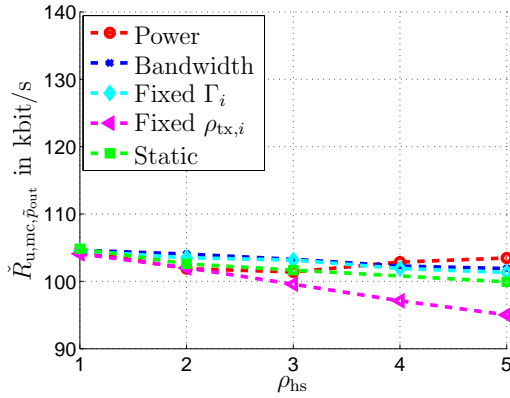
The second capacity optimization approach that does not yield to the minimum QoS requirement is the joint resource allocation with fixed PSDs $\rho_{tx,i}$, as can be seen from Figure 5.7(a) and Figure 5.7(c). In contrast to the joint resource allocation with constant power ratios Γ_i , however, the decrease in user QoS with increasing hotspot strength ρ_{hs} is linear, such that it cannot be corrected by a weighting of the QoS target. The reason for this behavior is found in the simulation approach, since the PBR- and PBN-Characteristics are determined from measurement data collected from the homogeneous scenario. For larger HS strengths, however, the situation that has to be adapted to deviates significantly from the situation in which the measurements were collected, such that the set of measurements, and consequently also the PBR- and



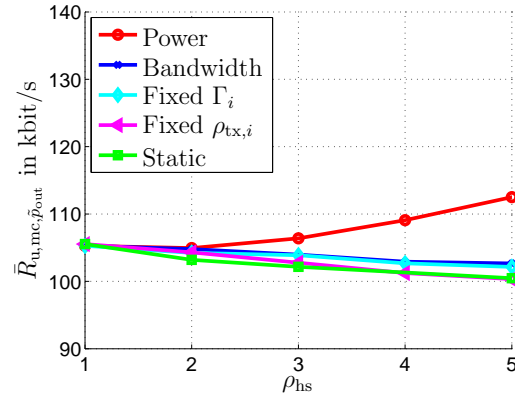
(a) Uncoordinated bandwidth allocations, minimum p_{out} -percentile.



(b) Uncoordinated bandwidth allocations, average p_{out} -percentile.



(c) Coordinated bandwidth allocations, minimum p_{out} -percentile.



(d) Coordinated bandwidth allocations, average p_{out} -percentile.

Figure 5.7. Average $\bar{R}_{u,mc,\bar{p}_{\text{out}}}$ and minimum $\check{R}_{u,mc,\bar{p}_{\text{out}}}$ of the p_{out} -percentile of the user bit rates of the cells for the maximization of the total number of users in the Single HS Scenario and for PF scheduling obtained from MC simulations.

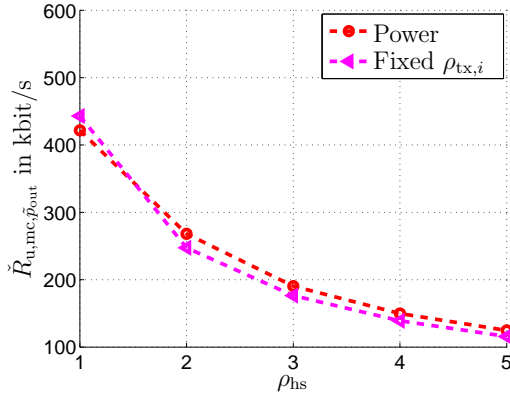
PBN-Characteristics, do not represent the current situation, such that errors result. In practical application, however, measurements are collected constantly, such that the formation of the HS is accompanied by the collection of measurements and, thus, represented by the set of measurements, which will reduce the inaccuracy significantly.

The high average QoS performance of the transmit power allocation, as it can be observed from Figures 5.7(b) and 5.7(d), is typical for transmit power allocation. It arises in cells that experience high capacity demand since they require high transmit power in order to assure the observation of the minimum QoS requirement also for users at the cell borders. The high transmit power leads to high SINR also for other users which, consequently, achieve high bit rates. Thus, the high average QoS performance is inherent to transmit power allocation. It is also a reason for the worse performance

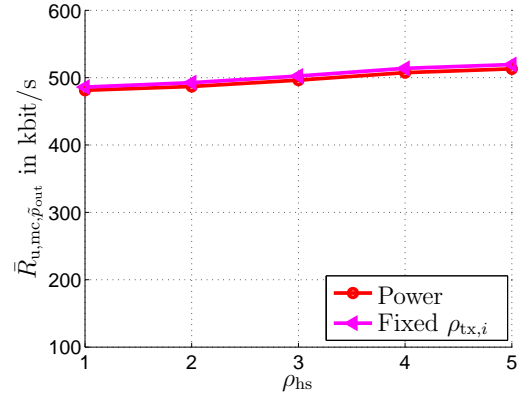
of the transmit power allocation with respect to capacity, as observed previously.

Maximum Network Throughput

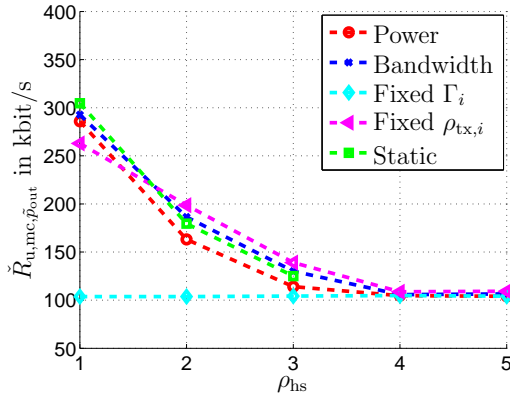
For the evaluation of the QoS performance of the network throughput optimization approaches, the results of the MC simulations are shown in Figure 5.8 for the Single HS Scenario and for PF scheduling, again in terms of the minimum $\check{R}_{u,mc,\tilde{p}_{out}}$ of the p_{out} -percentile of the user bit rates of the cells and the average $\bar{R}_{u,mc,\tilde{p}_{out}}$ of the p_{out} -percentiles of the user bit rates over all cells. Figure 5.8(a) and Figure 5.8(c) show that



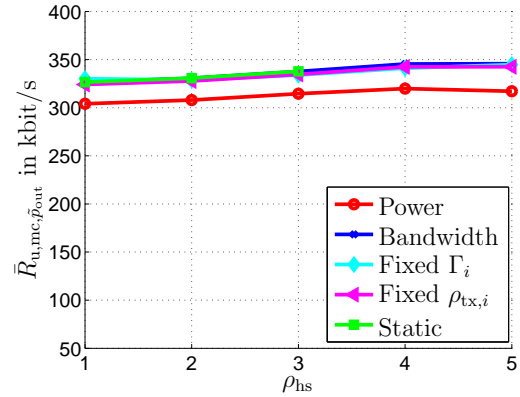
(a) Uncoordinated bandwidth allocations, minimum p_{out} -percentile.



(b) Uncoordinated bandwidth allocations, average p_{out} -percentile.



(c) Coordinated bandwidth allocations, minimum p_{out} -percentile.



(d) Coordinated bandwidth allocations, average p_{out} -percentile.

Figure 5.8. Average $\bar{R}_{u,mc,\tilde{p}_{out}}$ and minimum $\check{R}_{u,mc,\tilde{p}_{out}}$ of the p_{out} -percentile of the user bit rates of the cells for the maximization of the network throughput in the single HS Scenario and for PF scheduling obtained from MC simulations.

as long as the maximum HS strength that can be handled by the different resource

allocation techniques is not exceeded, the minimum QoS requirements are observed for all capacity optimization approaches and for coordinated as well as uncoordinated bandwidth allocations. The average QoS over all cells as shown by Figure 5.8(b) and Figure 5.8(d) is significantly higher than for the maximization of the number of users. The reason for this behavior is that large areas of the scenario experience a homogeneous capacity demand distribution, as already mentioned, while at the same time, the load in these areas is small, which is a consequence of the HS scenarios. Thus, the cells in the areas with homogeneous capacity demand distribution can provide high bit rates to their users, resulting in high average QoS.

Note that for sake of simplicity and clearness of presentation, only results for PF scheduling and the Single HS Scenario are shown in this section. The findings for the Cluster HS Scenario and for the Multi HS Scenario as well as the findings for FT scheduling, however, do not differ qualitatively. Appendix A.2.2 shows the performance results for PF scheduling and the Cluster HS Scenario and the Multi HS Scenario, Appendix A.2.3 shows the QoS performance results for FT scheduling and all HS scenarios.

5.3 Real-world Analysis

Additionally to the functional proof and the analysis of strength and weaknesses of the capacity optimization approaches and the corresponding resource allocation techniques, the performance evaluation of the capacity optimization approaches under real-world conditions in order to show the performance gain that can be expected in practical application is of great importance. This section presents an approach that establishes a real-world scenario based on throughput measurement data and uses the approach to obtain real-world simulation results. Section 5.3.1 introduces the simulation approach and describes which data is used for modeling and building of the real-world scenario. Section 5.3.2 presents the performance results. Parts of this section have been originally published by the author in [HKG⁺10].

5.3.1 Simulation Approach and Modeling Data

Real-world scenarios are very complex. A definition from scratch by considering every aspect arising from environmental and morphologic issues is not likely to achieve high sophistication and is, therefore, not recommended. As an alternative, this section

presents an approach that is based on throughput measurements, taken during operation from an existing network, and on prediction data, as it is used for planning and configuration of the respective part of the network, to define a real-world scenario.

For the real-world scenario of this section, a part of a real 2G/3G cellular mobile radio network is considered. The rectangular scenario is of size 5.4 km by 9.1 km, contains 126 sectors and is located in the downtown area of a big city. The sectors are distributed over 46 sites with one to three sectors per site. The simulation area is divided into a regular grid with a spacing of approximately 32 meters. The grid spacing is the smallest resolution in which data is available and in which calculations are carried out.

Cell areas and cell borders are determined based on predictions as they are used for the planning of the network. For this purpose, attenuation estimates are derived for each grid point and each sector based on predictions of the pilot power strength for each sector and grid point. The actual pilot power settings used in the operation of the network are not available, such that a uniform pilot power configuration is assumed throughout this section. Using the attenuation estimates and considering the pilot power, the areas covered by each of the sectors are obtained and cell areas and cell borders are derived. The user position probabilities, i.e. the distributions of the users within the areas covered by the cells or the sectors, respectively, are obtained based on an estimate of the user density over the scenario area as it is used for the planning of the network.

The capacity demand is determined based on downlink throughput measurements that are available for each sector in intervals of thirty minutes. Due to the combination of the user density estimation, which is specific for each grid point in the simulation area, and the traffic measurements, which are specific for the sectors but independent of the grid points, distribution and fluctuation of the inhomogeneous capacity demand can be modeled in detail. The throughput measurements are available over a duration of almost five days. In total, 229 different snapshots of the capacity demand are obtained. Note that with this method, the traffic that is actually served by the network, but not the offered traffic, is modeled. However, the method still provides a real-world situation concerning the inhomogeneous capacity distribution and the capacity variations, such that it is suited for the purpose of this section.

The proposed automatic capacity optimization approaches are carried out only for sectors that are located within an inner part of the scenario. The size of this inner part accounts for 22 % of the total area of the simulation scenario and contains approximately half of the sectors of the scenario. All sectors belonging to the outer area are assumed to have constant resource allocations and are used as source of interference

for the inner area such that border effects are avoided in the evaluation of the capacity optimization approaches. Table 5.2 summarizes the parameters of the real-world simulation approach.

Table 5.2. Simulation parameters for real-world analysis.

| Parameter | Value |
|---|------------------------------------|
| Scenario size | 5.4 km x 9.1 km |
| Total scenario area | 49 km ² |
| Size of the inner area | 11 km ² |
| Total number of sites | 46 |
| Total number of sectors | 126 |
| Number of sectors in the inner area | 60 |
| Grid spacing | 32 m |
| Carrier frequency | 1.9 GHz |
| System bandwidth B_{sys} | 10 MHz |
| Minimum user bit rate $R_{\text{u,min}}$ | 100 $\frac{\text{kbit}}{\text{s}}$ |
| Target cell outage probability \tilde{p}_{out} | 0.05 |
| Scheduling strategies | PF, FT |
| Total number of users | 2500-2700 |
| Target power ratio $\tilde{\Gamma}_i$ | 105 dB |

The simulations are carried out such that the capacity optimization approaches are applied to each of the snapshots independently. Thus, individual performance results are obtained for each snapshot and the simulation results are shown as a function of the snapshot index. As for the functional analysis, the central algorithms of Section 4.2 are applied for the solution of the capacity optimization problems.

In order to be able to better interpret the simulation results, the snapshots are analyzed with respect to their maximum HS strength of all HSs contained in the scenario. Figure 5.9(a) shows the result. The maximum HS strength is a figure of merit suited to identify snapshots with inhomogeneous capacity demand distributions and to classify the degree of inhomogeneity of the snapshot. Additionally, mean and standard deviation of the HS strength of all HSs of the snapshots are determined, as shown in Figure 5.9(b). They are used to identify snapshots with close to homogeneous capacity demand since low values in mean and standard deviation of the strengths of the HSs indicate low capacity demand inhomogeneity.

The range of forty snapshots considered in Figure 5.9, which covers a period of almost two days, is chosen for all analysis of this section. The range is selected such that different capacity demand distributions of interest for the evaluated approaches, such as almost homogeneous and strongly inhomogeneous distributions, are contained. Considering a broader range than the selected one shows that relevant distributions and

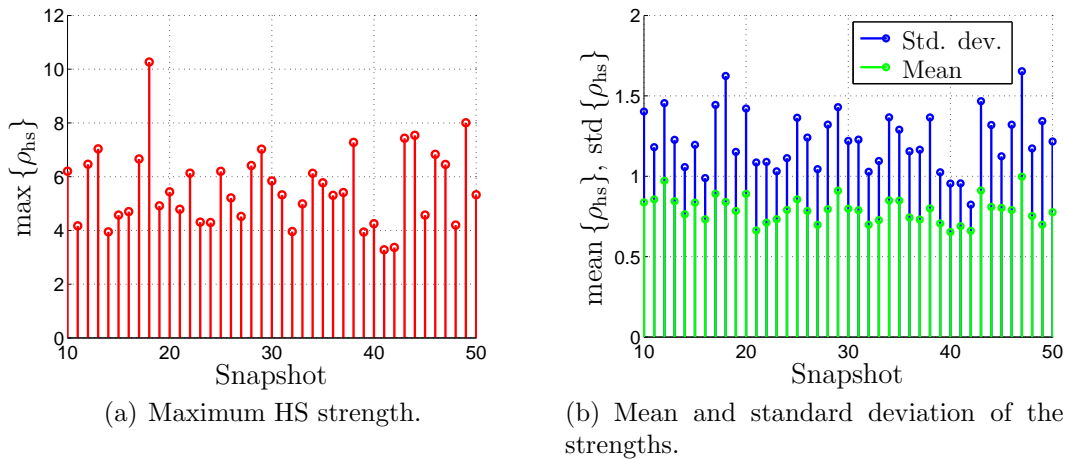


Figure 5.9. Maximum HS strength and mean and standard deviation of the HS strengths for the considered snapshots.

phenomena observed in the simulation results repeat. Furthermore, calculating average performance results over this range and over all 229 snapshots yields the same results. As a consequence, it can be concluded that a broader or different range does not reveal additional information and the snapshots considered in Figure 5.9 are sufficient for performance analysis and for the presentation of the results.

5.3.2 Performance Results

The performance results obtained for the real-world scenario in the considered snapshot range are shown in Figure 5.10 for the maximization of the number of users and for the maximization of the network throughput, both for PF scheduling as well as FT scheduling. The legend of Figure 5.10(b) holds for all plots of Figure 5.10. Transmit power allocation is not considered since it is expected to be problematic in practical application, as discussed in Section 5.2.2. In general, it can be observed from the figure that the network capacity is fluctuating less for network throughput maximization than for the maximization of the number of users since in network throughput maximization, non-HS cells contribute a large part to the overall network performance, as explained in Section 5.2.2. As before, the overall network capacity is lower for FT scheduling than for PF scheduling, since with FT scheduling, users with bad reception conditions have more influence on the overall performance than with PF scheduling.

Comparing uncoordinated bandwidth allocations and coordinated bandwidth allocations or state of the art scheduling based approaches and automatic capacity optimization approaches for SONS, respectively, with each other in Figure 5.10, a performance

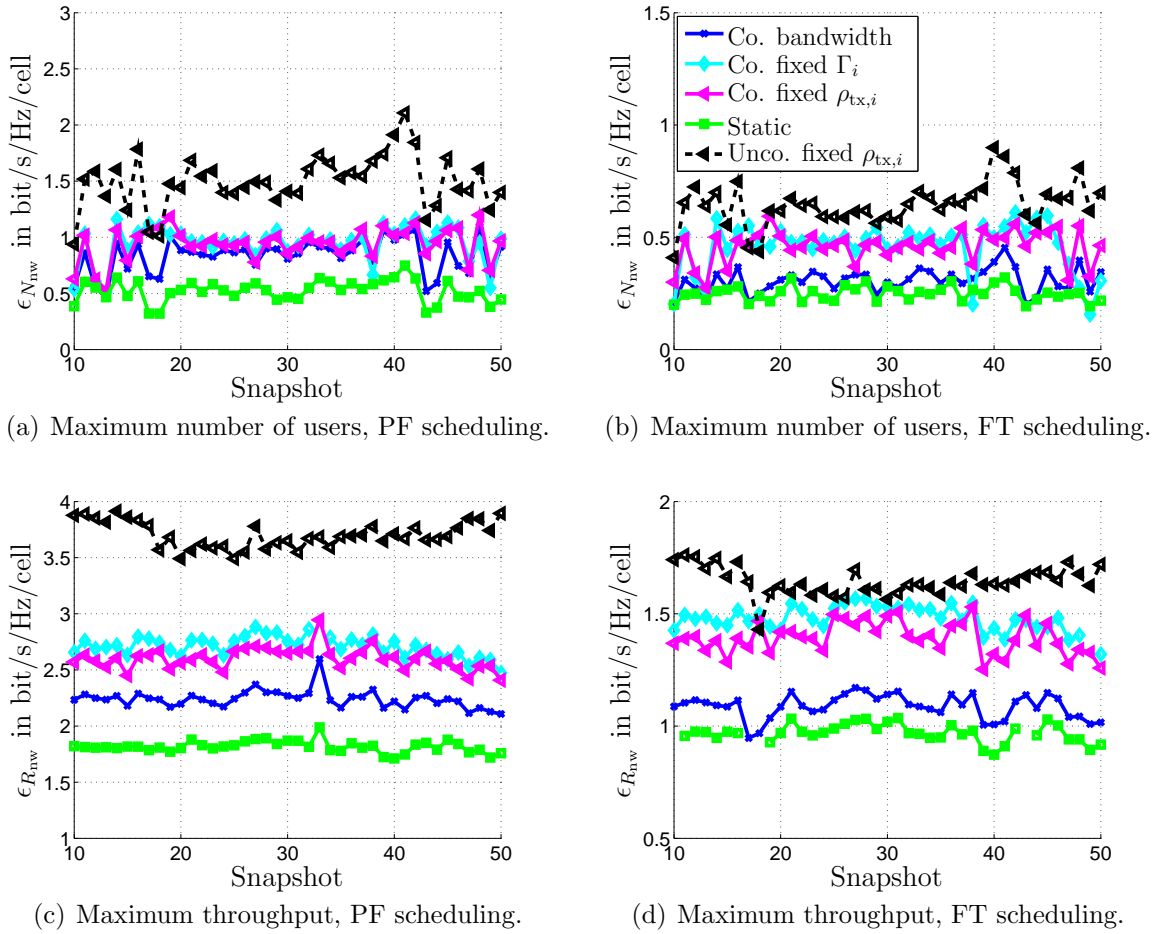


Figure 5.10. Performance results of the maximization of the total number of users and of the network throughput maximization, both for PF scheduling and FT scheduling.

gain of automatic capacity optimization approaches for SONs relative to state of the art scheduling based approaches can be observed for FT scheduling compared to PF scheduling. The large performance advantage of coordinated bandwidth allocations for FT scheduling, as identified in Section 5.2 where coordinated bandwidth allocations outperformed uncoordinated bandwidth allocations for FT scheduling, however, cannot be observed. Evaluating the real-world scenario with respect to the locations of the BSs and the user distribution of the scenario leads to the conclusion that the reason is a proper network planning, where sites are placed in or close to areas with high user density. As a consequence, less cell-edge users can be expected in real-world scenarios than in a uniform user distribution. The uniform user density assumed in Section 5.2 is, thus, usually not valid for real-world scenarios, such that the gain due to controlling ICI, as it is achieved by coordinated bandwidth allocations, can be expected to be less pronounced in real world-scenarios than in the functional analysis of Section 5.2.

Using Figure 5.9, snapshots that represent situations comparable to the scenarios and capacity demand distributions considered in Section 5.2 can be identified such that the results from the real-world simulations can be analyzed with respect to the behavior identified in the scope of the functional analysis of Section 5.2. In this context, hotspot situations are identified considering the maximum HS strength of the snapshots, as shown in Figure 5.9(a), such that snapshots 17-18, snapshot 38, snapshots 43-44 and snapshot 49, for example, are identified as snapshots that contain strong HSs.

Evaluating the performance results for the identified snapshots with strong HSs more in detail and according to the knowledge gained in Section 5.2 concerning the behavior of the different resource allocation techniques in the different HS scenarios allows to draw further conclusions. For snapshots 17-18 and 42-43, the simulation results show a significantly stronger performance drop for cell bandwidth allocation than for the other resource allocation techniques. As a consequence, it can be concluded that the most influencing HSs appear in clusters in these snapshots. Also, a relatively strong performance drop for uncoordinated bandwidth allocations can be noted, which lets even the joint resource allocation techniques with coordinated bandwidth allocations outperform the approaches with uncoordinated bandwidth allocations, as it was already observed in Section 5.2 for stronger HSs.

The situation is different for snapshots 38 and 49. Here, a performance drop can be observed, too. Cell bandwidth allocation, however, shows a relatively smaller performance drop than the other approaches, or performs even better. Furthermore, the performance drop for uncoordinated bandwidth allocations is much less pronounced than for the previously discussed snapshots, such that it can be concluded that the HSs in snapshots 38 and 49 are distributed over the scenario.

Additionally to inhomogeneous situations, homogeneous capacity demand distributions are of interest, too. The respective snapshots can best be identified by evaluating the average HS strength and its standard deviation as shown in Figure 5.9(b), such that snapshots 40-42 are identified as snapshots with quite homogeneous capacity demand distributions. Consequently, as it can be expected based on the knowledge gained from the results of Section 5.2, the network capacity achieves values that range among the highest over the considered snapshot range, as can be seen from Figure 5.10. Also the gain for uncoordinated bandwidth allocations compared to coordinated bandwidth allocations is found to be among the highest for the considered snapshots, which is typical for homogeneous scenarios, too.

In order to gain more knowledge concerning the local performance of the automatic capacity optimization approaches for SONs, rather than the performance in the whole

scenario, a more detailed analysis is carried out. For this purpose, the strongest HS, i.e. the HS with the highest HS factor ρ_{hs} , in the real-world scenario is identified for each snapshot. Using this HS, the HS area, which is defined as the HS cells of the HS together with all cells that belong to all NGs of which the HS cells are part of, is identified for each snapshot. Only this HS area is considered in the following for the performance evaluation of the automatic capacity optimization approaches, enabling the local performance evaluation of the capacity optimization approaches in areas with inhomogeneous capacity demand distributions.

Figure 5.11 shows for the considered snapshot range the performance results of the capacity optimization approaches for the HS areas of the strongest HSs in terms of the spectral efficiencies $\epsilon_{N_{\text{nw}}}$ and $\epsilon_{R_{\text{nw}}}$, respectively, and for PF scheduling as well as FT scheduling. The legend of Figure 5.11(b) holds for all plots of Figure 5.11. Comparing

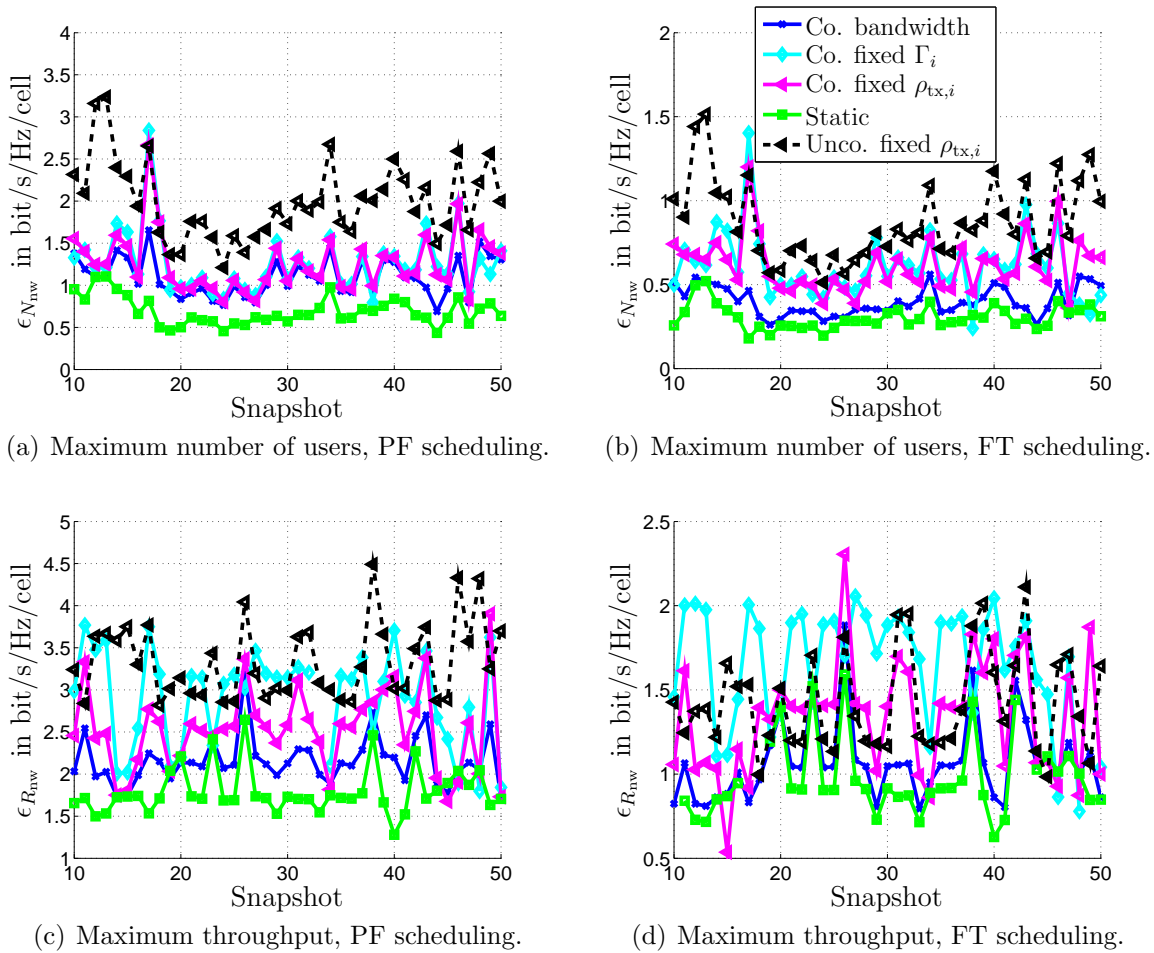


Figure 5.11. Performance results of the maximization of the total number of users and of the network throughput maximization for the HS areas of the strongest HSs and for PF scheduling and FT scheduling.

Figure 5.11 with Figure 5.10 shows that for the HS areas of the strongest HSs, the performance of the automatic capacity optimization approaches for SONs increases relative to state of the art scheduling based approaches, compared to the performance for the whole scenario. This effect is much more pronounced for the network throughput maximization than for the maximization of the total number of users. The largest difference between the performance for the HS area of the strongest HS and the performance for the whole scenario can be observed for the network throughput maximization and FT scheduling, according to Figure 5.10 and Figure 5.11.

The observation concerning the performance differences for the HS area of the strongest HSs and the performance for the whole scenario are completely according to the simulation results of Section 5.2, where it was shown that uncoordinated bandwidth allocations outperform coordinated bandwidth allocations for homogeneous and slightly inhomogeneous capacity demands, such that the performance of coordinated bandwidth allocations for the whole scenario, which also contains areas with homogeneous and low inhomogeneous capacity demand, must be lower than the performance of coordinated resource allocations for the HS area of the strongest HS. Also the larger performance differences that can be observed for the network throughput maximization compared to the maximization of the number of users are in accordance to the results of Section 5.2, since in network throughput maximization, a large part of the throughput comes from areas with homogeneous or low inhomogeneous capacity demand, such that the gain of the coordinated bandwidth allocations does not become obvious when considering large areas or a complete scenario. Finally, the performance gain for FT scheduling is larger than for PF scheduling since the controlling of ICI, as it is achieved by the coordinated bandwidth allocations, has more effect with FT scheduling than with PF scheduling, according to Section 5.2.

Thus, above observations and the results of Figure 5.11 make clear that automatic capacity optimization approaches are especially of interest for application to local areas that experience inhomogeneous and varying capacity demand. In order to strengthen this finding further and in order to investigate the gains of the implementation of automatic capacity optimization approaches for SONs in different areas with inhomogeneous capacity demand more in detail, the real-world scenario is further investigated with respect to the strongest HSs of the considered snapshots. In this context, the sectors of the scenario are analyzed with respect to their belonging to the HS areas of the strongest HSs. Figure 5.12(a) shows the result of this analysis in terms of the probability of each sector to belong to the HS area of the strongest HSs of the considered snapshots. Figure 5.12(b) provides more detail of this analysis by showing which sectors belong to the HS area of the strongest HS for each of the considered snapshots.

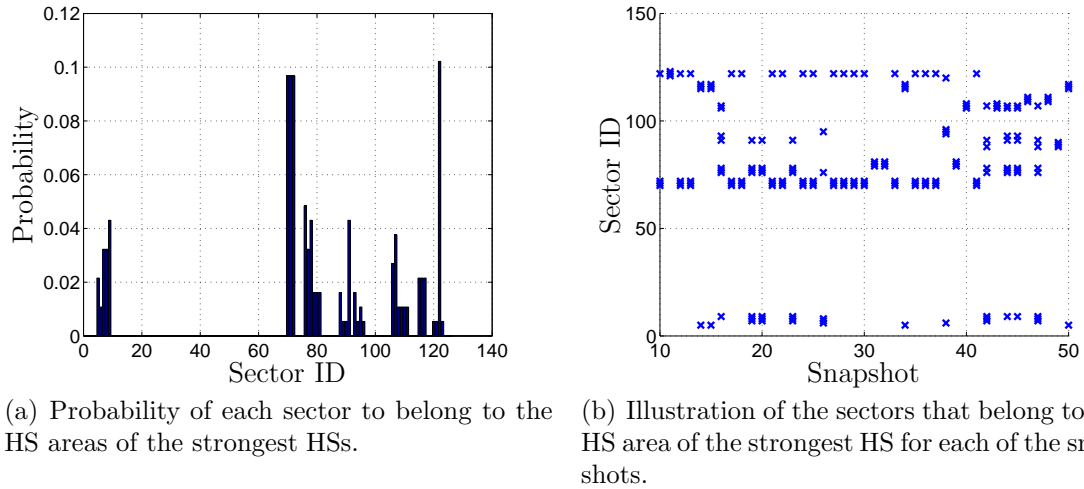


Figure 5.12. Analysis of the real-world scenario with respect to the strongest HSs of the considered snapshots.

Figure 5.12 allows interesting conclusions concerning the application of automatic capacity optimization approaches for SONs to the considered real-world scenario. Firstly, it is interesting to analyze the locations of the strongest HSs. Figure 5.12(a) shows that the strongest HSs in the real-world scenario appear preferably in the areas of certain sectors, such that it can be expected that the strongest HSs do not appear in many different places. This observation is supported by considering Table 5.3, which compiles the information from Figure 5.12 to relate different probabilities of a sector to belong to the HS area of the strongest HS with the number of sectors that have at least this probability to belong to the HS area of the strongest HSs and with the percentage of the HS areas of the strongest HSs that contain the respective sectors. The table

Table 5.3. Relation of the probability of a sector to belong to the HS area of the strongest HS with the number of sectors that have at least this probability to belong to the HS area of the strongest HS and with the percentage of the strongest HS that contain the respective sectors.

| HS probability | Number of sectors | Percentage of considered HSs |
|----------------|-------------------|------------------------------|
| <0.01 | 35 | 100% |
| 0.01 | 28 | 96% |
| 0.02 | 17 | 82% |
| 0.03 | 12 | 70% |
| 0.04 | 8 | 57% |
| 0.05 | 4 | 39% |

shows that only 35 sectors of the sectors of the inner area of the scenario, which is the part of the scenario that is considered for automatic capacity optimization, belong to

the HS area of at least one of the strongest HSs. This means, according to Table 5.2, that in the coverage area of almost fifty percent of the sectors of the inner area of the scenario, the strongest HS never appears. Another information that can be taken from Table 5.3 is, for example, that there are only 8 sectors that belong to the HS areas of at least four percent of the strongest HSs, and that these 8 sectors are part of the HS areas of 57 percent of the strongest HSs. Together with Figure 5.12(b), which shows the sectors that belong to the HS areas of the strongest HS of each snapshot, it can be concluded that the strongest HSs appear in only few areas repeatedly.

Secondly, it is interesting to relate the locations at which the strongest HSs appear with the performance results obtained for the HS areas of the strongest HSs. For this purpose, Figure 5.12(b) can be used to identify the location of the strongest HS for each of the snapshots. It can be seen from the figure that frequent locations of the strongest HS are, for example, the coverage areas of sectors 70, 71, 72 and 122, which will in the following be referred to as HS area 1. Another area in which the strongest HS is located frequently is the area covered by sectors 9, 76, 77, 78 and 91, which will in the following be referred to as HS area 2. Identifying the snapshots in which the strongest HS is located in each of the two mentioned areas and referring to Figure 5.11 to obtain the performance of the capacity optimization approaches for the respective snapshots allows to evaluate the performance of the automatic capacity optimization approaches for SONS for the two HS areas. This way, the different areas that exhibit inhomogeneous capacity demands and that are, consequently, of interest for the application of automatic capacity optimization approaches for SONS can be analyzed with respect to the gain that can be expected by the application of the new approaches and promising areas for the implementation of automatic capacity optimization approaches for SONS can be identified.

In order to illustrate this procedure, the snapshots with the strongest HS in HS area 1 and in HS area 2 are identified using Figure 5.12(b). The results are shown in Figure 5.13(a) for HS area 1 and in Figure 5.13(c) for HS area 2. The sector IDs given above to define the two HS areas can be read from the figures. It can be seen from Figure 5.13(c) that HS area 2 is actually larger than given above and that it changes over time. Figure 5.13(b) and Figure 5.13(d) show the performance results of the capacity optimization approaches for network throughput maximization and for FT scheduling in the respective HS area. The values are obtained from Figure 5.11(d) according to the snapshots identified by Figure 5.13(a) and Figure 5.13(c), respectively.

Thus, Figure 5.13(b) and Figure 5.13(d) contain the performance of the automatic capacity optimization approaches if the strongest HS is located in HS area 1 or in HS area 2, respectively. As a consequence, the figures show the performance of the

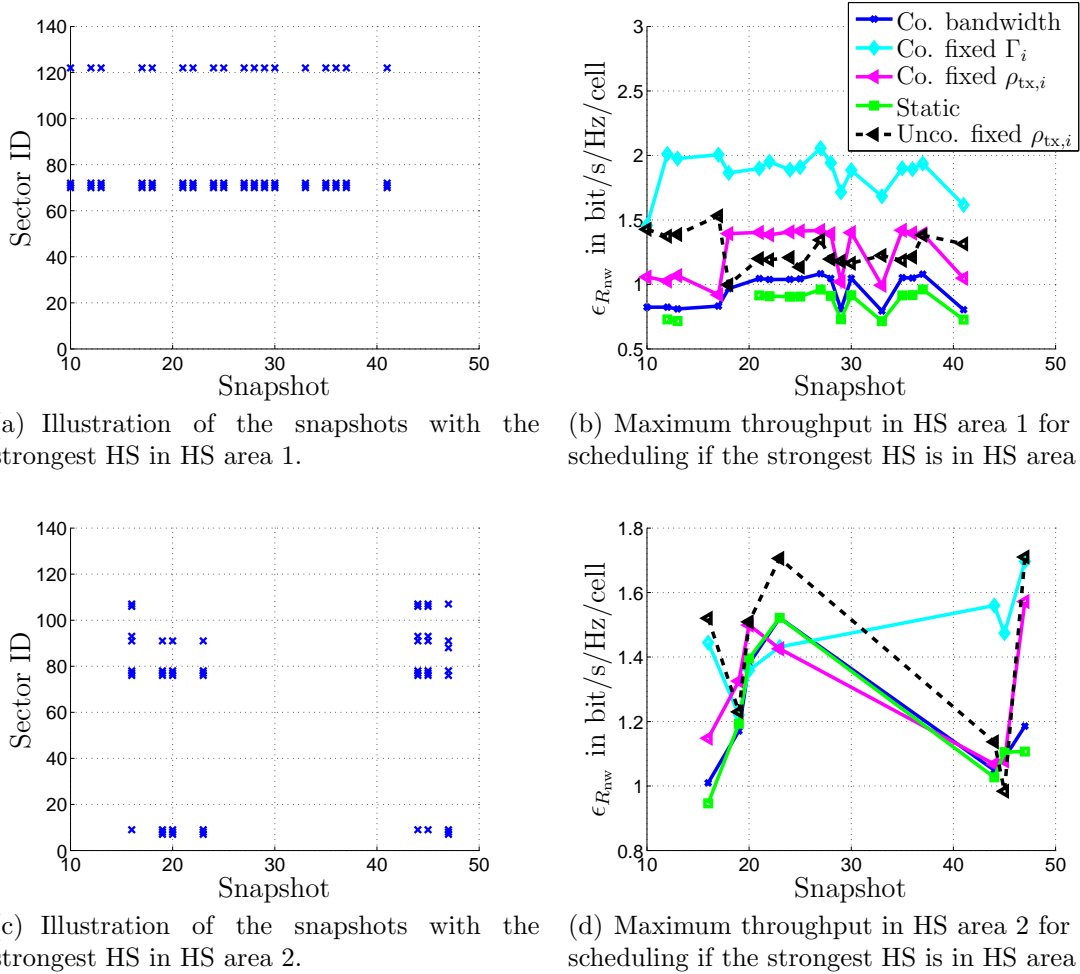


Figure 5.13. Performance analysis of the automatic capacity optimization approaches for HS area 1 and for HS area 2 if the strongest HS is in HS area 1 or in HS area 2, respectively.

automatic capacity optimization approaches for the two different HS areas. It can be seen that in HS area 1, automatic capacity optimization approaches for SONs clearly outperform state of the art scheduling based approaches, depending on the resource allocation technique, and achieve large gains, such that the implementation of automatic capacity optimization approaches for SONs is promising for HS area 1. In HS area 2, automatic capacity optimization approaches for SONs do not for all snapshots outperform state of the art scheduling based approaches. In average, however, automatic capacity optimization approaches for SONs achieve superior performance compared to state of the art scheduling based approaches, depending on the resource allocation technique.

Chapter 6

Summary and Outlook

In this thesis, automatic capacity optimization for SONs is investigated. The proposed automatic capacity optimization approaches for SONs adapt the network to changing and inhomogeneous capacity demands such that at all times and all places, only as much capacity as required is delivered. The capacity that is delivered by the network is adjusted by means of a capacity demand oriented allocation of the radio resources cell bandwidth and transmit power.

The challenge in the context of automatic capacity optimization for SONs is the combination of frequently made allocations of resources to the users in time intervals of milliseconds, as carried out by the schedulers of the cells, with the optimization of the capacity of the network, which needs to consider many cells at the same time. Chapter 2 presents an approach that solves this challenge. It proposes a hierarchic concept for the coordination of automatic capacity optimization and scheduling that separates the frequently carried out scheduling decisions and the capacity optimization decisions into two different planes. The concept is hierarchic since the capacity optimization approaches of the upper plane determine certain limits and requirements concerning the resource allocations of the cells such that the network capacity is optimized. These limits and requirements have to be observed by the scheduling carried out in the lower plane. This way, for each of the tasks of capacity optimization and scheduling, respectively, specific approaches can be applied that are designed with respect to the specific challenges of the task.

For the lower plane, state of the art scheduling approaches are well suited. Concerning the capacity optimization carried out in the upper plane, Chapter 2 presents a cell-centric modeling approach that models the relation between allocated resources and cell performance. The cell-centric network model focuses on the cells, rather than on the individual users, such that the modeling complexity is greatly reduced. At the same time, the distribution of the users, the QoS requirements of the users and the environment is considered in the model such that high accuracy is achieved. The cell-centric network model is derived for different scheduling strategies and approaches for the practical implementation of the model are given.

Using the cell-centric network model and the hierarchic concept for the coordination of automatic capacity optimization and scheduling, new automatic capacity optimization

approaches for SONs as well as state of the art scheduling based approaches can be considered in simulation and analysis, such that the new approaches can be compared to the state of the art scheduling based approaches.

Chapter 3 proposes different approaches for the automatic capacity optimization of a cellular radio network. The approaches consist of a method for the detection of the need for optimization and of several different optimization problems that optimize the capacity of the network. Detection of the need for optimization and the optimization problems for capacity optimization both use the cell-centric network model. The network is optimized with respect to the total network throughput and the total number of users that can be supported, respectively. The network optimization is achieved by the capacity demand oriented allocation of cell bandwidth, transmit power or both, cell bandwidth and transmit power, jointly.

The process of obtaining the solution of the proposed optimization problems is discussed in Chapter 4. Different algorithms for obtaining the solutions by a central instance and in a distributed way are presented. The central solving algorithms are especially of interest for simulation and analysis purposes. The Distributed algorithms are relevant for practical implementation. Due to the application of the cell-centric network model with low modeling complexity, the solutions can be found quickly and efficiently.

The automatic capacity optimization approaches for SONs are evaluated in Chapter 5. Two different analysis are carried out. The functional analysis verifies the automatic capacity optimization approaches and investigates their behavior and performance. For this purpose, a simulation approach with scenarios specifically for the evaluation of automatic capacity optimization for SONs in scenarios with inhomogeneous capacity demand is proposed. The functional analysis verifies the presented approaches for automatic capacity optimization for SONs and shows that automatic capacity optimization approaches for SONs outperform state of the art scheduling based approaches for inhomogeneous capacity demands and that the QoS of the users is observed using the cell-centric network model. Concerning the influence of the distribution and the size of the capacity demand HSs, it is shown that transmit power allocation is preferably to be used in scenarios with larger HSs that consist of several clustered HS cells. Cell bandwidth, on the other hand, achieves high performance in scenarios with several smaller HSs that are distributed over the scenario. Joint resource allocation is capable of exploiting the strengths of both, transmit power allocation and cell bandwidth allocation, to a certain degree.

The different optimization goals and different scheduling strategies do not influence

the performance of the automatic capacity optimization approaches for SONS qualitatively, as shown in the functional analysis. However, it is found that automatic capacity optimization for SONS provides higher gains with FT scheduling than with FR scheduling since users at the cell borders, which have more effect on the overall performance with FT scheduling than with PF scheduling, benefit more from automatic capacity optimization for SONS. Furthermore, it was found that transmit power allocation is of less relevance for practical application since it requires large transmit power differences in order to adapt a network to inhomogeneous capacity demands, such that low SINR values may result, which can be problematic with physical layer transmission techniques.

The second simulation approach pursued in Chapter 5 analyses the performance of the automatic capacity optimization approaches for SONS in a real-world scenario. For this purpose, a simulation approach that derives a real-world scenario using measurement data from a real network is presented. In the derivation of the real-world scenario, throughput measurement data is used to model the inhomogeneous capacity demand while predictions of the user distribution and the signal propagation conditions, as they are used in network planning, are used to determine cell areas and cell borders. The performance analysis carried out in this scenario confirms the results from the functional analysis. Furthermore, the real-world scenario is investigated with respect to the location of appearance of HSs and it is shown that the HSs usually appear in only few places repeatedly. Thus, the application of automatic capacity optimization approaches for SONS is especially in these areas of interest. The performance of the automatic capacity optimization approaches for SONS is evaluated especially in the areas of frequent appearance of HSs of the real-world scenario and it is shown that automatic capacity optimization for SONS is capable of achieving high performance gains locally.

Concerning further related research, the capability of the proposed cell-centric network model to express how efficient radio resources are used by the cells is of interest. This capability is already applied in this thesis in the optimization problems that are applied to carry out the capacity optimization of the network. The same way, the cell-centric network model could also be used in other planning and optimization processes by formulating the processes as optimization problems that use the cell-centric network model in objective functions and constraints. The capability of the cell-centric network model to express the efficiency of resource usage could, thus, be further exploited in the optimization and planning of parameters such as pilot power or BS locations, for example.

Furthermore, the capability of the cell-centric network model to assess the efficiency

of radio resource use can be applied to determine the cost of radio resources or, vice versa, the value of the radio resources for each cell individually. This information is available in real-time since it is obtained from system measurements. Based on such pricing information, the trading of radio resources or radio spectrum is enabled. Spectrum could then be traded analogously to stocks or energy at electronic markets, given an appropriate infrastructure. The trading would be fine-granular in time as well as in space, since the cell-centric model allows to determine real-time prices for each cell individually. Participants in such markets would be network operators that could temporarily sell or rent spectrum to each other, depending on their current and individual demand of spectrum and supply with spectrum. Pursuing this idea further, also regulators could enter the market, offering the spectrum to any participant in the market. Traditional regulation with the assignment of large parts of the spectrum to individual operators for long times would, thus, be obsolete. Instead, every market participant could supply itself with spectrum on demand, leading to a transparent and competitive market and, therefore, to an efficient use of the limited spectrum.

Note that the automatic capacity optimization approaches for SONs proposed in this thesis and the outlook concerning the further application of the cell-centric network model for planning and optimization tasks would require a time horizon of possibly several years to be implemented in cellular radio networks. The outlook concerning the trading of radio spectrum at electronic markets, as presented in the last paragraph, is visionary with prospects of being realized in even further future.

Appendix

A.1 Analytical Derivation of Achievable User Bit Rate and Required User Bandwidth

This section gives the full formulae of the analytical derivation of the pdf $f_{\mathbf{R}_u^{(i)}}(R_u^{(i)})$ of achievable user bit rate and the pdf $f_{\mathbf{B}_u^{(i)}}(B_u^{(i)})$ of required user bandwidth as introduced in Section 2.4.2. According to Section 2.4.2, the user position pdf holds for each user, such that user indices can be neglected for the user specific pdfs.

It is assumed that users are uniformly distributed over the circular shaped cell area as expressed by the user position pdf of (2.26). The pathloss between UE and BS depends on the distance r but not on the angle φ , such that the pdf of the radius is required, which is given by

$$\begin{aligned} p_{\mathbf{r}}^{(i)}(r) &= \int_0^{2\pi} p_{\mathbf{r},\varphi}^{(i)}(r, \varphi) d\varphi \\ &= \int_0^{2\pi} \frac{r}{\pi S_i^2} d\varphi \\ &= \frac{2r}{S_i^2}, \quad 0 < r < S_i. \end{aligned} \tag{A.1}$$

Considering the height h_i of BS i in the expression of the total distance $d = \sqrt{h_i^2 + r^2}$ that the signal has to travel, the pdf of the total distance d yields

$$\begin{aligned} f_{\mathbf{d}}^{(i)}(d) &= p_{\mathbf{r}}^{(i)}(r(d)) \cdot \left| \frac{\partial r(d)}{\partial d} \right| \\ &= p_{\mathbf{r}}^{(i)}\left(\sqrt{d^2 - h_i^2}\right) \cdot \frac{d}{\sqrt{d^2 - h_i^2}} \\ &= \frac{2d}{S_i^2}, \quad h_i < d < \sqrt{S_i^2 + h_i^2}. \end{aligned} \tag{A.2}$$

Using the pathloss model of (2.6) in a RV transformation of (A.2) leads to the pdf of the pathloss in dB

$$\begin{aligned} f_{\mathbf{a}_{\text{pl}}^{(i)}}(a_{\text{pl}}^{(i)}) &= f_{\mathbf{d}}^{(i)}\left(d(a_{\text{pl}}^{(i)})\right) \cdot \left| \frac{\partial d(a_{\text{pl}}^{(i)})}{\partial a_{\text{pl}}^{(i)}} \right| \\ &= f_{\mathbf{d}}^{(i)}\left(10^{\frac{a_{\text{pl}}^{(i)} - a_0}{10\alpha}}\right) \cdot \frac{\ln(10)}{10\alpha} 10^{\frac{a_{\text{pl}}^{(i)} - a_0}{10\alpha}} \\ &= \frac{\ln(10)}{5\alpha S_i^2} \cdot 10^{\frac{a_{\text{pl}}^{(i)} - a_0}{5\alpha}} \\ &= \frac{\ln(10)}{5\alpha S_i^2} \cdot e^{\frac{\ln(10)}{5\alpha}(a_{\text{pl}}^{(i)} - a_0)}, \quad a_{\text{pl}}^{(i)}(h_i) < a_{\text{pl}}^{(i)} < a_{\text{pl}}^{(i)}\left(\sqrt{S_i^2 + h_i^2}\right), \end{aligned} \tag{A.3}$$

and the pdf of the total signal attenuation in dB is obtained by the convolution of the pdf of the path loss in dB from (A.3) with the pdf of the independent slow fading process in dB from (2.7)

$$\begin{aligned}
f_{\mathbf{a}^{(i)}}(a^{(i)}) &= \int_{a_{\text{pl,min}}^{(i)}}^{a_{\text{pl,max}}^{(i)}} f_{\mathbf{a}_{\text{pl}}^{(i)}}(a_{\text{pl}}^{(i)}) \cdot f_{\mathbf{a}_{\text{sf}}}(a^{(i)} - a_{\text{pl}}^{(i)}) da_{\text{pl}}^{(i)} \\
&= \frac{\ln(10)}{5\alpha S_i^2} \cdot \frac{1}{\sigma_{\text{sf}}\sqrt{2\pi}} \cdot \int_{a_{\text{pl,min}}^{(i)}}^{a_{\text{pl,max}}^{(i)}} e^{\frac{\ln(10)}{5\alpha}(a_{\text{pl}}^{(i)} - a_0)} \cdot e^{-\frac{1}{2\sigma_{\text{sf}}^2}(a^{(i)} - a_{\text{pl}}^{(i)})^2} da_{\text{pl}}^{(i)} \\
&= \frac{\ln(10)}{5\alpha S_i^2} \cdot \frac{1}{\sigma_{\text{sf}}\sqrt{2\pi}} \cdot e^{-\frac{\ln(10)}{5\alpha}a_0} \cdot \int_{a_{\text{pl,min}}^{(i)}}^{a_{\text{pl,max}}^{(i)}} e^{\frac{\ln(10)}{5\alpha}a_{\text{pl}}^{(i)} - \frac{1}{2\sigma_{\text{sf}}^2}(a^{(i)} - a_{\text{pl}}^{(i)})^2} da_{\text{pl}}^{(i)}.
\end{aligned} \tag{A.4}$$

Defining for reasons of convenience the constants

$$\begin{aligned}
c_1 &= \frac{\ln(10)}{5\alpha S_i^2} \cdot \frac{1}{\sigma_{\text{sf}}\sqrt{2\pi}} \cdot e^{-\frac{\ln(10)}{5\alpha}a_0} \\
c_2 &= \frac{\ln(10)}{5\alpha} \\
c_3 &= \frac{1}{2\sigma_{\text{sf}}^2}
\end{aligned} \tag{A.5}$$

yields the final expression for the pdf of the total signal attenuation in dB

$$\begin{aligned}
f_{\mathbf{a}^{(i)}}(a^{(i)}) &= c_1 \int_{a_{\text{pl,min}}^{(i)}}^{a_{\text{pl,max}}^{(i)}} e^{c_2 a_{\text{pl}}^{(i)} - c_3 (a^{(i)} - a_{\text{pl}}^{(i)})^2} da_{\text{pl}}^{(i)} \\
&= \frac{c_1 \sqrt{\pi}}{2\sqrt{c_3}} \cdot e^{\frac{c_2^2}{4c_3} + c_2 a^{(i)}} \\
&\quad \left(\operatorname{erf} \left(\frac{c_2 + 2c_3 (a^{(i)} - a_{\text{pl,min}}^{(i)})}{2\sqrt{c_3}} \right) - \operatorname{erf} \left(\frac{c_2 + 2c_3 (a^{(i)} - a_{\text{pl,max}}^{(i)})}{2\sqrt{c_3}} \right) \right) \\
&= \frac{c_2}{2S_i^2} \cdot e^{\frac{c_2^2}{4c_3} + c_2 (a^{(i)} - a_0)} \\
&\quad \left(\operatorname{erf} \left(\frac{c_2 + 2c_3 (a^{(i)} - a_{\text{pl,min}}^{(i)})}{2\sqrt{c_3}} \right) - \operatorname{erf} \left(\frac{c_2 + 2c_3 (a^{(i)} - a_{\text{pl,max}}^{(i)})}{2\sqrt{c_3}} \right) \right).
\end{aligned} \tag{A.6}$$

Using the pdf of the SINR of (2.28) and considering the related assumptions concerning position independent ICI yields

$$\begin{aligned}
f_{\gamma^{(i)}}(\gamma^{(i)}) &= f_{\mathbf{a}^{(i)}} \left(10 \cdot \log_{10} \left(\frac{\Gamma_i}{\gamma^{(i)}} \right) \right) \cdot \frac{10}{\gamma^{(i)} \cdot \ln(10)} \\
&= \frac{5c_2}{S_i^2 \gamma^{(i)} \ln(10)} \cdot e^{\frac{c_2^2}{4c_3} + c_2 \left(10 \cdot \log_{10} \left(\frac{\Gamma_i}{\gamma^{(i)}} \right) - a_0 \right)} \\
&\quad \left(\operatorname{erf} \left(\frac{c_2 + 2c_3 \left(10 \cdot \log_{10} \left(\frac{\Gamma_i}{\gamma^{(i)}} \right) - a_{\text{pl,min}}^{(i)} \right)}{2\sqrt{c_3}} \right) \right. \\
&\quad \left. - \operatorname{erf} \left(\frac{c_2 + 2c_3 \left(10 \cdot \log_{10} \left(\frac{\Gamma_i}{\gamma^{(i)}} \right) - a_{\text{pl,max}}^{(i)} \right)}{2\sqrt{c_3}} \right) \right).
\end{aligned} \tag{A.7}$$

With (2.19) and defining $x = 2^{\frac{R_u^{(i)}}{B_u^{(i)}}} - 1$, the pdf of the achievable user bit rate

$$\begin{aligned}
f_{\mathbf{R}_u^{(i)}} \left(R_u^{(i)} \right) &= f_{\gamma}^{(i)} (x) \cdot 2^{\frac{R_u^{(i)}}{B_u^{(i)}}} \ln(2) \frac{1}{B_u^{(i)}} \\
&= \frac{5c_2}{S_i^2(x) \ln(10)} \cdot e^{\frac{c_2^2}{4c_3} + c_2(10 \cdot \log_{10}(\frac{\Gamma_i}{x}) - a_0)} \cdot 2^{\frac{R_u^{(i)}}{B_u^{(i)}}} \ln(2) \frac{1}{B_u^{(i)}} \\
&\quad \left(\operatorname{erf} \left(\frac{c_2 + 2c_3(10 \cdot \log_{10}(\frac{\Gamma_i}{x}) - a_{\text{pl,min}}^{(i)})}{2\sqrt{c_3}} \right) \right. \\
&\quad \left. - \operatorname{erf} \left(\frac{c_2 + 2c_3(10 \cdot \log_{10}(\frac{\Gamma_i}{x}) - a_{\text{pl,max}}^{(i)})}{2\sqrt{c_3}} \right) \right), \tag{A.8}
\end{aligned}$$

follows, and with (2.20), the pdf of the required user bandwidth is obtained

$$\begin{aligned}
f_{\mathbf{B}_u^{(i)}} \left(B_u^{(i)} \right) &= f_{\gamma}^{(i)} (x) \cdot 2^{\frac{R_u^{(i)}}{B_u^{(i)}}} \ln(2) \frac{R_u^{(i)}}{B_u^{(i)^2}} \\
&= \frac{5c_2}{S_i^2(x) \ln(10)} \cdot e^{\frac{c_2^2}{4c_3} + c_2(10 \cdot \log_{10}(\frac{\Gamma_i}{x}) - a_0)} \cdot 2^{\frac{R_u^{(i)}}{B_u^{(i)}}} \ln(2) \frac{R_u^{(i)}}{B_u^{(i)^2}} \\
&\quad \left(\operatorname{erf} \left(\frac{c_2 + 2c_3(10 \cdot \log_{10}(\frac{\Gamma_i}{x}) - a_{\text{pl,min}}^{(i)})}{2\sqrt{c_3}} \right) \right. \\
&\quad \left. - \operatorname{erf} \left(\frac{c_2 + 2c_3(10 \cdot \log_{10}(\frac{\Gamma_i}{x}) - a_{\text{pl,max}}^{(i)})}{2\sqrt{c_3}} \right) \right). \tag{A.9}
\end{aligned}$$

Note that the analytical derivation of mean

$$\mu_{\{R_u^{(i)}, B_u^{(i)}\}} = \int_0^\infty \{R_u^{(i)}, B_u^{(i)}\} \cdot f_{\{\mathbf{R}_u^{(i)}, \mathbf{B}_u^{(i)}\}} (\{R_u^{(i)}, B_u^{(i)}\}) d\{R_u^{(i)}, B_u^{(i)}\} \tag{A.10}$$

and variance

$$\sigma_{\{R_u^{(i)}, B_u^{(i)}\}}^2 = \int_0^\infty \left(\{R_u^{(i)}, B_u^{(i)}\} - \mu_{\{R_u^{(i)}, B_u^{(i)}\}} \right)^2 \cdot f_{\{\mathbf{R}_u^{(i)}, \mathbf{B}_u^{(i)}\}} (\{R_u^{(i)}, B_u^{(i)}\}) d\{R_u^{(i)}, B_u^{(i)}\} \tag{A.11}$$

could not be carried out. Instead, numerical methods can be used to determine mean and variance of achievable user bit rate and required user bandwidth.

A.2 Further Simulation Results

A.2.1 Influence of the HS Distribution

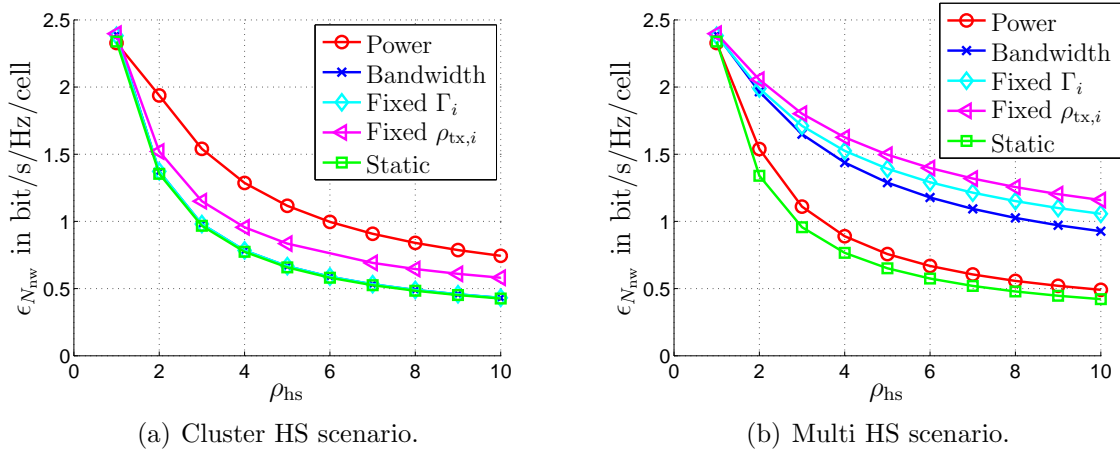


Figure A.1. Performance results of the maximization of the number of users in the Cluster HS Scenario and the Multi HS Scenario with coordinated bandwidth allocations and for PF scheduling.

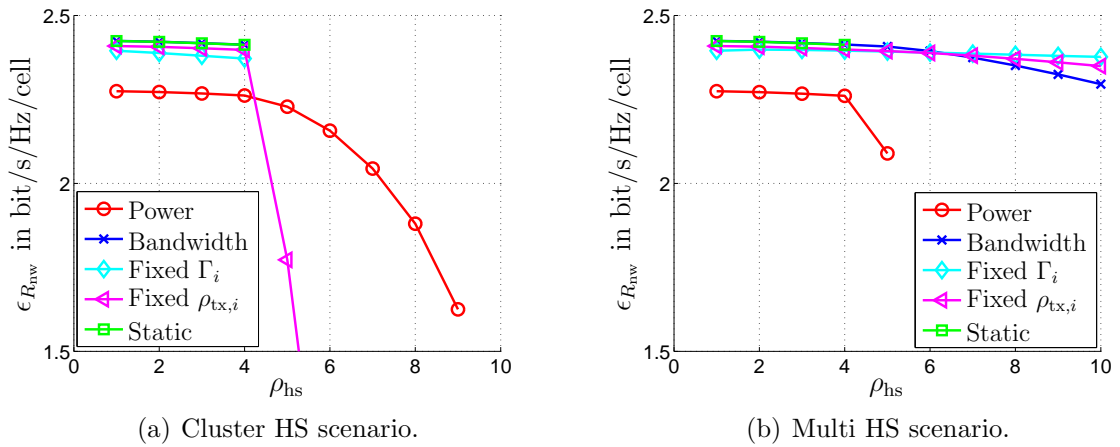
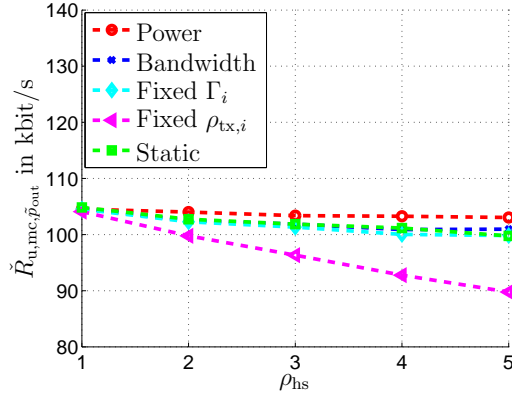
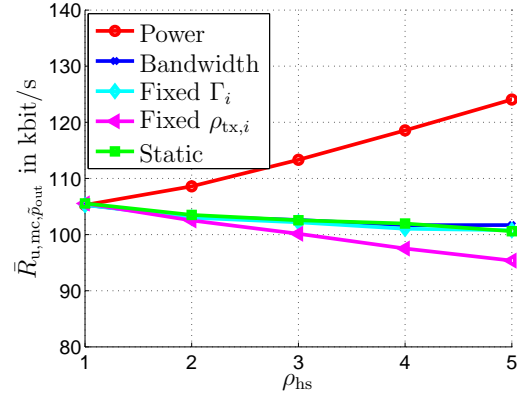


Figure A.2. Performance results of the network throughput maximization in the Cluster HS Scenario and the Multi HS Scenario with coordinated bandwidth allocations and for PF scheduling.

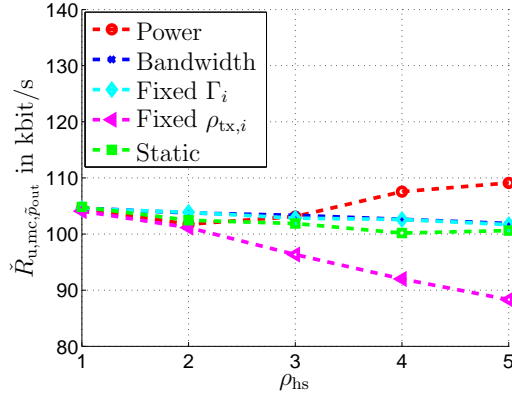
A.2.2 QoS Performance Evaluation for PF scheduling



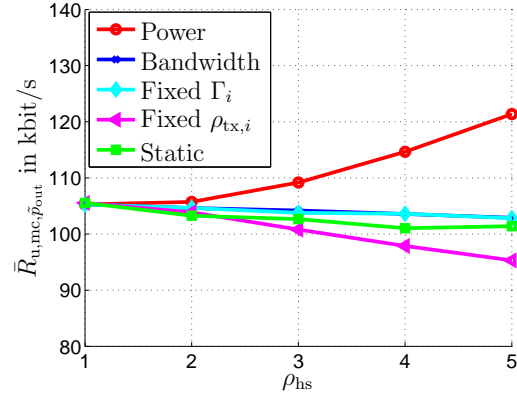
(a) Cluster HS scenario, minimum.



(b) Cluster HS scenario, average.

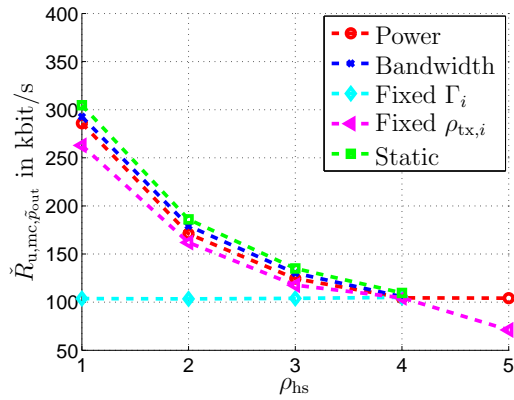


(c) Multi HS scenario, minimum.

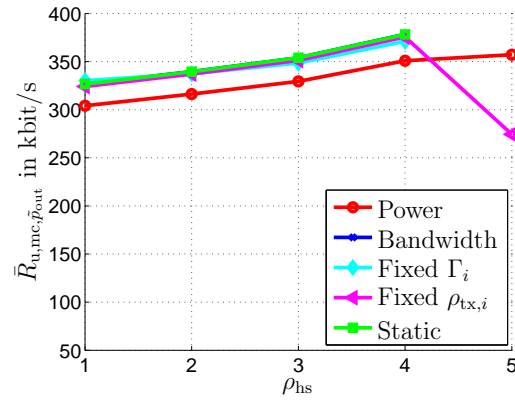


(d) Multi HS scenario, average.

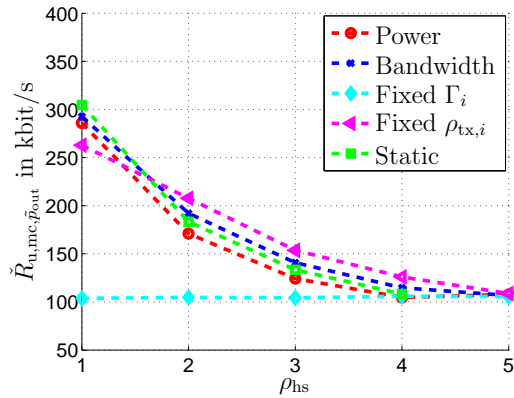
Figure A.3. Average $\bar{R}_{u,mc,\tilde{p}_{out}}$ and minimum $\hat{R}_{u,mc,\tilde{p}_{out}}$ of the p_{out} -percentile of the user bit rates of the cells for the maximization of the number of users with coordinated bandwidth allocations in the Cluster HS Scenario and the Multi HS Scenario and for PF scheduling obtained from MC simulations.



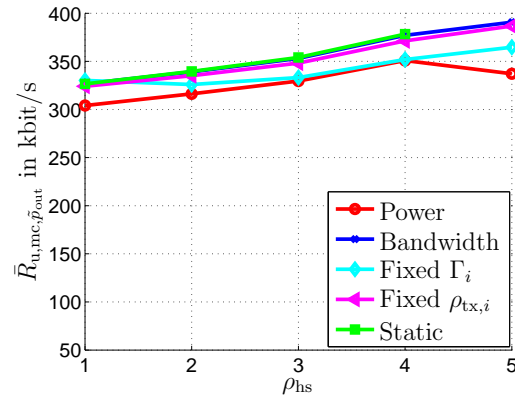
(a) Cluster HS scenario, minimum.



(b) Cluster HS scenario, average.



(c) Multi HS scenario, minimum.



(d) Multi HS scenario, average.

Figure A.4. Average $\bar{R}_{u,mc,\bar{p}_{out}}$ and minimum $\check{R}_{u,mc,\bar{p}_{out}}$ of the p_{out} -percentile of the user bit rates of the cells for the network throughput maximization with coordinated bandwidth allocations in the Cluster HS Scenario and the Multi HS Scenario and for PF scheduling obtained from MC simulations.

A.2.3 QoS Performance Evaluation for FT scheduling

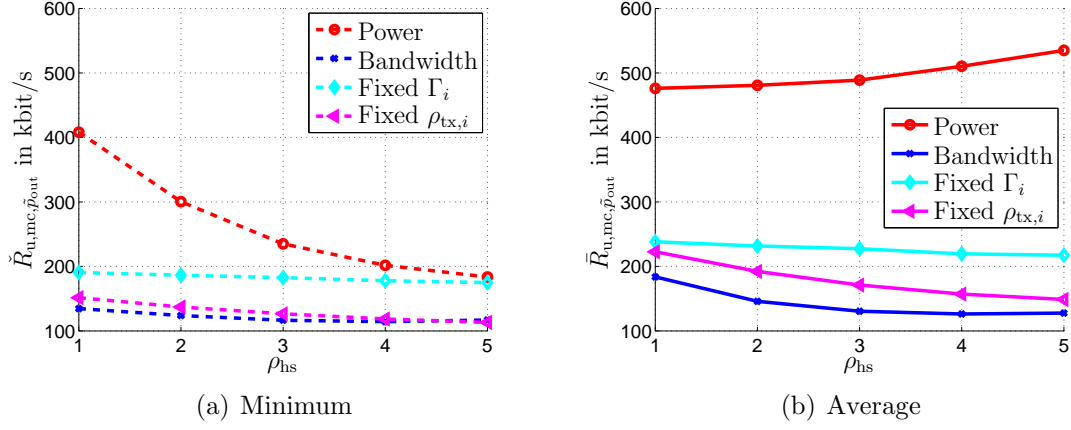


Figure A.5. Average $\bar{R}_{u,mc,\tilde{p}_{out}}$ and minimum $\check{R}_{u,mc,\tilde{p}_{out}}$ of the p_{out} -percentile of the user bit rates of the cells for the maximization of the total number of users with uncoordinated bandwidth allocations in the Single HS scenario obtained from MC simulations.

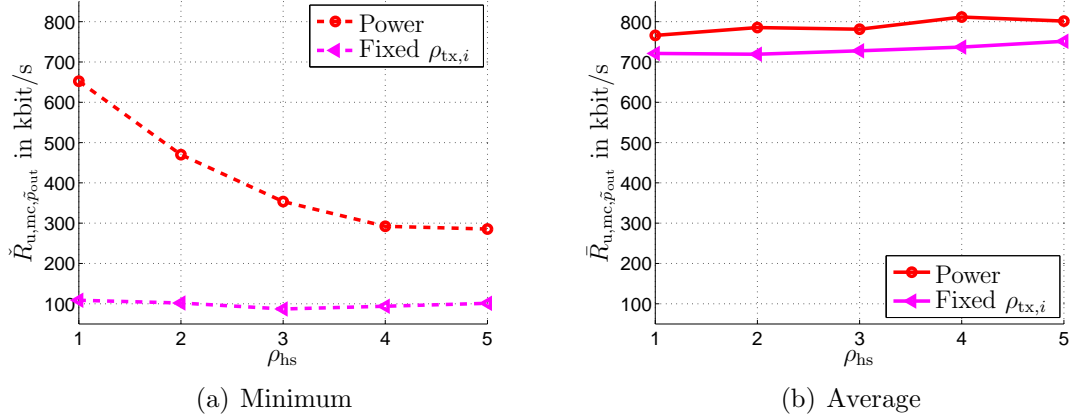
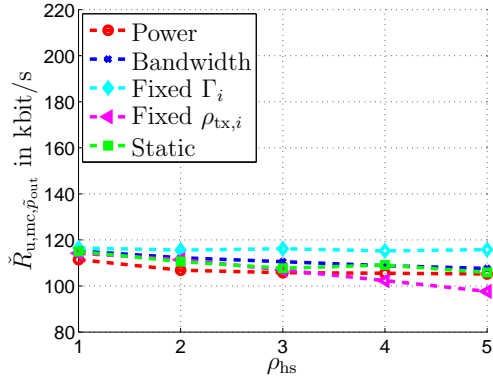
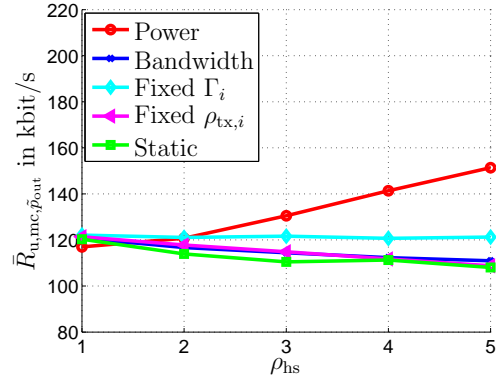


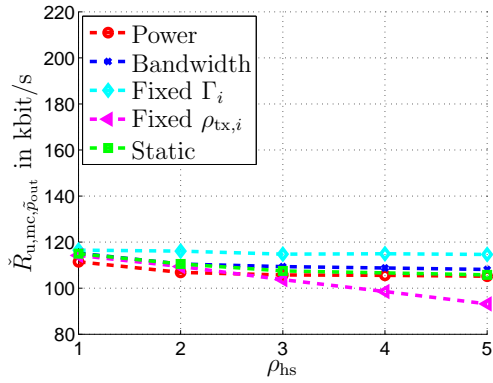
Figure A.6. Average $\bar{R}_{u,mc,\tilde{p}_{out}}$ and minimum $\check{R}_{u,mc,\tilde{p}_{out}}$ of the p_{out} -percentile of the user bit rates of the cells for the maximization of the network throughput with uncoordinated bandwidth allocations in the Single HS scenario obtained from MC simulations.



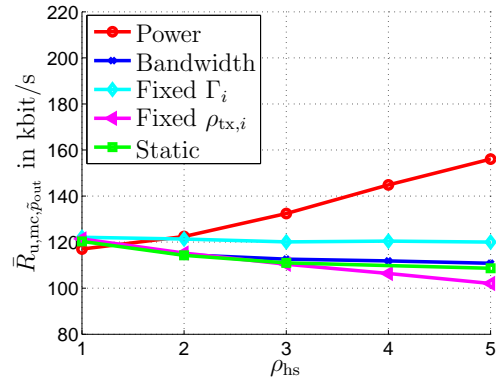
(a) Single HS scenario, minimum.



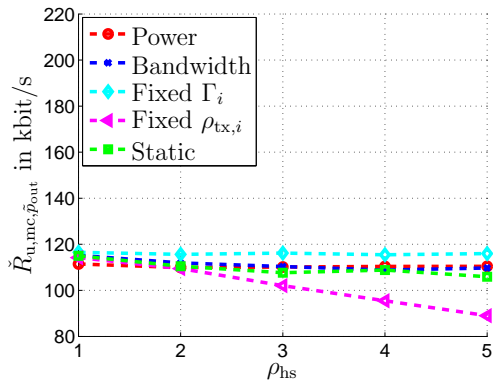
(b) Single HS scenario, average.



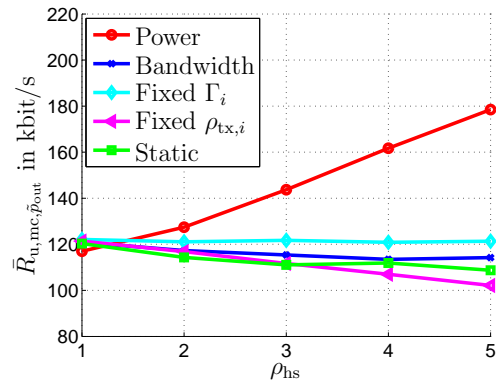
(c) Cluster HS scenario, minimum.



(d) Cluster HS scenario, average.

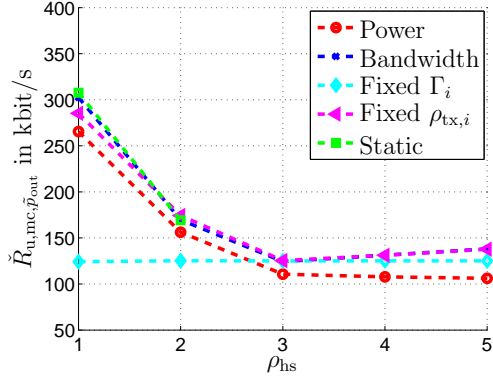


(e) Multi HS scenario, minimum.

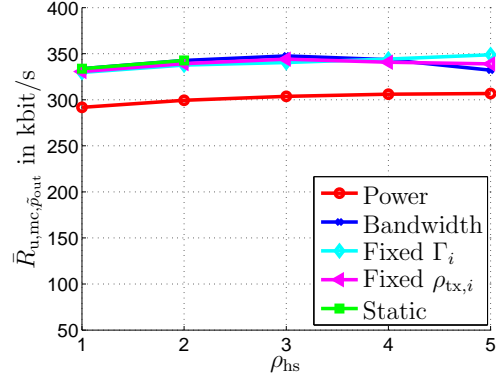


(f) Multi HS scenario, average.

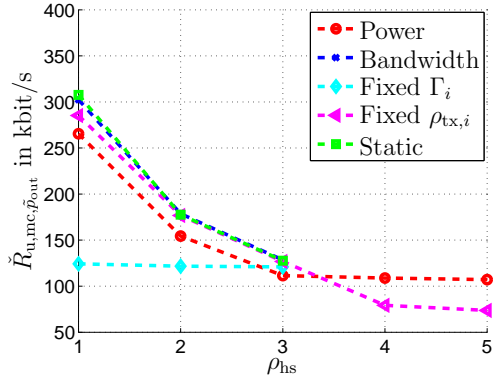
Figure A.7. Average $\bar{R}_{u,mc,\tilde{p}_{out}}$ and minimum $\hat{R}_{u,mc,\tilde{p}_{out}}$ of the p_{out} -percentile of the user bit rates of the cells for the maximization of the total number of users with coordinated bandwidth allocations obtained from MC simulations.



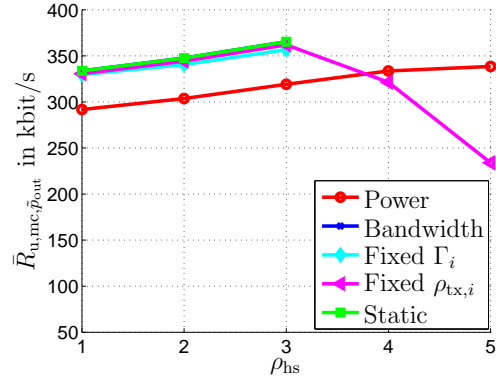
(a) Single HS scenario, minimum.



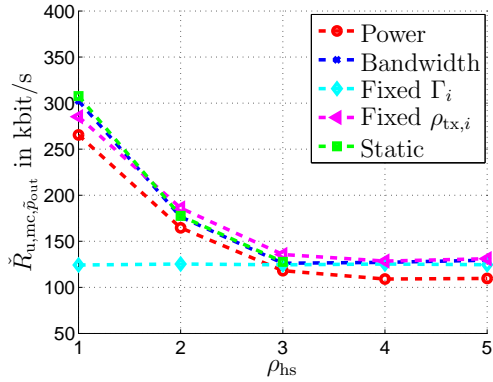
(b) Single HS scenario, average.



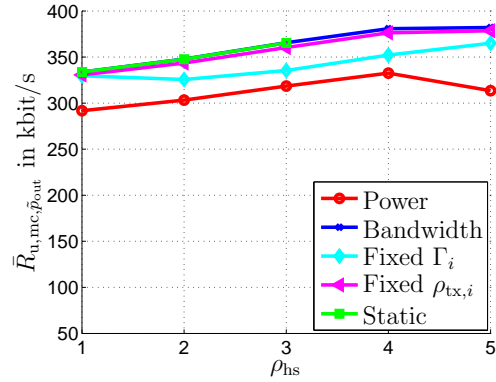
(c) Cluster HS scenario, minimum.



(d) Cluster HS scenario, average.



(e) Multi HS scenario, minimum.



(f) Multi HS scenario, average.

Figure A.8. Average $\bar{R}_{u,mc,\tilde{p}_{out}}$ and minimum $\hat{R}_{u,mc,\tilde{p}_{out}}$ of the p_{out} -percentile of the user bit rates of the cells for the maximization of the network throughput with coordinated bandwidth allocations obtained from MC simulations.

List of Acronyms

| | |
|--------------|--------------------------------------|
| 2G | 2 nd generation |
| 3G | 3 rd generation |
| 4G | 4 th generation |
| 3GPP | 3rd Generation Partnership Project |
| AMC | adaptive modulation and coding |
| BS | base station |
| CAPEX | capital expenditures |
| cdf | cumulative distribution function |
| CDMA | code division multiple access |
| CLT | Central Limit Theorem |
| DPC | Distributed Power Control |
| FR | Fair Resource |
| FT | Fair Throughput |
| FDMA | frequency division multiple access |
| HO | handover |
| HS | hotspot |
| ICI | inter-cell interference |
| ICIC | inter-cell interference coordination |
| IP | internet protocol |
| LP | linear program |
| LTE | Long Term Evolution |
| MIMO | multiple input multiple output |
| MC | Monte Carlo |
| MCS | Modulation and Coding Scheme |

| | |
|-------------|--|
| MSE | mean square error |
| NG | Neighborhood Group |
| NGMN | next generation mobile networks |
| OFDM | Orthogonal Frequency Division Multiplexing |
| OPEX | operational expenditures |
| UE | user equipment |
| PBR | Power-Bandwidth-Rate |
| PBN | Power-Bandwidth-Number-of-Users |
| PF | Proportional Fair |
| PSD | power spectral density |
| pdf | probability density function |
| QoS | Quality Of Service |
| RV | random variable |
| RRM | radio resource management |
| SAE | System Architecture Evolution |
| SCM | Spatial Channel Model |
| SINR | Signal to Interference plus Noise Ratio |
| SLP | Sequential Linear Programming |
| SNR | Signal to Noise Ratio |
| SON | self-organizing network |
| TDMA | time division multiple access |

List of Symbols

| | |
|----------------------------|--|
| $a_{ij}(r, \varphi)$ | average channel attenuation from cell j to position (r, φ) in cell i |
| \mathbf{b} | cell bandwidth vector |
| \mathbf{b}^* | optimum cell bandwidth vector |
| $\mathbf{b}^{(l)}$ | cell bandwidth vector of iteration l |
| B_i | cell bandwidth of cell i |
| \tilde{B}_i | outage bandwidth at cell-level of cell i |
| B_{sys} | total system bandwidth |
| $B_{u,n}^{(i)}$ | bandwidth of user n of cell i |
| $\tilde{B}_{u,n}^{(i)}$ | user bandwidth target for user n of cell i |
| $B_{u,\text{th}}^{(i)}$ | user bandwidth threshold to assign users to inner and outer area of cell i in fractional frequency reuse |
| $B_{u,k}^{(i)'}$ | user bandwidth resulting from the k -th SINR measurement of cell i |
| $\mathbb{B}_u^{(i)}$ | set of user bandwidths resulting from SINR measurements of cell i |
| β_i | relative cell bandwidth of cell i |
| \mathbf{C} | interference coupling matrix |
| D | reuse distance |
| \mathbf{E} | effective interference coupling matrix considering coordination |
| ϵ_i | cell spectral efficiency of cell i in bits/s/Hz |
| $\epsilon_{N_{\text{nw}}}$ | spectrum efficiency of the system for the maximization of the number of users in bits/s/Hz/cell |
| $\epsilon_{R_{\text{nw}}}$ | spectrum efficiency of the system for the network throughput maximization in bits/s/Hz/cell |
| g_{ij} | expected value of the channel gain from cell j over the cell area of cell i |
| $g_{\text{pf}}^{(i)}$ | PF scheduling power gain of cell i |
| \mathbf{G} | coupling gain matrix |
| \mathbb{G} | set of all Neighborhood Groups |
| $\gamma_n^{(i)}$ | SINR of user n of cell i |
| $\gamma_{\text{th}}^{(i)}$ | user SINR threshold to assign users to inner and outer area of cell i in fractional frequency reuse |
| $\gamma_k^{(i)'}$ | k -th user SINR measurement of cell i |
| $\mathbf{\Gamma}$ | power ratio vector |
| $\mathbf{\Gamma}^*$ | optimum power ratio vector |
| Γ_i | power ratio of cell i |

| | |
|--|---|
| $\Gamma_{0,k}^{(i)'}$ | power ratio value at the time of the k -th user SINR measurement of cell i |
| $\tilde{\Gamma}$ | power ratio target vector |
| $\tilde{\Gamma}_i$ | power ratio target of cell i |
| $\check{\Gamma}$ | modified power ratio target vector |
| $\check{\Gamma}_i$ | modified power ratio target of cell i |
| i | cell index |
| j | cell index |
| k | measurement value index |
| l | iteration index |
| μ_{B_i} | mean of the cell bandwidth of cell i |
| $\mu_{B_{u,n}^{(i)}}$ | mean of the user bandwidth of user n of cell i |
| $\mu_{B_u^{(i)} R_u^{(i)}=1}$ | mean of the bandwidth required by a user of cell i to transmit one bit/s |
| μ_{R_i} | mean of the cell throughput of cell i |
| $\mu_{R_{u,n}^{(i)}}$ | mean of the user bit rate of user n of cell i |
| $\mu_{R_u^{(i)} B_u^{(i)}=1}$ | mean of the bit rate achieved by a user of cell i for one Hertz of user bandwidth |
| n | user index |
| \mathbf{n} | noise power vector |
| N_c | number of cells |
| N_0 | number of users in a non-HS cell |
| N_i | number of users of cell i |
| N'_i | linear approximation of the number of users of cell i |
| N_{hs} | number of users in a HS cell |
| N_{ng} | number of Neighborhood Groups |
| N_{nw} | total number of users in the network |
| \mathbf{N} | Neighborhood Group matrix |
| \mathbf{p} | transmit power vector |
| \mathbf{p}^* | optimum transmit power vector |
| $\mathbf{p}^{(l)}$ | transmit power vector of iteration l |
| $p_{\text{out},i}$ | outage probability of cell i at cell-level |
| $p_{\mathbf{r},\varphi}^{(i)}(r, \varphi)$ | pdf of user position of cell i |
| $\bar{P}_{1,i}$ | reference interference power of cell i |
| P_{max} | maximum transmit power |
| P_{N} | receiver noise power |

| | |
|--|---|
| $P_{\text{tx},i}$ | transmit power of cell i |
| $P_{\text{tx},i}^{(l)}$ | transmit power of cell i of iteration l |
| r | frequency reuse factor |
| \bar{R}_{u} | average user bit rate |
| $R_{\text{u},\text{min}}$ | minimum user bit rate |
| R_i | cell throughput of cell i |
| R'_i | linear approximation of the cell throughput of cell i |
| \tilde{R}_i | outage capacity at cell-level of cell i |
| R_{nw} | total network throughput |
| $R_{\text{u},n}^{(i)}$ | bit rate of user n of cell i |
| $\tilde{R}_{\text{u},n}^{(i)}$ | user bit rate target for user n of cell i |
| $R_{\text{u},\text{mc},n}^{(i)}$ | user bit rate achieved by user n in MC simulation |
| $R_{\text{u},\text{th}}^{(i)}$ | user bit rate threshold to assign users to inner and outer area of cell i in fractional frequency reuse |
| $R_{\text{u},k}^{(i)'}$ | user bit rate resulting from the k -th SINR measurement of cell i |
| $\mathbb{R}_{\text{u}}^{(i)}$ | set of user bit rates resulting from SINR measurements of cell i |
| $\rho(\mathbf{X})$ | spectral radius of matrix \mathbf{X} |
| ρ_{hs} | HS strength |
| $\rho_{\text{in},i}$ | relative size of the inner area of cell i for fractional frequency reuse |
| $\rho_{\text{rel},i}$ | number of users of cell i relative to the total number of users |
| ρ_{slp} | interpolation parameter for SLP |
| $\rho_{\text{tx},i}$ | transmit PSD of cell i |
| S_i | size of cell i , distance from the BS to the most remote point within the cell area |
| $\mathbb{S}_{\text{u}}^{(i)}$ | set of user SINR measurements from cell i |
| $\sigma_{B_i}^2$ | variance of the cell bandwidth of cell i |
| $\sigma_{B_{\text{u},n}^{(i)}}^2$ | variance of the user bandwidth of user n of cell i |
| $\sigma_{B_{\text{u}}^{(i)} R_{\text{u}}^{(i)}=1}^2$ | variance of the bandwidth required by a user of cell i to transmit one bit/s |
| $\sigma_{R_i}^2$ | variance of the cell throughput of cell i |
| $\sigma_{R_{\text{u},n}^{(i)}}^2$ | variance of the user bit rate of user n of cell i |
| $\sigma_{R_{\text{u}}^{(i)} B_{\text{u}}^{(i)}=1}^2$ | variance of the bit rate achieved by a user of cell i for one Hertz of user bandwidth |
| T_{coup} | interference coupling threshold |

Bibliography

- [3GP09] 3GPP, “TR 25.996: Spatial channel model for multiple input multiple output (MIMO) simulations,” 3GPP, Tech. Rep., 2009.
- [3GP11a] —, “TR 36.902: Evolved universal terrestrial radio access network (e-utran); self-configuring and self-optimizing network (son) use cases and solutions (release 9),” 3GPP, Tech. Rep., 2011.
- [3GP11b] —, “TS 36.300: Evolved universal terrestrial radio access (e-utra) and evolved universal terrestrial radio access network (e-utran); overall description; stage 2 (release 10),” 3GPP, Tech. Rep., 2011.
- [ABB⁺08] S. Avis, S. Baines, D. Bevan, D. Chandler, S. Hall, P. Myerscough-Jackopson, N. Scully, and S. Thiel, “Final project report (public version),” MONOTAS, Tech. Rep. Deliverable 7.2, Jan. 2008.
- [ADSK03] G. Auer, A. Dammann, S. Sand, and S. Kaiser, “On modeling cellular interference for multi-carrier based communication systems including a synchronization offset,” in *Proc. Wireless Personal Multimedia Communications WPMC03*, 2003.
- [ALS⁺08] M. Amirijoo, R. Litjens, K. Spaey, M. Döttling, T. Jansen, N. Scully, and U. Türke, “Use cases, requirements and assessment criteria for future self-organising radio access networks,” in *International Workshop on Self-Organizing Systems IWSOS 2008*, Dec. 2008.
- [AvK⁺01] K. I. Aardal, S. P. M. van Hoesel, A. M. C. A. Koster, C. Mannino, and A. Sassano, “Models and solution techniques for frequency assignment problems,” Konrad-Zuse-Zentrum für Informationstechnik Berlin, Tech. Rep. ZIB-Report 01-40, Dec. 2001.
- [AYM06] M. H. Ahmed, H. Yanikomeroglu, and S. Mahmoud, “Interference management using basestation coordination in broadband wireless access networks,” *Wireless Communications and Mobile Computing*, vol. 6, pp. 95–103, Jan. 2006.
- [BBD⁺05] S. C. Burst, A. Buvanewari, L. M. Drabeck, M. J. Flanagan, J. M. Graybeal, G. K. Hampel, M. Haner, W. M. MacDonald, P. A. Polakos, G. Rittenhouse, I. Saniee, A. Weiss, and P. A. Whiting, “Dynamic optimization in future cellular networks,” *Bell Labs Technical Journal*, vol. 10, no. 2, pp. 99–119, Aug. 2005.
- [BBP05] T. Bonald, S. Borst, and A. Proutiere, “Inter-cell scheduling in wireless data networks,” in *Proc. European Wireless Conference*, Cyprus, Apr. 2005.
- [BSMM08] I. N. Bronstein, K. A. Semendjajew, G. Musiol, and H. Mühlig, *Taschenbuch der Mathematik*, 7th ed. Harri Deutsch, 2008.
- [BV08] S. Boyd and L. Vandenberghe, *Convex Optimization*, 6th ed. Cambridge University Press, 2008.

- [CL01] Y. Cao and V. O. K. Li, "Scheduling algorithms in broad-band wireless networks," in *Proceedings of the IEEE*, vol. 89, no. 1, Jan. 2001, pp. 76–87.
- [CQ99] K. Chawla and X. Qiu, "Quasi-static resource allocation with interference avoidance for fixed wireless systems," *IEEE Journal on Selected Areas in Communications*, vol. 17, no. 3, pp. 493–504, mar 1999.
- [DAD⁺05] H. Dubreil, Z. Altman, V. Diascorn, J.-M. Picard, and M. Clerc, "Particle swarm optimization of fuzzy logic controller for high quality rrm auto-tuning of umts networks," in *Proc. IEEE 61rd Vehicular Technology Conference VTC 2005-Spring*, May 2005, pp. 1865–1869.
- [Dav81] H. A. David, *Order Statistics*, 2nd ed. John Wiley & Sons, 1981.
- [EGJ⁺03] A. Eisenblätter, H.-F. Geerdes, D. Junglas, T. Koch, T. Kürner, and A. Martin, "Final report on automatic planning and optimisation," IST MOMENTUM, Tech. Rep. Deliverable D4.7, Oct. 2003.
- [FCS07] M. Feng, L. Chen, and X. She, "Uplink adaptive resource allocation mitigating inter-cell interference fluctuation for future cellular systems," in *Proc. 2007 IEEE International Conference on Communications*, Jun. 2007, pp. 5519–5524.
- [Fer10] A. Fernekeß, "Low-complexity performance evaluation methodologies for OFDMA-based packet-switched wireless networks," Ph.D. dissertation, Technische Universität Darmstadt, 2010.
- [FHL⁺98] T. K. Fong, P. S. Henry, K. K. Leung, X. Qiu, and N. K. Shankaranarayanan, "Radio resource allocation in fixed broadband wireless networks," *IEEE Transactions on Communications*, vol. 46, no. 6, pp. 806–818, Jun. 1998.
- [FM93] G. J. Foschini and Z. Miljanic, "A simple distributed autonomous power control algorithm and its convergence," *IEEE Transactions on Vehicular Technology*, vol. 42, no. 4, pp. 641–646, Nov. 1993.
- [Gam86] A. Gamst, "Some lower bounds for a class of frequency assignment problems," *IEEE Transactions on Vehicular Technology*, vol. 35, no. 1, pp. 8–14, Feb. 1986.
- [GC97] A. J. Goldsmith and S.-G. Chua, "Variable-rate variable-power mqqam for fading channels," *IEEE Transactions on Communications*, vol. 45, no. 10, Oct. 1997.
- [GC98] ———, "Adaptive coded modulation for fading channels," *IEEE Transactions on Communications*, vol. 46, no. 5, May 1998.
- [Gee08] H.-F. Geerdes, "UMTS radio network planning: Mastering cell coupling for capacity optimization," Ph.D. dissertation, Technische Universität Berlin, 2008.

- [GKGO07] D. Gesbert, S. G. Kiani, A. Gjendemsjo, and G. E. Oien, “Adaptation, coordination, and distributed resource allocation in interference-limited wireless networks,” *Proceedings of the IEEE*, vol. 95, no. 12, pp. 2393–2409, Dec. 2007.
- [GZ94] S. A. Grandhi and J. Zander, “Constrained power control in cellular radio systems,” in *Proc. IEEE 44th Vehicular Technology Conference*, Jun. 1994, pp. 824–828.
- [Hal80] W. K. Hale, “Frequency assignment: Theory and applications,” *Proc. IEEE, Vol. 68*, pp. 1497–1514, Dec. 1980.
- [Hal83] S. W. Halpern, “Reuse partitioning in cellular systems,” in *Proc. 1983 IEEE 33rd Vehicular Technology Conference*, May 1983, pp. 322–327.
- [Hän01] E. Hänsler, *Statistische Signale - Grundlagen und Anwendungen*. Springer-Verlag, 2001.
- [Hat80] M. Hata, “Empirical formula for propagation loss in land mobile radio services,” *IEEE Transactions on Vehicular Technology*, vol. 29, no. 3, pp. 317–325, Aug. 1980.
- [HK08] P. P. Hasselbach and A. Klein, “An analytic model for outage probability and bandwidth demand of the downlink in packet switched cellular mobile radio networks,” in *Proc. 2008 IEEE International Conference on Communications (ICC 2008)*, May 2008.
- [HKG08] P. P. Hasselbach, A. Klein, and I. Gaspard, “Dynamic resource assignment (DRA) with minimum outage in cellular mobile radio networks,” in *Proc. 2008 IEEE 67th Vehicular Technology Conference: VTC2008-Spring*, May 2008.
- [HKG09a] —, “Self-organising radio resource management for cellular mobile radio networks using power-bandwidth characteristics,” in *Proc. ICT-MobileSummit 2009*, Jun. 2009.
- [HKG09b] —, “Transmit power allocation for self-organising future cellular mobile radio networks,” in *Proc. 2009 IEEE 20th International Symposium on Personal, Indoor and Mobile Communications (PIMRC09)*, Sep. 2009.
- [HKG⁺10] P. P. Hasselbach, A. Klein, I. Gaspard, D. von Hugo, and E. Bogenfeld, “Performance evaluation of self-optimising mobile radio networks in realistic scenarios,” *Frequenz - Journal of RF-Engineering and Telecommunications*, vol. 64, pp. 164–168, Sep. 2010.
- [HKS08] P. P. Hasselbach, A. Klein, and M. Siebert, “Interdependence of transmit power and cell bandwidth in cellular mobile radio networks,” in *Proc. 2008 IEEE 19th International Symposium on Personal, Indoor and Mobile Communications (PIMRC08)*, 2008.

- [HS94] J. K. Ho and R. P. Sundarraj, "On the efficacy of distributed simplex algorithms for linear programming," *Computational Optimization and Applications*, vol. 3, no. 4, pp. 349–363, Oct. 1994.
- [JBT⁺10] T. Jansen, I. Balan, J. Turk, I. Moerman, and T. Kürner, "Handover parameter optimization in LTE self-organizing networks," in *Vehicular Technology Conference Fall (VTC 2010-Fall)*, 2010 IEEE 72nd, sept. 2010.
- [JK00] R. Jäntti and S.-T. Kim, "Second-order power control with asymptotically fast convergence," *IEEE Journal on Selected Areas in Communications*, vol. 18, no. 3, pp. 447–457, Mar. 2000.
- [Kel97] F. Kelly, "Charging and rate control for elastic traffic," *European Transactions on Telecommunications*, vol. 8, no. 1, pp. 33–37, Jan-Feb 1997.
- [KK98] K. D. Kammeyer and K. Kroschel, *Digitale Signalverarbeitung*. B. G. Teubner Stuttgart, 1998.
- [KN96] I. Katzela and M. Naghshineh, "Channel assignment schemes for cellular mobile telecommunication systems: A comprehensive survey," *IEEE Personal Communications*, vol. 3, no. 3, pp. 10–31, Jun. 1996.
- [LCS03] X. Liu, E. K. P. Chong, and N. B. Shroff, "A framework for opportunistic scheduling in wireless networks," *Computer Networks*, vol. 41, no. 4, Mar. 2003.
- [Leh07a] F. Lehser, "Next generation mobile networks use cases related to self organising network, overall descriptions," NGMN Alliance, Tech. Rep., Dec. 2007.
- [Leh07b] —, "Use cases related to self organising network, overall description," NGMN Alliance, Tech. Rep., May 2007.
- [Leh08] —, "Recommendations on SON and o&m requirements," NGMN Alliance, Tech. Rep., Dec. 2008.
- [LL06] G. Li and H. Liu, "Downlink radio resource allocation for multi-cell ofdma system," *IEEE Transactions on Wireless Communications*, vol. 5, no. 12, pp. 3451–3459, Dec. 2006.
- [LS99] K. Leung and A. Srivastava, "Dynamic allocation of downlink and uplink resource for broadband services in fixed wireless networks," *IEEE Journal on Selected Areas in Communications*, vol. 17, no. 5, pp. 990–1006, may 1999.
- [LSJB10] A. Lobinger, S. Stefanski, T. Jansen, and I. Balan, "Load balancing in downlink lte self-optimizing networks," in *Vehicular Technology Conference (VTC 2010-Spring)*, 2010 IEEE 71st, may 2010.
- [LWN02] J. Laiho, A. Wacker, and T. Novosad, *Radio Network Planning and Optimisation for UMTS*. John Wiley & Sons, 2002.

- [LZ06] K. B. Letaief and Y. J. Zhang, "Dynamic multiuser resource allocation and adaptation for wireless systems," *IEEE Wireless Communications Magazine*, vol. 13, no. 4, pp. 38–47, Aug. 2006.
- [MNK⁺07] P. Mogensen, W. Na, I. Kovacs, F. Frederiksen, A. Pokhariyal, K. Pedersen, T. Kolding, K. Hugl, and M. Kuusela, "LTE capacity compared to the shannon bound," in *Vehicular Technology Conference, 2007. VTC2007-Spring. IEEE 65th*, april 2007, pp. 1234–1238.
- [Moi06] H. Moiin, "Next generation mobile networks beyond HSPA & EVDO," NGMN Alliance, Tech. Rep., Dec. 2006.
- [Mol03] A. F. Molisch, *Wireless Communications*. Wiley & Sons, November 2003.
- [NAD06] R. Nasri, Z. Altman, and H. Dubreil, "Fuzzy q-learning based autonomic management of macrodiversity algorithms in umts networks," *Annals of Telecommunications*, vol. 61, no. 9-10, pp. 1119–1135, Sep. 2006.
- [NADN06] R. Nasri, Z. Altman, H. Dubreil, and Z. Nour, "Wcdma downlink load sharing with dynamic control of soft handover parameters," in *Proc. IEEE 63rd Vehicular Technology Conference VTC 2006-Spring*, May 2006, pp. 942–946.
- [NDA06] M. J. Nawrocki, M. Dohler, and A. H. Aghvami, *Understanding UMTS Radio Network Modelling, Planning and Automated Optimisation*. John Wiley & Sons, 2006.
- [Nec08] M. Necker, "Interference coordination in cellular ofdma networks," *IEEE Network*, vol. 22, no. 6, pp. 12–19, november-december 2008.
- [PB05] C. Prehofer and C. Bettstetter, "Self-organization in communication networks: Principles and design paradigms," *IEEE Communications Magazine*, vol. 43, no. 7, pp. 78–85, Jul. 2005.
- [PB09] M. Pischella and J.-C. Belfiore, "Resource allocation for qos-aware ofdma using distributed network coordination," *IEEE Transactions on Vehicular Technology*, vol. 58, no. 4, pp. 1766–1775, May 2009.
- [PP02] A. Papoulis and U. Pillai, *Probability, Random Variables and Stochastic Processes*, 4th ed. McGraw Hill Higher Education, 2002.
- [Rap02] T. S. Rappaport, *Wireless Communications*, 2nd ed. Prentice Hall, 2002.
- [S⁺08a] L. C. Schmelz *et al.*, "Requirements for self-organising networks," FP7 SOCRATES, Tech. Rep. Deliverable D2.2, May 2008.
- [S⁺08b] N. Scully *et al.*, "Use cases for self-organising networks," FP7 SOCRATES, Tech. Rep. Deliverable D2.1, Mar. 2008.
- [S⁺08c] K. Spaey *et al.*, "Assessment criteria for self-organising networks," FP7 SOCRATES, Tech. Rep. Deliverable D2.3, Jun. 2008.

- [SAD⁺05] P. Stuckmann, Z. Altman, H. Dubreil, A. Ortega, R. Barco, M. Toril, M. Fernandez, M. Barry, S. McGrath, G. Blyth, P. Saidha, and L. M. Nielsen, “The EUREKA gandalf project: monitoring and self-tuning techniques for heterogeneous radio access networks,” in *Proc. IEEE 61st Vehicular Technology Conference*, May 2005.
- [SCR05] C. Stimming, T. Chen, and H. Rohling, “Flexible self-organized resource allocation in cellular ofdm systems,” in *Proc. 10th International OFDM-Workshop*, 2005.
- [Sha48] C. Shannon, “A mathematical theory of communication,” *Bell Systems Technical Journal*, 1948.
- [SPI05] C. Shen, D. Pesch, and J. Irvine, “A framework for self-management of hybrid wireless networks using autonomic computation principles,” in *3rd Annual Communication Networks and Services Research Conference*, May 2005.
- [SV08] A. Stolyar and H. Viswanathan, “Self-organizing dynamic fractional frequency reuse in ofdma systems,” in *INFOCOM 2008: The 27th IEEE Conference on Computer Communications*, Apr. 2008, pp. 1364–1372.
- [SWB06] S. Stanczak, M. Wiczanowski, and H. Boche, *Resource Allocation in Wireless Networks - Theory and Algorithms*. Springer-Verlag, 2006.
- [SWB09] ———, *Fundamentals of Resource Allocation in Wireless Networks*. Springer-Verlag, 2009.
- [TV05] D. Tse and P. Viswanath, *Fundamentals of Wireless Communication*. Cambridge University Press, 2005.
- [TVZ04] V. Tralli, R. Veronesi, and M. Zorzi, “Power-shaped advanced resource assignment (psara) for fixed broadband wireless access systems,” *IEEE Transactions on Wireless Communications*, vol. 3, no. 6, pp. 2207–2220, nov. 2004.
- [Van01] R. J. Vanderbei, *Linear Programming: Foundations and Extensions*, 2nd ed. Kluwer Academic Publishers, 2001.
- [Var10] R. S. Varga, *Matrix Iterative Analysis*, 2nd ed. Springer-Verlag, 2010.
- [vLE⁺08] J. L. van den Berg, R. Litjens, A. Eisenblätter, M. Amirijoo, O. Linnell, C. Blondia, T. Kürner, N. Scully, J. Oszmianski, and L. C. Schmelz, “Self-organisation in future mobile communication networks,” in *ICT-Mobile Summit 2008*, Jun. 2008.
- [VTL02] P. Viswanath, D. N. C. Tse, and R. Laroia, “Opportunistic beamforming using dumb antennas,” *IEEE Transactions on Information Theory*, vol. 48, no. 6, pp. 1277–1294, Jun. 2002.

- [VTZZ06] R. Veronesi, V. Tralli, J. Zander, and M. Zorzi, "Distributed dynamic resource allocation for multicell sdma packet access networks," *IEEE Transactions on Wireless Communications*, vol. 5, no. 10, pp. 2772–2783, oct. 2006.
- [XW10] Z. Xie and B. Walke, "Performance analysis of reuse partitioning techniques in OFDMA based cellular radio networks," in *Proc. 2010 IEEE 17th International Conference on Telecommunications*, Apr. 2010, pp. 272–279.
- [Yar01] G. Yarmish, "A distributed implementation of the simplex method," Ph.D. dissertation, Polytechnic University of New York, 2001.
- [Yv09] G. Yarmish and R. van Slyke, "A distributed, scaleable simplex method," *The Journal of Supercomputing*, vol. 49, no. 3, pp. 373–381, Sep. 2009.
- [Zan92a] J. Zander, "Distributed cochannel interference control in cellular radio systems," *IEEE Transactions on Vehicular Technology*, vol. 41, no. 3, pp. 305–311, Aug. 1992.
- [Zan92b] —, "Performance of optimum transmitter power control in cellular radio systems," *IEEE Transactions on Vehicular Technology*, vol. 41, no. 1, pp. 57–62, Feb. 1992.
- [Zem71] G. Zemke, *Lineare Optimierung - Lineare Programmierung*. Friedrich Vieweg & Sohn, 1971.
- [ZK01] J. Zander and S.-L. Kim, *Radio Resource Management for Wireless Networks*. Artech House, April 2001.
- [ZTH⁺10] S. Zheng, H. Tian, Z. Hu, L. Chen, and J. Zhu, "Qos-guaranteed radio resource allocation with distributed inter-cell interference coordination for multi-cell ofdma systems," in *Proc. 2010 IEEE 71st Vehicular Technology Conference: VTC 2010-Spring*, May 2010.

Lebenslauf

Name: Philipp Paul Hasselbach

Geburtsdatum: 4. März 1980

Geburtsort: Wetzlar

Familienstand: ledig

Schulausbildung

08/1986 - 07/1990 Grundsule Aßlar

08/1990 - 07/1996 Freiherr-vom-Stein-Schule Wetzlar
Integrierte Gesamtschule, gymnasialer Bildungsgang

08/1996 - 07/1999 Goetheschule Wetzlar
Oberstufengymnasium, Abschluss: Abitur

Studium

10/2000 - 06/2006 Studium der Elektrotechnik und Informationstechnik
an der Technischen Universität Darmstadt
Abschluss: Diplom-Ingenieur

Berufstätigkeit

seit 11/2006 wissenschaftlicher Mitarbeiter am
Fachgebiet Kommunikationstechnik,
Institut für Nachrichtentechnik,
Technische Universität Darmstadt

Darmstadt, 22. September 2011

Erklärung laut §9 der Promotionsordnung

Ich versichere hiermit, dass ich die vorliegende Dissertation allein und nur unter Verwendung der angegebenen Literatur verfasst habe. Die Arbeit hat bisher noch nicht zu Prüfungszwecken gedient.

Darmstadt, 22. September 2011

